LOW-TEMPERATURE PLATINUM THERMOMETRY AND VAPOUR PRESSURES OF NEON AND OXYGEN

J. L. TIGGELMAN

LOW-TEMPERATURE PLATINUM THERMOMETRY AND VAPOUR PRESSURES OF NEON AND OXYGEN

INSTITUUT-LORENTZ
voor theoretische natuurkunde
Nieuwsteeg 18-Leiden-Nederland

LOW-TEMPERATURE PLATINUM THERMOMETRY AND VAPOUR PRESSURES OF NEON AND OXYGEN

PROEFSCHRIFT

TER VERKRIJGING VAN DE GRAAD VAN DOCTOR IN DE WISKUNDE EN NATUURWETENSCHAPPEN AAN DE RIJKSUNIVERSITEIT TE LEIDEN, OP GEZAG VAN DE RECTOR MAGNIFICUS DR. A. E. COHEN, HOOGLERAAR IN DE FACULTEIT DER LETTEREN, VOLGENS BESLUIT VAN HET COLLEGE VAN DEKANEN TE VERDEDIGEN OP WOENSDAG 13 JUNI 1973 TE KLOKKE 15.15 UUR

DOOR

JAN LEENDERT TIGGELMAN

GEBOREN TE 'S-GRAVENHAGE IN 1942

1973

DRUKKERIJ J. H. PASMANS, 'S-GRAVENHAGE

PROMOTOR: PROF. DR. C.J. GORTER

DIT PROEFSCHRIFT IS BEWERKT ONDER TOEZICHT VAN

DR. M. DURIEUX

STELLINGEN

1. Grassie, Swallow, Williams en Loram vergelijken voor verdunde Pd-legeringen de afname van de specifieke elektrische weerstand ten gevolge van magnetische ordening door een uitwendig magnetisch veld met die ten gevolge van magnetische ordening door temperatuurverlaging zonder uitwendig veld. De argumenten op grond waarvan zij dan concluderen tot een niet-ferromagnetische toestand bij het absolute nulpunt zijn onjuist.

   A.D.C. Grassie, G.A. Swallow, G. Williams en J.W. Loram, Phys. Rev. B 3, 4154 (1971).

2. Waarden voor de soortelijke warmte bij constante druk, C_p, van vast neon kunnen worden verkregen uit correlaties met de dampspanning en andere thermodynamische grootheden van neon. Bij het tripelpunt stemmen deze waarden beter overeen met recente door Fugate en Swenson uit C_v berekende waarden dan met de direkt gemeten waarden voor C_p.

   R.Q. Fugate en C.A. Swenson, J. Low Temp. Physics 10, 317 (1973).
   Dit proefschrift, Hoofdstuk 2.

3. De waarden van Debije temperaturen, die o.a. door Van Duyneveldt en Pouw en door Lijphart, De Vroomen en Poulis zijn afgeleid uit spin-rooster relaxatiemetingen, blijken voor sommige ionische kristallen niet onafhankelijk van de temperatuur te zijn. Men dient bij analyses daarom rekening te houden met het temperatuurgebied waarin de metingen zijn uitgevoerd.

   A.J. van Duyneveldt en C.L.M. Pouw, XVIIth Congress Ampère, Univ. of Turku, Turku, Finland, Aug. 1972, paper M4.
   E.E. Lijphart, A.C. de Vroomen en N.J. Poulis, ibid., paper M2 (II).

4. Een recente bepaling van het kookpunt van water met een gas-thermometer heeft de waarde t = 99.97 °C opgeleverd. Dit zou betekenen, dat men in 1954 voor het ijspunt T = 273.23 K had moeten kiezen in plaats van T = 273.15 K. De laatste waarde berustte op een grote hoeveelheid nauw overeenstemmende gegevens. Een nieuwe bepaling van het kookpunt van water, ook niet-gas-thermometrisch, is daarom zeker gewenst.

L.A. Guildner, R.L. Anderson en R.E. Edsinger, Procès-Verbaux du Comité Consultatif de Thermométrie (C.C.T.), Sèvres, France, 1971, Annexe T13.
Procès-Verbaux du C.C.T., Sèvres, France, 1952.
Dixième Conférence Générale des Poids et Mesures, 1954.

5. Het is wenselijk de temperatuurverdeling, zoals die bijvoorbeeld optreedt langs capillairen in gasthermometers en dampspannings-thermometers, onder verschillende experimentele omstandigheden te onderzoeken.

R.D. Goodwin en L.A. Weber, J. Res. Natl. Bur. Stands. 73A, 1 (1969).
J.P. Compton, Metrologia 6, 103 (1970).
Dit proefschrift, Hoofdstukken 2 en 3.

6. Het door sommige auteurs gesignaleerde optreden van zg. X-punten - karakteristieke golflengten waarbij de optische reflectie- of emissie-coëfficiënt van metalen onafhankelijk van de temperatuur is - heeft meer een toevallige dan een principiële betekenis.

R.E. Hummel, Optische Eigenschaften von Metallen und Legierungen (Springer, Berlin, 1971) p. 190 e.v.

7. Er zijn drie vaste punten aan te geven in het temperatuurgebied tussen 4.2 K en 13.81 K waarmee, met de germanium-thermometer als interpolatie-instrument, op eenvoudige wijze een nauwkeurige praktische temperatuurschaal in dit gebied kan worden vastgelegd.

8. Volgens Sullivan en Sonntag is er een verschil van ongeveer een factor 3 tussen hun resultaten voor de tweede viriaalcoëfficiënt van neon en die van Crommelin, Palacios Martinez en Kamerlingh Onnes. In werkelijkheid bedraagt het verschil slechts ongeveer 10%.

C.A. Crommelin, J. Palacios Martinez en H. Kamerlingh Onnes, Commun. Phys. Lab., Leiden, No. 154a (1921).
J.A. Sullivan en R.E. Sonntag, Advances in Cryog. Eng. 12, 706 (1967).

9. De relatie $1\ \mathrm{Oe} = \frac{1000}{4\pi}\ \frac{\mathrm{A}}{\mathrm{m}}$, die door Alonso-Finn en door Strumia wordt gegeven voor de omrekening van het niet-gerationaliseerde magnetische veld in oersted naar het gerationaliseerde magnetische veld in SI-eenheden, is om twee redenen onjuist.

M. Alonso en E.J. Finn, Fund. Univ. Physics, Addison-Wesley Publ. Co., 1st ed., 1969.
F. Strumia, Metrologia 8, 85 (1972).

10. Er bestaat een grote discrepantie tussen enerzijds de hoeveelheid werk, die vele gebruikers en instituten voor metrologie verrichten om veranderingen, die kunnen optreden in de calibratie van germanium-thermometers, op te vangen, en anderzijds de hoeveelheid werk, die wordt gedaan ter verbetering van de stabiliteit van deze thermometers.

J.L. Tiggelman

Leiden, 13 juni 1973

Aan Alma en Jeroen

Aan mijn moeder

Aan de nagedachtenis van mijn vader

CONTENTS

CHAPTER 1

INTRODUCTION

1 General introduction

This thesis deals with measurements of vapour pressures of solid and liquid neon between 19 K and 30 K and of liquid oxygen between 54 K and 99 K and with a study of the behaviour of platinum resistance thermometers in the range between 2 K and 273.15 K. Although in the chapters on neon and oxygen vapour pressures also correlations of thermophysical data for these gases are discussed, and in the chapter on platinum thermometry below 13.81 K the problem of deviations from Matthiessen's rule for samples of pure platinum is touched upon, the main theme of the thesis is precision thermometry which is the physics of temperature measurements and the establishment of international practical temperature scales. This justifies the rather extensive treatment of such topics as the realization of the triple points and boiling points of neon and oxygen with sub-millikelvin precision and the differences between temperatures as measured with different platinum thermometers, topics which may not be of much interest from the point of view of general physics, but are of high importance for the definition of reproducible practical temperature scales.

2 Objectives of this research

The objectives of the research described in this thesis can conveniently be discussed in the frame of the International Practical Temperature Scale of 1968 (IPTS-68). A short description of this scale, which became effective on January 1, 1969, is given in the Appendix at the end of this thesis.

In the low temperature range, which is of interest for the present research, IPTS-68 is based on the platinum thermometer which has to be calibrated at a number of fixed points. The conditions to realize fixed

point temperatures with the accuracy and reproducibility which are required in the calibration of platinum thermometers on IPTS-68 are studied for the triple points and boiling points of neon and oxygen in Chapters 2 and 3.

The vapour-pressure temperature relations of solid neon between 19 K and 24.56 K and of liquid neon between 24.56 K and 30 K and of liquid oxygen between 54 K and 99 K have been determined. The temperatures have been measured, for the first time, on IPTS-68. In the past, measurements were made on so-called national or laboratory scales which, in nearly all cases, lack the reproducibility of measurements in different laboratories which is inherent in IPTS-68.

The obtained vapour-pressure equations may serve as alternatives to the platinum thermometer to measure temperatures. The vapour-pressure equations are also of interest from a more general point of view; this is demonstrated in their correlation with other thermophysical properties such as latent heat of vaporization and heat of fusion, heat capacities of the condensed and gaseous phases and virial coefficients of the gas. The thermodynamic consistency of available data is discussed; in some cases quantities for which no experimental data exist could be calculated.

Vapour-pressure temperature relations of solid and liquid ^{20}Ne and ^{22}Ne between 19 K and 30 K are presented, which are derived from the present results on neon of normal isotopic composition and from available data on differences between vapour pressures of the pure isotopes. The advantage of replacing the boiling point of neon of normal isotopic composition (T_{68} = 27.102 K) by that of the pure isotope ^{20}Ne is discussed.

In Chapter 4, the small differences between realizations of IPTS-68 with different platinum thermometers are studied below 0°C for a group of nine thermometers from different sources. It is found that these differences are for seven thermometers within ± 1 mK over the full range from 13.81 K to 0°C.

In Chapter 5, measurements of the temperature dependence of the resistances of ten platinum thermometers between 2 K and 15 K are presented and discussed. It is demonstrated that platinum thermometers can be used even below 13.81 K with a reasonable precision (1.5 mK at 4.2 K). Specific calibration procedures for the temperature range between 4.2 K

and 13.81 K are suggested. The results are also discussed in their relation to Matthiessen's rule; significant deviations from this rule are detected.

It is gratifying that, as a by-product of the research described in this thesis, the laboratory has now the disposal of nine standard platinum thermometers calibrated between 2 K and 273.15 K. In the range above 13.81 K, this calibration is on the International Practical Temperature Scale of 1968. Some of these thermometers have gone to other laboratories as standards for temperature measurements and some will be used for an international intercomparison of realizations of IPTS-68, which is being planned, and for future calibrations in our laboratory of standard platinum thermometers below 273.15 K.

Finally, I would like to mention here that the present research in several essential ways has benefitted from work of Van Rijn in this laboratory. In the first place, his apparatus designed for helium and hydrogen vapour-pressure measurements could be used for the experiments on neon and oxygen described in Chapters 2 and 3. Secondly, his calibrations of thermometers at the fixed points at liquid hydrogen temperatures were used to obtain the IPTS-68 calibrations of the thermometers, and, thirdly, his magnetic temperature measurements provided the temperature scale used in Chapter 5.

CHAPTER 2

VAPOUR PRESSURES OF NEON

1 Introduction

The vapour-pressure temperature relations of liquid neon between the triple point (24.562 K) and 30 K and of solid neon between the triple point and 19 K have been determined. Temperatures were directly measured on the International Practical Temperature Scale of 1968 (IPTS-68) [1] with two platinum thermometers.

The dependence of the accuracy and reproducibility of realizations of the triple point and the normal boiling point upon the experimental conditions, which is of importance for the use of these points as fixed points in thermometry, has been investigated.

The measurements have been made with neon of natural isotopic composition.

Vapour-pressure temperature relations of the pure isotopes ^{20}Ne and ^{22}Ne have been calculated from those of neon of normal isotopic composition, which is shown to obey closely Raoult's law, and from literature data for differences between isothermal vapour pressures of the isotopes.

The measured vapour pressures have been correlated with other thermophysical properties of neon.

2 Experimental method

2.1 *Apparatus and procedure of measurement*

The apparatus, which was originally built for the calibration of germanium and platinum thermometers against helium and hydrogen vapour pressures [2], has been used for realizations of all fixed points of IPTS-68 below 0 °C and for measurements of vapour pressures of solid and liquid neon and of liquid oxygen. It is sketched in fig. 2.1.

In a copper block K, of about 700 g, there are twelve holes N in

which germanium thermometers can be inserted, two holes L to accommodate platinum thermometers and a central cavity J which is the reservoir of the vapour-pressure thermometer. The block is suspended by the stainless-steel capillary H (I.D. 1.6 mm, O.D. 2.0 mm) which connects the vapour-pressure bulb to the manometers. D is a radiation trap in this capillary. The block is surrounded by a copper thermal shield G. On top of the thermal shield there is a second vapour-pressure bulb F; it is connected to the manometers by the stainless-steel tube C (I.D. 2.4 mm) which surrounds capillary H. In the present experiments, C is usually employed as vacuum jacket around capillary H. The assembly is suspended in the brass can E, which is sealed with an indium O-ring. B is the pumping line. A is one of four platinum-glass seals, in each of which there are nine platinum wires, soldered into german silver tubes in the top plate of the vacuum can.

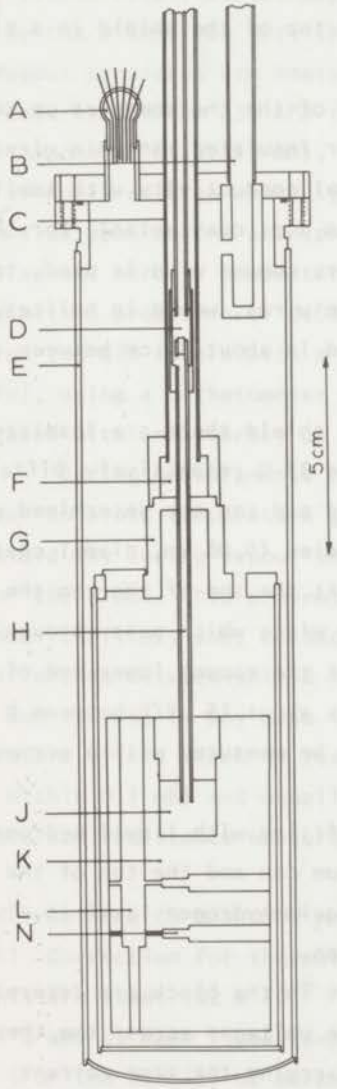

Fig. 2.1
Apparatus for measurements of vapour pressures and calibrations of platinum and germanium thermometers.

To ensure good thermal contact between the resistance

thermometers and the copper block, Apiezon N grease and copper shims are used. For germanium thermometers it is known (see e.g. Blakemore [3]) that about 70% of the heat exchange between the germanium crystal and the thermometer surroundings occurs along the lead wires. Therefore the four (potential and current) wires of each thermometer are glued to the block surface with GE 7031 over a distance of at least 5 cm. The lead wires are thermally anchored to the top of the shield in a similar way.

For the extension of the lead wires of the thermometers up to the top of the vacuum can, in general lacquer insulated manganin wire (0.1 mm) is used. Manganin combines low thermal conductivity with small thermal EMF versus copper (in contrast to e.g. constantan). For the current leads of the platinum thermometers copper wire is used, to minimize joule heating. The length of the wires, wound in helices, is between block and shield about 10 cm, and is about 30 cm between shield and platinum-glass seals.

Around the block and the top of the shield there are insulated constantan heater wires (0.1 mm) of 84 Ω and 33 Ω respectively. Differences between the temperatures of block, shield and can are determined with Au-0.03 at.% Fe versus chromel thermocouples (0.08 mm, diamel coated wires, Johnson, Matthey and Co., Ltd.). At the top of the can the Au-Fe and chromel wires are soldered to copper wires which pass through B, the junctions being thermally anchored at the copper lower end of B. The sensitivity of these thermocouples is about 15 μV/K between 4 K and 273 K. The temperature of the shield can be measured with a germanium thermometer.

The apparatus is placed in a dewar filled with liquid hydrogen. The distance between the top of the vacuum can and the top of the dewar is 67 cm. During the measurements the liquid-hydrogen level is always about 6 cm above the top of the vacuum can.

D.c. resistances of the thermometers in the block are determined potentiometrically, by intercomparing the voltages across the thermometers and across a standard resistor, carrying the same current. About 99.9% of the voltage is counterbalanced using the first two dials of a modified precision Diesselhorst potentiometer, developed by Dr. H. van

Dijk. The remaining signal goes into a Keithley model 140 precision nanovolt d.c. amplifier (amplification factor 10^5, accuracy 10^{-4}, linearity 5×10^{-6}, input impedance > 50 MΩ), and is then displayed on a digital voltmeter (Hewlett Packard 3450 A) and read to 0.5 mV when necessary. The standard resistors have been calibrated and related to $\Omega_{69\text{-}BI}$ with a relative accuracy of 2×10^{-6} (for resistances up to 50 Ω) by the Dienst van het Ijkwezen in the Hague in 1972.

Vapour pressures are measured with a mercury manometer (I.D. 25 mm) for pressures between 233 kPa (1750 torr) and 6.7 kPa (50 torr) and with an oil manometer (I.D. 13 mm), filled with Octoil-S, for pressures below 6.7 kPa. For pressures above 130 kPa the manometer is used with the vacuum side open to the atmosphere. The atmospheric pressure is measured with a second mercury manometer. Readings of the mercury levels are performed with a precision of 0.01 mm (corresponding to 1.3 Pa) or better, those of the oil levels with a precision of 0.02 mm (corresponding to 0.18 Pa), using a cathetometer and an invar scale. The invar scale is calibrated with an accuracy of 2 μm, and is mounted next to the manometers.

During measurements the heater around the block is never used, in order to avoid temperature gradients in the block. The temperature of the shield is, during vapour-pressure measurements, kept slightly above that of the block. This prevents the occurrence of cold spots [4] along the inner capillary and, consequently, errors in measured pressures. The difference between shield and block temperature is usually between 20 mK and 100 mK, in any case it is such that the rate of change of temperature of the block is less than 4 mK/hour. This allows precise (i.e. within 0.1 mK) and usually linear interpolation in time of vapour-pressure and resistance measurements.

2.2 *Corrections to measured pressures*

1) Correction for thermal expansion. As mean cubic expansion coefficients are used: 182×10^{-6} °C^{-1} for mercury and 785×10^{-6} °C^{-1} for Octoil-S and as mean linear expansion coefficient for invar 1×10^{-6} °C^{-1}. (For the density of mercury at 0 °C the value 13.5951 g/cm^3 is used and for that of Octoil-S at 25 °C 0.9103 g/cm^3.)

2) Correction for the deviation of the local value of the accel-

eration of gravity (9.81276 m/s^2) [5] from the standard value (9.80665 m/s^2).

3) Correction for the aerostatic pressure head due to the difference in weight of the gas columns above the condensed neon and above the mercury or oil level in the manometer. The temperature distribution along the capillary in the cryostat was not measured, but had to be estimated (5 cm of the capillary, between block and shield, was at constant temperature, while the temperature gradient existed over 73 cm of the capillary between the shield and the top of the hydrogen dewar). The estimate was made from the geometry of the apparatus, and by comparison with data obtained in this laboratory by El Hadi en Ter Harmsel for capillaries where temperature distributions were measured with thermocouples. The aerostatic pressure head correction for the gas in the capillary up to the top of the H_2 dewar, which is applied in the present work, varies from 0.65 Pa (equivalent to 0.5 mK) at 19 K to 59 Pa (1.1 mK) at 30 K. The uncertainty in the correction is estimated to be less than 25%.

4) Correction for the thermomolecular-pressure effect (see also Chapter 3). It is only applied at temperatures near 19 K (even there the correction is equivalent to only 0.1 mK).

5) Correction for the deviation of the samples' composition from the normal isotopic composition of neon: equivalent to 0.8 mK at all temperatures (see sections 3 and 7).

2.3 *Neon samples and purification*

Neon samples were taken from research grade neon supplied in metal cylinders by Messer Griesheim GmbH, a member of the Hoechst group (W. Germany), and by Matheson Gas Products (U.S.A.). Samples are denoted H and M respectively. According to the manufacturer, neon H contained less than 500 ppm of He, while other impurities were not detectable. Neon M contained, according to the manufacturer, 30 ppm of He and less than 1 ppm of each of other impurities. Since these amounts of helium could have an appreciable influence upon the vapour pressure, the samples were purified.

The neon gas from a cylinder was solidified in a small glass bulb

in a separate hydrogen dewar at 14 K and pumped for half an hour or longer. Virtually no neon is lost since the vapour pressure of neon at 14 K is 0.1 torr. Thereafter, the neon was evaporated into glass bulbs with volumes of 2 ℓ and 4 ℓ, from which controlled amounts were condensed into the vapour-pressure bulb.

Occasionally, small samples, taken from the vapour above the condensed neon, were analyzed mass spectrometrically. Negligible amounts of impurities were found (see table 2.2).

3 Isotopic composition

Atmospheric neon is a mixture of the isotopes ^{20}Ne; ^{21}Ne and ^{22}Ne. The pure isotopes have different vapour pressures, or boiling points, and thus the boiling point of the mixture will depend on the isotopic composition.

Recent data for the isotopic composition of atmospheric neon have been reported by Eberhardt, Eugster and Marti [6] and by Walton and Cameron [7]. They differ from data reported earlier by Nier [8] (see table 2.1); the differences have been explained [6] by assuming a

Table 2.1

Natural abundance of neon isotopes[a]

Author	at.% ^{20}Ne	at.% ^{21}Ne	at.% ^{22}Ne
Nier [8]	90.92 ± 0.04	0.257± 0.001	8.82 ± 0.04
Eberhardt et al. [6]	90.50 ± 0.07	0.268± 0.002	9.23 ± 0.07
Walton and Cameron [7]	90.514± 0.031	0.266± 0.005	9.220± 0.029
normal composition according to the text in IPTS-68 [1]	90.9	0.26	8.8

[a] Quoted uncertainties are taken from the original publications.

possible fractionation of Nier's sample.

The composition of atmospheric neon given in the text of IPTS-68 is close to that given by Nier (it is also close to the composition of the sample used by Grilly [9] in his vapour-pressure measurements). Recently used samples (viz. Furukawa [10] and table 2.2) of commercial atmospheric neon have isotopic compositions which are closer to those reported by Eberhardt et al. and Walton and Cameron.

The composition and purity of samples, taken from the vapour above the liquid and from the gas cylinders in the present experiments, are given in table 2.2. The data were obtained mass-spectrometrically.*

Table 2.2

Isotopic composition and purity of neon samples

sample[a]	source	at.% ^{20}Ne	at.% ^{21}Ne	at.% ^{22}Ne	at.% ^{22}Ne in liquid phase[b]	H_2	He
H	gas cylinder[c]	90.6	0.264	9.15	-	-	<500 ppm
H	triple point 22.6	90.69	0.265	9.04	9.41	4 ppm	15 ppm
H	boiling point 31	90.61	0.264	9.12_5	9.43_5	6 ppm	-
H	boiling point 32	90.43_5	0.268	9.30	9.61	7 ppm	-
M	gas cylinder	90.36	0.269	9.37	-	4 ppm	-
M2	boiling point 34	90.62	0.265	9.11_5	9.42_5	4 ppm	-
M2	evaporated liquid after completion of measurements	90.11	0.281	9.60_5	9.60_5	7 ppm	4 ppm

[a] Samples are indicated as described in section 2.3; the numbers in column 2 refer to series numbers (see sections 5 and 6)

[b] Values in this column have been calculated from those in the preceding column (see Appendix 1).

[c] Manufacturer's analysis

* The mass-spectrometrical analyses were carried out at the FOM-Instituut voor Atoom-en Molecuulfysica in Amsterdam. We are obliged to Mr. A. Haring for his helpful cooperation.

The precision of the data is 0.5% in the ratio $^{22}Ne/^{20}Ne$ and 1% in the ratio $^{21}Ne/^{20}Ne$. The mass spectrometer was assumed to be equally sensitive to all isotopes. Systematic errors probably do not exceed 1%.

The normal boiling point of ^{22}Ne is 127 mK higher than that of ^{20}Ne. If, therefore, the ratio of the mole fractions of ^{22}Ne and ^{20}Ne, which is about 0.1, is uncertain by 1% (and the ratio $^{21}Ne/^{20}Ne$ is assumed to be sufficiently known; ^{21}Ne is a minor component), the uncertainty in the mole fractions of ^{20}Ne and ^{22}Ne is 0.0009 and the uncertainty in the temperature determination by means of vapour-pressure thermometry is 0.11 mK.

The relative abundances of the isotopes in the liquid and vapour phases differ slightly. It is shown in Appendix 1 to this Chapter that the mole fraction of ^{22}Ne near the triple point is 0.0037 higher in the liquid than in the vapour; near the normal boiling point this difference is 0.0031.

In IPTS-68 it is not specified whether the stated "normal" composition applies to the liquid or the vapour phase. This implies, as remarked also by Compton [11], that there is an uncertainty of 0.4 mK in the specification of the normal boiling point of neon. In the present research it is assumed that the normal composition given in the text of IPTS-68 (see table 2.1) applies to the liquid phase; the experimental results were corrected for deviations of the liquid composition from that in IPTS-68. The uncertainty in the temperature corrections due to uncertainties in the determinations of the composition of the gas and to a possible non-equilibrium distribution of the isotopes over the two phases is estimated to be 0.2 mK.

4 Temperature measurements on IPTS-68

Temperatures were measured with the two platinum thermometers, 164956 (to be referred to as B2) and T4. Thermometer B2 was calibrated by Van Rijn et al. [2] at the hydrogen fixed points 13.81 K, 17.042 K and 20.28 K and, in fact, against hydrogen vapour pressures also at a number of other temperatures. After these measurements, also T4 was placed in the apparatus and compared with B2 at the hydrogen fixed points. The resistance at 4.2 K of B2 was checked, and appeared to be within the

experimental error the same as found by Van Rijn et al. (The difference was 2×10^{-8} in the reduced resistance $R_{4.2\ K}/R_{0\ °C}$.)

In the present measurements B2 and T4 were calibrated at the neon normal boiling point (see section 5). Later (see Chapter 3), these two thermometers were calibrated at the oxygen triple point and normal boiling point. The two thermometers were repeatedly calibrated at the triple point of water and at the steampoint (see Chapter 4). The accuracy of the calibrations at the fixed points is estimated to be 0.2 mK at the oxygen triple point, 0.5 mK at the other fixed points below 273.15 K, 1 mK at 273.15 K and 3 mK at 373.15 K. From these figures it can be calculated that the uncertainties in the calibration of the thermometers do not exceed 0.8 mK between 19 K and 30 K.

In several of the graphs in the subsequent sections, which show the experimental results, the data for the two thermometers are given separately. However, for all final calculations of the experimental results the average of the T_{68} values for the two thermometers has been taken. It can be seen in Chapter 4 that this average is, between 19 K and 30 K, within ± 0.2 mK equal to the average for seven platinum thermometers with $\alpha > 0.003926\ °C^{-1}$.

5 Normal boiling point of neon

5.1 *Introduction*

The normal boiling point (NBP) of neon of the isotopic composition given in the last row of table 2.1, hereafter called normal neon, is a defining fixed point of IPTS-68. Its value of 27.102 K is based on data of Grilly [9], (27.092 ± 0.003) K, and on a preliminary value of Furukawa [12], (27.0986 ± 0.0007) K, both on the NBS-55 temperature scale. The average value of 27.095 K (on NBS-55) was increased with 7 mK, to be in agreement with a smoothed average of the four "national scales" which was fitted to the fixed points at 13.81 K, 20.28 K, 54.361 K and 90.188 K (for details, see Bedford et al. [13,14]).

Recent values on the NBS-55 scale are close to the average value 27.095 K given above: Furukawa et al. [15] reported (27.096 ± 0.001) K on NBS-55. This value must be decreased with 0.6 mK to account for the deviation of the sample from normal neon. Compton [11] reported (27.096$_1$ ±

0.00026) K on NBS-55; the exact sample composition is unknown (the quoted compositions are relative to that of a "standard cylinder" which was assumed to contain normal neon, although the occurrence of normal neon seems to be exceptional rather than normal, see section 3).

It may be pointed out here that the value 27.095_4 K for the NBP of normal neon, calculated from the data of Furukawa et al. [15], yields 6.6 mK for the difference between the NBS-55 scale and IPTS-68 at 27.1 K, which is in close agreement with the value 7.1 mK given by Bedford et al. [14].

The realization of the NBP of neon is essential for the accurate calibration of platinum thermometers down to 20 K on IPTS-68. The reproducibility and the accuracy of the realization of the NBP have been investigated.

5.2 *Experiment*

The temperature of the block T_B is, during the measurements, within 10 mK of 27.102 K. The temperature of the shield T_S is kept between 30 and 70 mK above T_B. Under these conditions T_B increases with about 3 mK per hour.

Temperatures T_{68} are measured with the platinum thermometers B2 and T4; the agreement between these is in general within 0.1 mK (see table 2.3). Observed vapour pressures are converted into temperatures T_p by means of the vapour-pressure equation in IPTS-68 (eq. (2.1), section 7). Differences T_{68}-T_p obtained are given in table 2.3 and fig. 2.2. (A correction of 0.9 mK is applied for the aerostatic head in the capillary, but the data are not corrected for deviations of the isotopic composition from that of normal neon).

As a check on the purity of the neon, portions of the vapour (of about 600 cm^3 NTP) were pumped off several times. When He or H_2 would be present, a decrease in the vapour pressure and an increase of T_{68}-T_p would occur. For pure neon a small similar effect must be expected: because ^{20}Ne is more volatile than ^{22}Ne, the concentration of ^{22}Ne will increase if gas is pumped off and, consequently, the vapour pressure will decrease. The increase of the mole fraction of ^{22}Ne is noticable from series 31 to series 32 (see table 2.2); the effect on the vapour pressure would cause a decrease in T_p of 0.2 mK; this is not reflected

Table 2.3

Realization of the normal boiling point of neon

series	sample	$T_{68} - T_p$ (mK)	$T_{68}^{(T4)} - T_{68}^{(B2)}$ (mK)	liquid volume (cm^3)	liquid-vapour mass ratio
1	M1	0.2	0.0	1.5	5.0
2		0.1_5	0.1	1.0	3.3
3		0.1	0.0_5	1.0	3.3
4		0.0_5	-0.3	1.0	3.3
5		0.0_5	0.1	1.0	3.3
6		-0.1	-0.0_5	1.0	3.3
10	H	-0.5	-0.0_5	1.5	5.0
11		0.5	0.0	1.0	3.3
12		0.1	-0.0_5	0.7	2.3
13		-0.0_5	-0.1	0.7	2.3
14		-0.2	0.0	0.7	2.3
27		0.0	-0.0_5	0.7	2.3
30		0.1_5	0.0	0.7	2.3
31		0.1	0.0_5	0.7	2.3
32		0.1_5	0.1	0.4	1.3
33		0.2_5	-	0.1_5	0.5
34	M2	-0.0_5	-	1.8	6.0
35		0.0	-0.0_5	1.8	6.0
36		-0.3	0.0	1.5	5.0

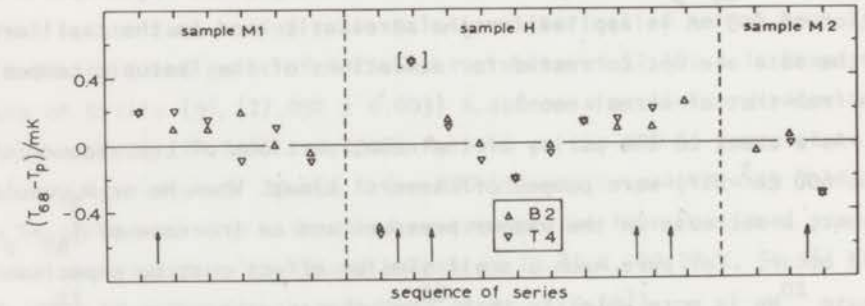

Fig. 2.2. Reproducibility of the normal boiling point of neon. Arrows indicate pumping off of about 600 cm^3 NTP of neon. Series 11 is unreliable. The zero has been arbitrarily chosen.

in fig. 2.2, probably because it hardly exceeds the experimental error.

Impurities found for series 31, 32 and 34 are negligible (see table 2.2; an amount of 10 ppm of volatile impurities in the vapour increases the observed pressure with the equivalent of 0.025 mK). The decrease of T_p after run 10 to a "normal" value is possibly associated with the removal of impurities: neon H originally had contained 500 ppm of He, which would have caused T_p to increase with 10 mK for our experimental conditions; the purification would thus have removed only 95% of the He impurity.

The result for series 11 is probably due to an error, as indicated by an inconsistency in the sum of the mercury heights in the manometer.

As the final value of the NBP of neon, which was used for the calibration of the platinum thermometers, the base line in fig. 2.2, corrected with 0.8 mK for the deviations of the isotopic composition of the samples from that of normal neon, has been chosen.

5.3 *Conclusions*

In the present experiments the NBP of neon could be realized with a reproducibility of ± 0.2 mK (see fig. 2.2).

The absolute accuracy is estimated to be 0.5 mK. This includes an uncertainty in the aerostatic head correction (0.25 mK) and an uncertainty in the isotopic composition (0.2 mK). The latter effect also affects the reproducibility of the data and the spread of the points in fig. 2.2, but the first effect does not, because the level of the liquid hydrogen in the dewar and, consequently, the temperature distribution along the capillary and the aerostatic head correction were nearly the same for all series.

These results may be compared with those of Furukawa et al. [15] (uncertainty of the NBP on the NBS-55 scale ± 1 mK) and Compton [11,16] (reproducibility ± 0.25 mK; overall accuracy ± 0.23 mK, see however section 5.1).

The NBP of normal neon appears to be excellently suitable as defining fixed point of IPTS-68. The aerostatic head correction should be taken into account. Also the isotopic composition must be known. If, in the vapour-pressure measuring system, the liquid to vapour mass ratio

is large enough, the composition of the liquid will be practically equal to that of the neon supply from which the sample is taken, which makes it unnecessary to determine the composition of the sample in situ. Recently, it was suggested [9] that a replacement of the NBP of normal neon by that of ^{20}Ne as a fixed point of IPTS-68 should be seriously considered. This would, of course, eliminate the errors due to uncertainties in the distribution of the isotopes entirely; however, if suitable precautions are taken, this error is not likely to exceed 0.2 mK.

6 Triple point of neon

6.1 *Introduction*

The triple point (TP) of natural neon has been measured. The dependence of the observed TP temperature and vapour pressure upon experimental conditions has been investigated, and values for these quantities in the limit of zero heat influx into the sample have been determined.

The TP of neon is not a defining fixed point in IPTS-68, but the present study has been considered worthwhile in view of a possible relation to the phenomena found at the TP of argon [17] and of oxygen ([18], Chapter 3) and because of its use as a secondary fixed point.

A comparison with measurements of the TP of neon, oxygen, nitrogen and argon by different authors will be given in Chapter 3, section 5.5.

6.2 *Experiment*

The copper block, with about 1.5 cm^3 of condensed neon in the vapour-pressure bulb, and the surrounding shield are cooled below TP. This can be done by evaporating neon from the vapour-pressure bulb, because the heat of fusion (334 J/mol) is much lower than the heat of vaporization (1795 J/mol), and because the heat capacities of the apparatus (11 J/K) and of the neon (3.2 J/K) are relatively small. To cool the system from 25 K to just below TP, about 20% of the neon has to be evaporated. This has been done once. Normally cooling of the block below TP is achieved by heat exchange with the liquid hydrogen bath, after admission of some helium gas into the vacuum can. When the block has reached a temperature between 19 K and 22 K, the can is evacuated to

10^{-5} torr; thereafter the block is heated till just below TP. Then the heat input is so much reduced that the temperature of the block rises about 1 mK per minute until TP is reached. This is displayed on a recorder, which shows a small uncompensated and amplified part of the signal from a platinum thermometer.

Since the normal cooling procedure could cause neon to solidify in the capillary between block and shield, the shield was heated a few kelvin above the TP temperature (this was done before the TP temperature was reached or just thereafter). After a slow increase of the vapour pressure due to heating of the top layer of liquified neon in the capillary, a sharp decrease eventually indicated that the capillary was open. Thereafter, the shield was allowed to cool down, mainly by heat conduction along the outer capillary between vacuum can and shield, to slightly above the temperature of the block; the rate of cooling was about 1 K/hour.

Because it appeared that the temperature and the vapour pressure are dependent upon the heat influx into the sample, actual measurements of T and p were made at very low heat influx and, to investigate the dependence of T and p upon the fraction of melted neon, controlled amounts of heat were applied to the block between measurements.

In order to prevent condensation of neon in the capillary, the shield temperature T_S was kept above the block temperature T_B during the TP transition; a current through the shield heater of about 4.5 mA, corresponding to 500 μW, was sufficient to compensate for heat losses, mainly along the outer capillary, to the bath.

The heat influx into the block due to the temperature difference T_S-T_B was about 8 μW per 0.1 K; this was found from the heat capacity of the system and the observed rate of change of T_B for T_S-T_B = 0.3 K, at a temperature just above TP, after correcting for the steady heat influx of 3.6 μW produced by the current of 3 mA through the platinum thermometers.

Usually, during measurements, T_S-T_B was kept small (see table 2.4), so that the heat influx was small, e.g. for T_S-T_B = 0.1 K the complete melting of the sample would take about 20 days.

Especially near the end of a TP passage, when a large fraction of

the neon had melted, the temperature of the block rose far above the TP temperature during heating periods and, in these cases, it was necessary to wait after the heating periods for more than an hour before the temperature became constant and the measurements of T and p could be started.

To investigate the dependence of the observed TP temperature and vapour pressure upon the heat influx at different fractions of melted neon, $T_S - T_B$ was occasionally varied between certain limits.

Twice a TP was realized with one sample of neon H and four times with two samples of neon M.

6.3 *Discussion of the results*

In table 2.4 the results of the measurements are given and in fig. 2.3 the observed temperatures are plotted versus the fractional amount of melted neon (the ratio of the number of moles of liquid and the total number of moles of neon in the vapour-pressure bulb). For fractions of melted neon smaller than 0.07, the observed TP temperature is dependent upon the amount of melted neon, at least for the samples M1 and H. This can be attributed to very small quantities of impurities which are more soluble in the liquid than in the solid neon. For example, 1 ppm of an impurity which is soluble in the liquid and not in the solid gives a decrease of the freezing point of less than 0.02 mK when (nearly) 100 per cent of the solid is melted, but of about 0.8 mK when only 2 percent of the solid is melted; 1 or 2 ppm of such an impurity are then sufficient to explain the observed effect. In the case of oxygen, Ancsin [18] reported Ar and, to a small extent, He to elevate the TP temperature and Ne, Kr and especially Xe to lower it.

The observed TP temperature depends, especially for larger fractions of melted neon, upon the heat influx (see fig. 2.3; the platinum-thermometer current is equivalent to an extra temperature difference $T_S - T_B$ of about 40 mK, see paragraph 6.2). For a small fraction of melted neon no increase in temperature is found, even for $T_S - T_B = 1.4$ K, corresponding to a heat influx of about 100 μW.

It can be seen from the last column in table 2.4 that nearly in all circumstances the observed vapour pressures are in agreement with the temperatures, even if these differ from the TP temperature. For the

Table 2.4

Triple-point transition data[a] for neon of normal isotopic composition

neon sample	series number	time (min)	% melted	$T_S - T_B$ (mK)	p[b] (Pa)	$T_{68}^{(B2)}$ (K)	$T_{68}^{(T4)}$ (K)	$T_{(p)} - T_{68}$[c] (mK)
M1	9.1	30	∿ 0.1	500	43320	24.5597	24.5595	-1.0
	.2	30	∿ 0.3	80	43320	24.5597	24.5596	-1.0_5
H	22.1	25	4.7	60	43355	24.5610_5	24.5607	-0.0_5
	.2	10	6.4	300	43363 / 43360 [d]	24.5614	24.5613	-0.1_5
	.3	15	24.6	350	43371 / 43368	24.5620_5	24.5617	-0.2
	.4	10	34.6	400	43371 / 43376	24.5620	-	0.0_5
	.5	10	48.1	500	43376	24.5622_5	-	-0.1
	.6[e]	4	∿99	550	43372	24.5621	-	-0.2
	23.1	20	0.7	80	43338 / 43347	24.5605	24.5602	-0.3_5
	.2	25	45	40	43374	24.5620	24.5618	0.1
	.3	35	74	50	43373	24.5620	24.5617	0.0_5
	.4	20	75	220	43381	24.5625	-	0.0_5
	.5	10	75	30	-	24.5620	-	-
M2	37.1	20	3.1	85	43368	24.5617	24.5614	0.0_5
	.2	15	6.7	80	43370	24.5617	24.5615	-0.1_5
	.3	25	60	80	43374	24.5621_5	24.5618	0.0
	.4	20	60	500	43384	24.5630	24.5629	-0.3
	.5	25	60	50	43372 / 43374	24.5623	24.5619	-0.1
	38.1	25	?	50	43376	24.5621	24.5618	0.1_5
	.2	20	33	50	43378	24.5624	24.5620	0.0
	.3	30	33	- 0	43359	24.5619	24.5617	-0.7_5
	39.1	20	1.8	50	43370	24.5619	24.5615	0.0
	.2	10	2.7	1400	43372	24.5618_5	-	0.1_5
	.3	20	40.2	10	43375	24.5620	24.5617	0.2
	.4	10	90	10	43378	24.5623	-	0.0
	.5[f]	8	90	500	43414 / 43431	24.56^{69}_{78}	-	∿-2.5
	.6	5	90	25	-	24.5629	-	-

[a] The actually measured data have been corrected for the deviation of the liquid isotopic composition of the samples (see table 2.2) from the composition of normal neon as defined in IPTS-68 (see table 2.1): the measured pressures have been decreased with 2 Pa (0.01_5 torr), the measured temperatures with 0.8 mK (see, e.g., Furukawa [10]). All other necessary corrections have been applied to the measured pressures; the aerostatic head correction has been taken equal to 12.8 Pa (0.096 torr).

[b] 1 Pa (= 1 N/m^2) is equal to 1/101325 standard atmosphere.

[c] $T_{(p)}$ has been derived from p using the experimental vapour-pressure equation for liquid neon given in section 7 (eq. (2.4)).
[d] In cases where two values are given, the measured quantity drifted during the series between the two values.
[e] Series H-22.6 which lasted only 4 minutes, was measured shortly after evaporation of 0.007 cm^3 of liquid neon. This explains the relatively low values for p and T; $T_{(p)}-T_{68}$ illustrates the good thermal equilibrium which nevertheless existed.
[f] Under these conditions no thermal equilibrium could be achieved.

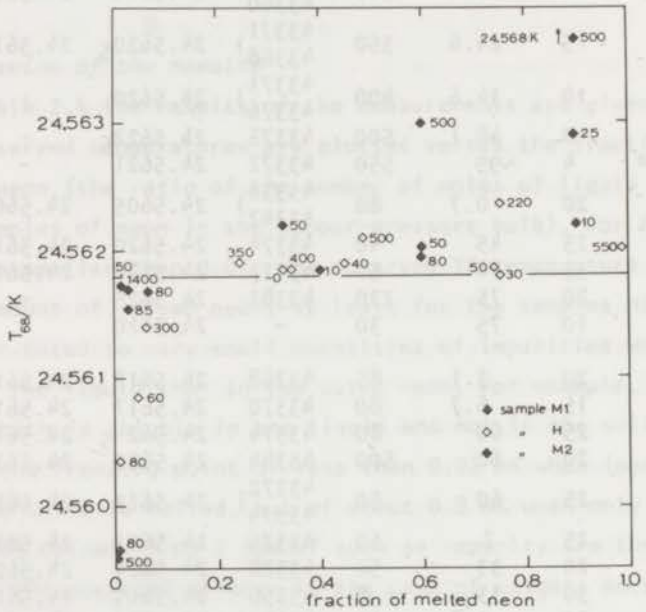

Fig. 2.3. The measured temperature at the triple point of neon versus the fractional amount of melted neon. The numbers near the points indicate the temperature differences in mK between the shield and the block ($T_{shield}-T_{block}$).

points at small fractions of melted neon for which the temperature is smaller than the TP temperature, the agreement between T and p can be expected if the impurity concentrations are negligible in the vapour phase. (In this case the decrease of the vapour pressure due to impurities can be estimated from Henry's law, and is negligibly small for im-

purity contents of 1 or 2 ppm.) In cases where the temperatures are larger than the TP temperature, the fact that the observed vapour pressures follow the temperatures means, that there is temperature equilibrium between block and liquid neon surface in the vapour-pressure bulb, so that the increase in the temperatures must be due to temperature gradients in the liquid neon.

The correct values for the TP temperature and pressure were determined from the data at the lower fractions of melted neon, and from extrapolation to zero heat input of the data at larger fractions of melted neon.

The overheating is, at constant fraction of melted neon, roughly proportional to the heat influx into the block (see fig. 2.4); this is to be expected if it is due to temperature gradients in the liquid neon. In fig. 2.5 the overheating is plotted versus the fractional amount of melted neon, for a heat influx of 30 μW (data for this figure are ob-

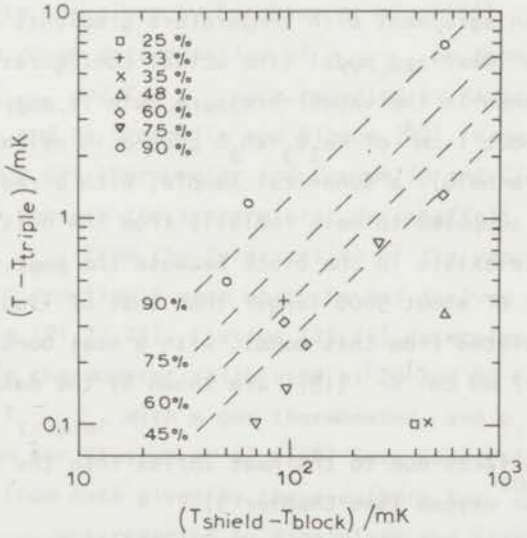

Fig. 2.4. Overheating during triple point transitions as a function of $T_{shield}-T_{block}$ for various fractions of melted neon. The actual values of $T_{shield}-T_{block}$ have been increased with 40 mK to account for the heat input due to the thermometer current. The dashed lines have been calculated from a crude model.

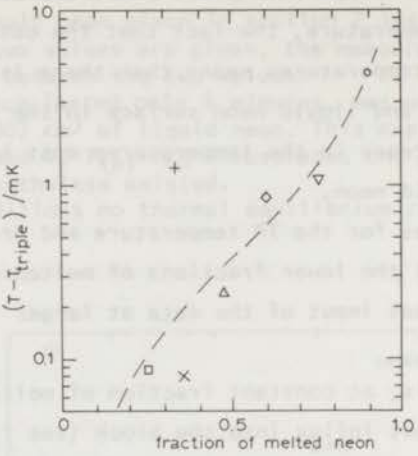

Fig. 2.5. Overheating as a function of the fractional amount of melted neon for a heat influx of 30 μW, determined by rough interpolation of the experimental points in fig. 2.4.

tained by interpolation of the experimental points in fig. 2.4). The data are roughly in agreement with temperature gradients calculated from the following idealized model (the actual configuration of the liquid and solid neon in the vapour-pressure bulb is not known, due to the presence of about 1 cm^3 of $Fe_2O_3 \cdot xH_2O$ packed in nylon stocking in the vapour-pressure bulb): a spherical sample, with a radius of 5 mm, of condensed neon is supposed to melt radially from the outside; no temperature difference exists in the block because the heat conduction of copper is a factor of about 5000 larger than that of liquid neon. The overheatings calculated from this model, with a heat conductivity for liquid neon of 1.17 mW $cm^{-1}K^{-1}$ [19], are shown by the dashed lines in fig. 2.4.

Overheating effects due to the heat influx into the sample have also been found for oxygen (see Chapter 3).

It may finally be mentioned that during the TP passage the isotopic compositions in the liquid and the solid phase, which are slightly different, change. It is shown in Appendix 1 to this Chapter that due to this change the TP temperature increases with 0.11 mK and the TP pressure with 0.3 Pa during melting.

The results of the TP determinations, corrected to zero heat influx, are

$$T_{68\ \text{triple}} = (24.5618 \pm 0.0008)\ \text{K}$$
$$p_{\text{triple}} = (43371 \pm 7)\ \text{Pa}$$
$$= (325.31 \pm 0.05)\ \text{torr}$$

The uncertainty in $T_{68\ \text{triple}}$ includes the accuracy of the TP realization for the different samples (± 0.1 mK) and the accuracy of the calibration of the thermometers on IPTS-68 (± 0.7 mK). The value for $T_{68\ \text{triple}}$ quoted is the average for the two platinum thermometers, the values for each thermometer being: 24.5619 K for B2 and 24.5617 K for T4.

The uncertainty given for p_{triple} includes the accuracy of the pressure measurement itself (± 3 Pa) and the uncertainty in the aerostatic head correction (± 4 Pa).

6.4 *Comparison with previous data*

Data published by different authors are given in table 2.5 (a compilation of data was given by Furukawa et al. [15]).

After the rough determination of p_{triple} by Kamerlingh Onnes [20], values for p_{triple} and T_{triple} were reported by Kamerlingh Onnes and Crommelin [21] and by Crommelin and Gibson [22]. Kamerlingh Onnes and Crommelin used a gas thermometer and Crommelin and Gibson a platinum thermometer to measure the temperature. Verschaffelt [23] calculated p_{triple} and T_{triple} from the intersection of the vapour-pressure equations for solid and liquid neon which he had derived after an analysis of various data [21,22,24]. Clusius [25,26] determined T_{triple} with a lead resistance thermometer calibrated at 20 and 80 K. Henning and Otto [27] measured T_{triple}, with a gas thermometer, and p_{triple}. The data in table 2.5 given for Clusius et al. [28] have been calculated by linear interpolation from data given by these authors for ^{20}Ne and ^{22}Ne. A value for p_{triple} was reported by Bigeleisen and Roth [29]. The temperatures given by all these authors cannot be converted to a current temperature scale, which prevents accurate comparison with later data.

Recent measurements were made by Grilly [9], Furukawa et al. [15] and Compton [11]; the temperatures were given on the NBS-55 scale and

Table 2.5

Data for the triple-point temperature and pressure given by different authors

Investigator	year	T/K	temperature scale	T_{68}/K	p/kPa
Kamerlingh Onnes [20]	1909	-	-	-	47
Kamerlingh Onnes and Crommelin [21]	1915	24.42_5[a]	-	-	43.13
Crommelin and Gibson [22]	1927	24.57_5[a]	-	-	43.13
Verschaffelt [23]	1928	24.40_5	-	-	39.9_2
Clusius [25]	1929	24.59	-	-	-
Clusius [26]	1936	24.55	-	-	-
Henning and Otto [27]	1936	24.56[b]	-	-	43.3
Clusius et al. [28]	1960	24.68	-	-	43.372
Bigeleisen and Roth [29]	1961	24.59_5[c]	ref.22	-	43.338±0.013
Grilly [9]	1962	24.544 ±4	NBS-55	24.552	43.300±0.048
Furukawa et al. [15]	1970	24.552_4[d] ±1	NBS-55	24.560_4	43.331±0.013
Compton [11]	1970	24.552[e] ±2	NBS-55	24.560	-
This research		24.5618 ±0.8	IPTS-68	24.5618	43.371±0.007

[a] The temperatures have been increased by 5 mK for conversion from the scale with 0 °C = 273.09 K to a scale with 0 °C = 273.15 K.

[b] Uncorrected for the assumed ice-point value of 273.16 K (the correction of 1 mK is much smaller than the uncertainty in the data).

[c] Temperature deduced from the measured vapour pressure and the vapour-pressure equation of Crommelin and Gibson [22].

[d] Temperature and pressure quoted are corrected with -0.6 mK and -1 Pa respectively for the deviation of the composition of the neon from the normal isotopic composition.

[e] No correction for deviation from the normal isotopic composition applied.

have been converted to IPTS-68 [14]. Furukawa et al. attributed the low value of T_{triple} found by Grilly to errors in the calibration of the thermometer; it can be seen, however, that also his value for p_{triple} is rather low. The values for T_{triple} given by Furukawa et al. and by Compton differ slightly from the present result. This may be caused by the uncertainty in the recalculation of the results of these authors from the NBS-55 scale to IPTS-68. The differences are, however, within the experimental uncertainties. The difference between the value of p_{triple} given by Furukawa et al. and the present value is somewhat larger;

it is equivalent to about 3 mK.

Furukawa [10] has measured values for T_{triple} and p_{triple} of ^{20}Ne and ^{22}Ne (see also section 9.2). Interpolation of these to a normal neon mixture yields $T_{68\ triple}$ = 24.561 K and p_{triple} = 43356 Pa. These values agree even better with the present results than the data of Furukawa et al. for normal neon.

7 The vapour-pressure equation of liquid neon between 24.5 K and 30 K

7.1 *Introduction*

Vapour pressures of liquid neon of natural isotopic composition have been measured at 13 temperatures between the triple point (24.562 K) and 30 K. From the data a vapour-pressure equation is derived; the results are compared with previous data.

7.2 *Experimental results*

The experimental procedure was similar to that described for the normal boiling point. Vapour pressures have been determined with the mercury manometers and temperatures T_{68} with the two thermometers T4 and

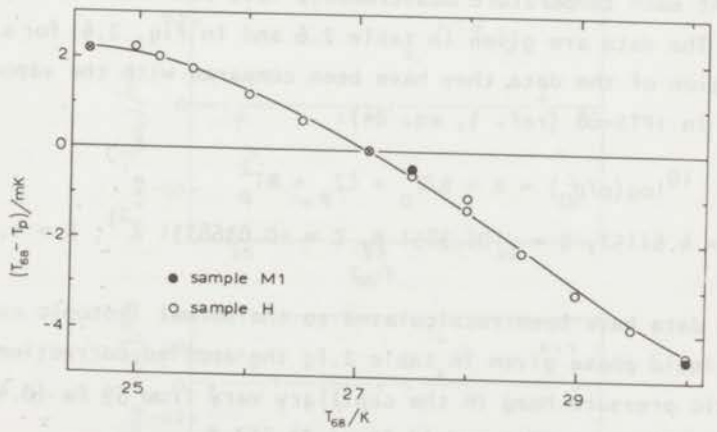

Fig. 2.6. Differences between experimental vapour-pressure temperature data for liquid neon and eq. (2.1). The data points at the triple point and the normal boiling point are averages of several series. The curve represents eq. (2.4).

Table 2.6

Experimental vapour-pressure vs. temperature data for liquid neon.

series number	neon sample	T_{68}[a] (K)	$T_{68}-T_p$[b] (mK)	$T_{68}^{(T4)}-T_{68}^{(B2)}$ (mK)
TP	H,M2	24.5618	2.2	-0.2
18	H	24.97	2.2_5	-0.2
24	H	25.19	2.0_5	-0.2_5
19	H	25.48	1.8	-0.2
25	H	25.99	1.2	-0.4
26	H	26.48	0.6_5	-0.1
NBP	H,M1,2	27.102	0	0
28	H	27.51	-0.5_5	-0.1_5
7	M1	27.51	-0.4	-0.4
15	H	28.00	-1.2_5	0.0
29	H	28.00	-1.0	0.0
16	H	28.50	-2.2	-0.2
17	H	28.95	-3.1	0.0
20	H	29.46	-3.8_5	-0.1
8	M1	30.00	-4.5_5	0.0
21	H	30.00	-4.4_5	0.0

[a] In this column rounded-off values of the series temperature are given.
[b] T_{68} is the average of the temperatures $T_{68}^{(B2)}$ and $T_{68}^{(T4)}$, T_p is derived from the vapour pressures by using eq. (2.1).

B2; the agreement between the two thermometers was always 0.4 mK or better. At each temperature measurements have been made during about half an hour. The data are given in table 2.6 and in fig. 2.6; for a convenient presentation of the data, they have been compared with the vapour-pressure equation in IPTS-68 (ref. 1, eq. 24):

$$^{10}\log(p/p_0) = A + B/T_p + CT_p + DT_p^2 \qquad (2.1)$$

where $A = 4.61152$, $B = -106.3851$ K, $C = -0.0368331$ K^{-1}, $D = 4.24892 \times 10^{-4}$ K^{-2}.

The data have been recalculated to the normal isotopic composition in the liquid phase given in table 2.1; the applied corrections for the aerostatic pressure head in the capillary vary from 59 Pa (0.44 torr) at 30 K to 27 Pa at 27 K and 13 Pa at 24.562 K.

The results with different samples at 27.5 K and 30 K agree within 0.15 mK and the two values for one sample at 28 K within 0.25 mK. The overall precision is about 0.2 mK.

7.3 *Representation of data*

The relationship between vapour pressure and temperature is usually represented by the equation

$$\ln(p/p_0) = \sum_{n=0}^{k-1} A_n T^{n-1} + B \ln(T/T_0) \qquad (2.2)$$

or by

$$\ln(p/p_0) = \sum_{n=0}^{k} A_n T^{n-1} \qquad (2.3)$$

Expressing $\ln(p/p_0)$ in a series of powers of 1/T is suggested by thermodynamical calculations, i.e. integration of Clapeyron's equation in its simplest form yields the expression $\ln(p/p_0) = C_1 + C_2/T$ or, if a linear change with temperature of the enthalpy of the vapour is assumed, $\ln(p/p_0) = C_1 + C_2/T + C_3 \ln T$ (see also section 10).

Fits of eqs. (2.2) and (2.3) to the experimental data give nearly identical results for equal value of k. Fig. 2.7 shows the differences between experimental points and a fit of eq. (2.3) with k = 2; systematic differences are apparent. The small scatter of the points around a smooth curve through the points confirms the precision of 0.2 mK. The

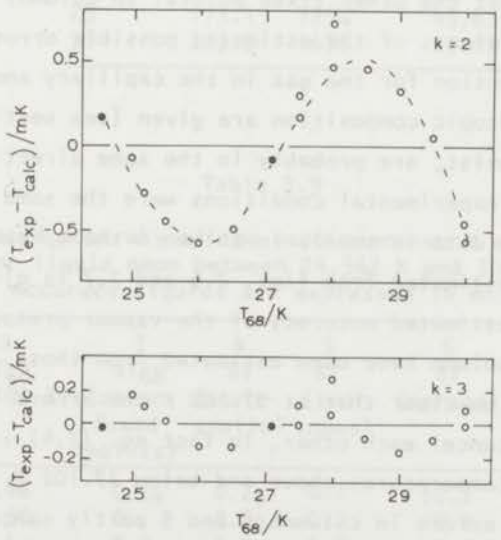

Fig. 2.7. Differences between the experimental data for liquid neon in table 2.6 and fits with eq. (2.3) for k = 2 and k = 3.

deviations of the experimental points from a fit of eq. (2.3) with k = 3 are, with the exception of one point, smaller than 0.2 mK (see fig. 2.7). The RMS value of $(p_{calc}-p_{exp})/p_{calc}$ is 3.3×10^{-5} and the maximum value is 8.6×10^{-5}. No better fit is found with k = 4.

Eq. (2.3) with k = 3 was chosen as the final representation of the data; coefficients are given in table 2.7. The coefficients A and B are within 10% and 25%, respectively, in agreement with the values obtained by integrating Clapeyron's equation; such agreement was also found with k = 2, but not with k = 4.

For convenience, a list of values of T, p and dp/dT calculated from eq. (2.4) in table 2.7 is given in table 2.8.

7.4 *Accuracy of the experimental vapour-pressure equation*

The accuracy of eq. (2.4) depends on the accuracy of the measurements of T_{68} and the vapour pressure. The figures in table 2.9 should show the factors which determine these accuracies, and give an impression of the final accuracy which is obtained. In column 2 the systematic error in T_{68} due to a possible error in the calibration at 27.102 K is given (see section 5), and in column 3 the systematic error due to errors in the calibrations at the other fixed points. In columns 4 and 5 the temperature equivalents of the estimated possible errors in the aerostatic head correction for the gas in the capillary and the uncertainty in the isotopic composition are given (see section 3); these errors, if they exist, are probably in the same direction at all temperatures since the experimental conditions were the same and, moreover, the spread in the data is small. In column 6 the spread (precision) of the p-T data as estimated from figs. 2.6 and 2.7 is given. Column 7 gives the total estimated accuracy of the vapour-pressure equation. The numbers in this column have been estimated from those in columns 2, 3, 4, 5 and 6; it will be clear that at 27.102 K the errors in T_{68} and in the vapour pressure cancel each other, in fact eq. (2.4) is exact at this temperature; at temperatures above and below 27.102 K the errors in column 2 and the errors in columns 4 and 5 partly cancel each other.

As mentioned before, the temperature T_{68} in eq. (2.4) is derived from the average for the two platinum thermometers used in this experi-

Table 2.7

The vapour-pressure equation for liquid normal neon[a] between the triple point (24.562 K) and 30 K derived from the present experiments

$$\ln(p/p_0) = A + B/T_{68} + CT_{68} + DT_{68}^2 \qquad (2.4)$$

$$A = 10.1531987$$
$$B = -240.780122 \quad K$$
$$C = -6.7969444 \times 10^{-2} \quad K^{-1}$$
$$D = 7.802784 \times 10^{-4} \quad K^{-2}$$

[a] Composition in the liquid phase as specified in IPTS-68, see table 2.1.

Table 2.8

Values of T, p and dp/dT calculated from eq. (2.4) in table 2.7

T_{68}/K	p/kPa	p/torr	dp/dT_{68} kPa/K
24.562	43.37	325.3	16.02
25	50.84	381.4	18.12
26	71.59	537.0	23.54
27	98.24	736.8	29.91
27.102	101.3	760	30.61
28	131.7	988.1	37.26
29	173.1	1298	45.63
30	223.3	1675	55.03

Table 2.9

Estimated accuracy of the vapour-pressure equation for liquid neon between 24.562 K and 30 K. Accuracy figures are expressed in mK.

1 T_{68}	2 δT_{68} (27.102 K)	3 δT_{68} (other fixed points)	4 δT (aero-static)	5 δT (iso-topes)	6 δT (spread)	7 δT (total)	8 δT (IPTS-68 spread)
24.562 K	0.46	0.2_4	0.2_0	0.2	±0.2	0.7	±0.3
27.102 K	0.50	0	0.2_2	0.2	±0.2	0.0	0.0
30 K	0.4_6	0.2_5	0.2_8	0.2	±0.2	0.7	±0.2

ment. The maximum difference with the average of the seven standard platinum thermometers with $\alpha > 0.003926\ K^{-1}$ used in Chapter 4 is only 0.1 mK (at 30 K). An impression of how much temperatures measured with individual platinum thermometers can differ from this average, is given by the total spread among the seven thermometers used in Chapter 4 (column 8).

7.5 *Comparison with previous data*

Data of different authors are compared with the present results in fig. 2.8. Most of the early measurements were made in Leiden. Kamerlingh Onnes and Crommelin [21] reported data between the triple point and the normal boiling point, Cath and Kamerlingh Onnes [24] between the normal boiling point and the critical point (44.4 K). The vapour-pressure equation fitted by Crommelin [30] to selected data (black points in fig. 2.8) from these authors differs considerably (up to 0.2 K) from the experimental points. This is probably due to the spread in the data and to unequal weighing of the points (and not to typographical errors as suggested by

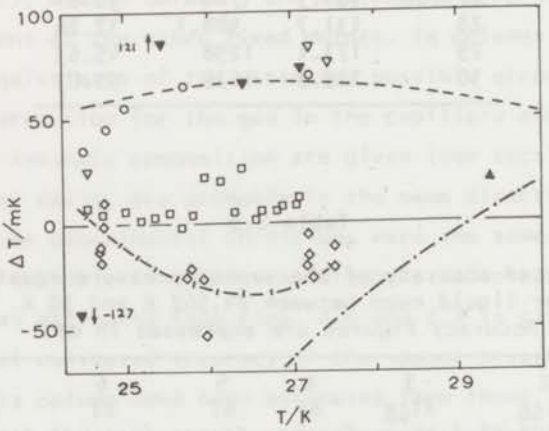

Fig. 2.8. Deviations of data of previous authors from the present vapour-pressure equation (eq. (2.4)) for liquid neon. The base line represents eq. (2.4).

▽▼ Kamerlingh Onnes and Crommelin [21] - - - Verschaffelt [23]

▲ Cath and Kamerlingh Onnes [24] □ Haantjes [31]

—·—·— Crommelin [30] —◇—◇— Henning and Otto [27]

○ Crommelin and Gibson [22]

Furukawa [10]). Verschaffelt [23] derived from data of Crommelin and Gibson [22] between the triple point and the normal boiling point, and from the older data, a vapour-pressure equation valid up to 44.4 K. The data reported by Haantjes [31], of which the spread is only about 0.01 K, differ not more than 0.01 K from the present relation. The spread in the data of Henning and Otto [27] is about 0.03 K.

The data presented sofar were not (and, with a few exceptions, could not be) converted to IPTS-68. Where necessary, they were corrected for deviations of the ice-point from 273.15 K.

More recent data are compared with the present results in fig. 2.9. Grilly [9] has given a vapour-pressure equation of neon between the triple point and 44.40 K, in which temperatures are on the NBS-55 scale. The equation recalculated to IPTS-68, with scale differences given in ref. 14, differs less than 3.3 mK from the present results.

The vapour-pressure equation for liquid neon in IPTS-68 (this is eq. (2.1) and is the base line in fig. 2.6) has been derived in 1968 from Grilly's equation by recalculation from the NBS-55 scale to IPTS-68, and making some slight adjustments to let the normal boiling point coin-

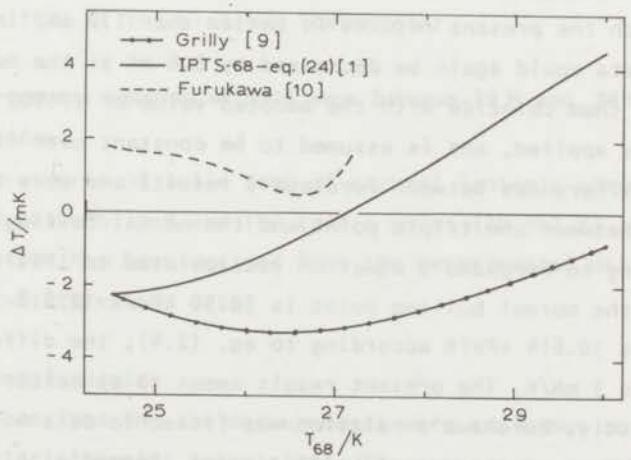

Fig. 2.9. Differences between recent vapour-pressure equations for liquid neon. The base line represents eq. (2.4.). The equations of Grilly and Furukawa have been recalculated to IPTS-68.

cide with the adopted value 27.102 K. At the time that this recalculation and the adjustments were made, the conversion tables in ref. 14 were not yet published; the adjustments of the normal boiling point and the use of slightly different values for the scale differences explain the differences between Grilly's equation recalculated to IPTS-68 and the IPTS-68 equation (see fig. 2.9).

The slope of the vapour-pressure equation derived from the present results differs from that in the IPTS-68 equation by a nearly constant amount of 1 mK/K between 25 K and 30 K. (This difference is so small that the small-range inverse vapour-pressure equation in IPTS-68 (eq. (19) of ref. 1) differs from the present results by only 0.12 mK at 27.0 K and 27.2 K.)

Measurements of the vapour pressure of liquid neon were also made by Furukawa. The data were represented by a vapour-pressure equation from the triple point to slightly above the normal boiling point, in which temperatures are on the NBS-55 scale [10]. The equation has been recalculated to IPTS-68; the differences with the present equation are shown in fig. 2.9. For a better comparison with the present results, Furukawa's data must be corrected by -0.6 mK for the deviation of the isotopic composition of his sample from the IPTS-68 normal composition. Then the agreement with the present results is better than 1.2 mK. In fact, Furukawa's data could again be decreased by 0.6 mK at the normal boiling point to let them coincide with the adopted value of 27.102 K; if this correction is applied, and is assumed to be constant over the temperature range, the differences between Furukawa's results and ours become less than 0.7 mK between the triple point and the normal boiling point.

According to Furukawa's equation recalculated to IPTS-68, the value of dp/dT at the normal boiling point is 30.50 kPa/K (228.8 torr/K) whereas it is 30.614 kPa/K according to eq. (2.4); the difference is equivalent to 3 mK/K. The present result seems to be better for two reasons. Firstly, Furukawa's relation was fitted to data which extended to only 0.05 K above the normal boiling point. Secondly, his results for ^{20}Ne as well as for ^{22}Ne yield dp/dT = 30.60 kPa/K.

The recent vapour-pressure data of Cetas [32] between the triple point and the normal boiling point (presented in a small graph) are pre-

cise to ± 1 mK and show no significant differences with Furukawa's recalculated data and the present results.

7.6 *Conclusion*

The equation in table 2.7 which represents the present vapour-pressure data is in good agreement with recent other data; it has the advantage of being derived from measurements directly on IPTS-68. The equation, in terms of T_{68}, is exact by definition at 27.102 K; the accuracy is estimated to vary from 0.7 mK at 24.56 K to 0 mK at 27.102 K and 0.7 mK at 30 K. The equation is derived for neon of the normal isotopic composition as defined in table 2.1, but it can easily be recalculated to other compositions. Remarks about the accuracy in terms of thermodynamic temperatures are made in section 10.

The liquid-neon vapour-pressure thermometer may serve for accurate temperature measurements between 24.5 K and 30 K in such cases where the use of the platinum thermometer is less convenient, or where experiments are made with liquid neon itself. Automatic pressure measuring equipment can to some extent overcome the relative inconvenience of accurate pressure measurements. The sensitivity of the neon vapour-pressure thermometer is excellent and its accuracy for measuring temperatures on IPTS-68 is comparable to that of the platinum thermometer.

8 The vapour-pressure equation of solid neon between 19 K and 24.5 K

8.1 *Introduction*

Vapour pressures of solid neon of natural isotopic composition have been measured between 19 K and the triple point (24.562 K). A vapour-pressure equation has been derived from the experimental data; the results are compared with previous data.

8.2 *Experimental results*

The preparations for the measurements were analogous to those outlined for the triple-point transitions. The same care was taken that the capillary did not become blocked with solid neon during cooling of the sample. In some cases this cooling was achieved by pumping on the solid neon in the vapour-pressure bulb, and in other cases by heat exchange

with the liquid hydrogen bath through admission of gas into the vacuum can. The measurements were made in a similar way as those for liquid neon. The shield temperature was kept about 70 mK higher than the block temperature. The temperature drift of the block due to heat influx was about 3 mK/hour and linear, which permitted precise interpolation and smoothing of the data acquired in series of at least half an hour.

Vapour pressures have been measured with the mercury manometer for pressures above 7 kPa and with the oil manometer for the lower pressures. The applied correction for the aerostatic pressure head for gas in the capillary varied from 0.6 Pa (equivalent to 0.5 mK) at 19 K to 13 Pa (0.7 mK) at the triple point. The correction for the thermomolecular pressure effect amounts to only 0.1 Pa (0.1 mK) at the lowest pressure. The data have been recalculated to the normal isotopic composition in the solid phase as given in IPTS-68 (see table 2.1). The results are given in table 2.10.

Table 2.10

Vapour pressures of solid neon of normal isotopic composition

series	T_{68}/K [a]	p/Pa	$(T_{68}^{(T4)} - T_{68}^{(B2)})$/mK
TP	24.5618	43371	-0.2
41	23.8503	31477	-0.3
40	23.8482_5	31449	-0.3
43	23.0297	21254	-0.4
42	23.0248	21202	-
44	22.1997	13892	-0.3_5
47	22.1890_5	13811	-0.5
45	21.5064_5	9504	-0.4_5
46	20.7137	5981.6	-0.1_5
50	20.3722_5	4848.2	-0.1_5
49	20.3298	4718.8	-
48	20.2722	4551.7	-0.2
51	18.9596_5	1875.0	0.4_5

[a] T_{68} is the mean of the temperatures $T_{68}^{(T4)}$ and $T_{68}^{(B2)}$. The data at the triple point is the average of several series (see section 6).

8.3 *Representation of data*

As in the case of liquid neon, fits of eqs. (2.2) and (2.3) to the experimental data were nearly indistinguishable. Differences between the experimental data and fits with eq. (2.3) for k = 2 and k = 3 are shown in fig. 2.10. The data point near 19 K (see table 2.10) has been shifted by -1.5 mK before making the fits (see section 10); in fig. 2.10 the deviation for the shifted point is given. The deviations for k = 2 are systematic and slightly larger than the estimated precision of the data (0.1 mK in T_{68} and 0.01 and 0.02 mm for mercury and oil manometer readings respectively). For k = 3 and k = 4 they are non-systematic and within the experimental precision; for k = 4 the coefficients of the fits deviate widely from those which can be calculated from Clapeyron's equation and thermal data, for k = 3 the first two coefficients agree with the calculated values within 20%. Eq. (2.3) with k = 3 was chosen as representation of the data. The coefficients are given in table 2.11; calculated values of p and dp/dT at integral temperatures and at the triple point are given in table 2.12.

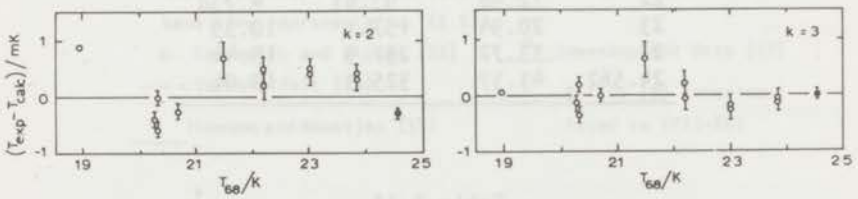

Fig. 2.10. Differences between the experimental data for solid neon in table 2.10 and fits with eq. (2.3) for k = 2 and k = 3. For the data point at 19 K T_{exp} has been corrected with -1.5 mK.

8.4 *Accuracy of the experimental vapour-pressure equation*

As in the case of liquid neon (section 7.4), the influence of the different factors which determine the accuracies of the measured temperatures and vapour pressures have been evaluated and the final accuracy of eq. (2.5) has been estimated. After the description in section 7.4 table 2.13 will be self-explanatory.

Table 2.11

The vapour-pressure equation for solid normal[a] neon between 19 K and the triple point (24.562 K) derived from the present experiments

$$\ln(p/p_0) = A + B/T_{68} + CT_{68} + DT_{68}^2 \qquad (2.5)$$

$A = 10.275895$

$B = -261.18205$ K

$C = -4.540820 \times 10^{-2}$ K^{-1}

$D = 10.35289 \times 10^{-4}$ K^{-2}

$p_0 = 101325$ Pa

[a] Composition in the solid phase as specified in IPTS-68, see table 2.1.

Table 2.12

Values of T, p and dp/dT for solid neon calculated from eq. (2.5)

T_{68}/K	p/kPa	p/torr	dp/dT_{68} kPa/K
19	1.932	14.49	1.386
20	3.823	28.68	2.481
21	7.099	53.25	4.191
22	12.48	93.63	6.738
23	20.94	157.1	10.39
24	33.72	252.9	15.44
24.562	43.37	325.3	19.01

Table 2.13

Accuracy estimate of the vapour-pressure equation for solid neon between 19 K and 24.562 K. Accuracy figures are expressed in mK.

1 T_{68}	2 δT_{68} (27.102 K)	3 δT_{68} (other fixed points)	4 δT (aero-static)	5 δT (iso-topes)	6 δT (spread)	7 δT (total)	8 δT (IPTS-68 spread)
19 K	0.17	0.65	0.13	0.2	±1.0	2.0	±0.3
21 K	0.14	0.51	0.13	0.2	±0.4	0.9	±0.2
23 K	0.39	0.34	0.18	0.2	±0.2	0.7	±0.3
24.562 K	0.46	0.24	0.20	0.2	±0.2	0.7	±0.3

8.5 *Comparison with previous results*

Data of different authors are compared with the present results in fig. 2.11. The data of Crommelin and Gibson [22] differ above 19 K up to

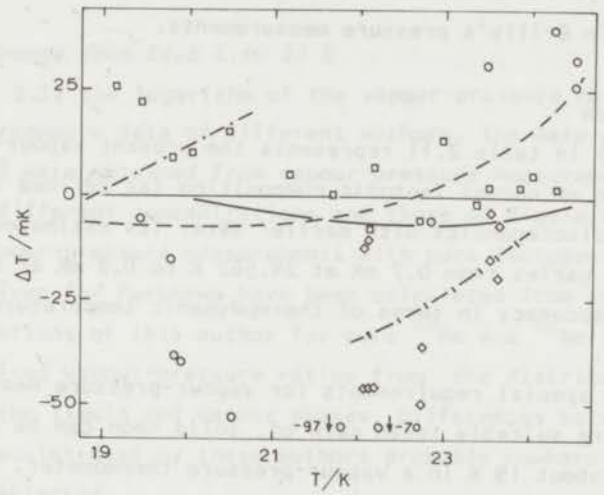

Fig. 2.11. Deviations of data of previous authors from the present vapour-pressure equation (eq. (2.5)) for solid neon. The base line represents eq. (2.5).

o Crommelin and Gibson [22]
– – – Verschaffelt [23]
□ } Keesom and Haantjes [33]
◇ } Henning and Otto [27]
——— Grilly [9] (recalculated to IPTS-68)

0.1 K with the present vapour-pressure equation; the equation fitted to these data by Verschaffelt [23] is below 23.5 K within 10 mK in agreement with the present equation. The spread of the data of Keesom and Haantjes [33] and also their deviations from the present equation are, at least above 20 K, in general smaller than 10 mK. The data of Henning and Otto [27] spread 35 mK near 22 K.

The data of the authors mentioned sofar were not recalculated to IPTS-68 because the differences with the original temperature scales are not known. Moreover, the spread in the data is often as large as estimates of these scale differences.

The temperatures in the vapour-pressure equation given by Grilly [9]

were on the NBS-55 scale; the equation has been recalculated to IPTS-68. Near 20.3 K and near the triple point the differences with the present equation are 2 mK and in between these temperatures they reach a maximum of 7 mK, Grilly's recalculated equation giving the lower temperatures (see fig. 2.11). The differences can easily be explained from the inaccuracies in Grilly's pressure measurements.

8.6 *Conclusion*

Eq. (2.5) in table 2.11 represents the present vapour-pressure data for solid neon of normal isotopic composition (as defined in table 2.1); there are no discrepancies with earlier data. Its estimated accuracy, in terms of T_{68}, varies from 0.7 mK at 24.562 K to 0.8 mK at 21 K and 2 mK at 19 K. The accuracy in terms of thermodynamic temperatures is discussed in section 10.

When the special requirements for vapour-pressure measurements of a solid phase are suitably taken care of, solid neon can be used between 24.562 K and about 19 K in a vapour-pressure thermometer. The precision and accuracy of the solid-neon vapour-pressure thermometer are high near 24.562 K (see tables 2.12 and 2.13) but go down gradually towards lower temperatures.

9 Vapour-pressure equations of ^{20}Ne and ^{22}Ne on IPTS-68

9.1 *Introduction*

Vapour-pressure equations for the liquid isotopes ^{20}Ne and ^{22}Ne between the triple points and the normal boiling points have been determined by Furukawa [10]; the temperatures were expressed on the NBS-55 scale. For the liquid phase above 27 K and for the solid phase accurate vapour-pressure equations on well-defined temperature scales have not been published for ^{20}Ne and ^{22}Ne. However, vapour-pressure differences $p^0_{20}-p^0_{22}$, or ratios p^0_{20}/p^0_{22}, have been determined from 19 K to 30 K by several authors. It seemed worthwhile to combine the available data for p^0_{20}/p^0_{22}, including Furukawa's data between 24.5 K and 27 K, with the vapour-pressure equations for liquid and solid normal neon derived in the preceding sections, to produce equations for the liquid isotopes from the triple points to 30 K and for the solid isotopes from 19 K to

the triple points, with temperatures on IPTS-68.

It is shown in Appendix 1 to this Chapter that Raoult's law for the mixture, with effective mole fractions of ^{20}Ne and ^{22}Ne, is sufficiently accurate to be used for the calculations. This law has also experimentally been verified by Furukawa between 24.5 K and 27 K [10].

9.2 *Liquid range from 24.5 K to 30 K*

In fig. 2.12 the logarithm of the vapour-pressure ratio p^0_{20}/p^0_{22} is used to intercompare data of different authors. The data of Keesom and Haantjes [34] were obtained from vapour-pressure measurements of isotopic mixtures of different concentrations and those of Bigeleisen and Roth [29] from vapour-pressure measurements with pure isotopes. The data in the figure given for Furukawa have been calculated from the vapour-pressure equations of this author for pure ^{20}Ne and ^{22}Ne [10]. Boata et al. [35] derived vapour-pressure ratios from the distribution of the isotopes in the liquid and vapour phases. Differences between the various temperature scales used by these authors probably nowhere exceed 0.03 K and may be neglected.

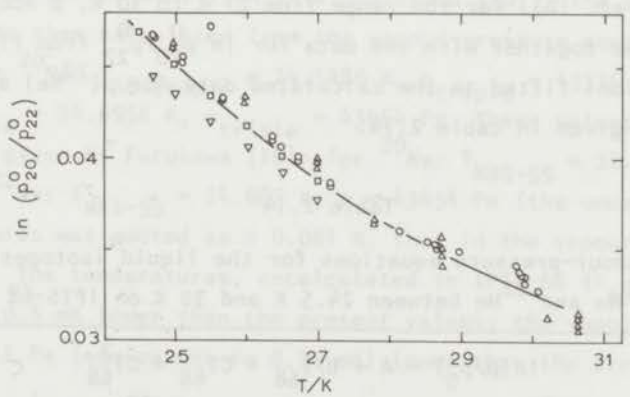

Fig. 2.12. Vapour-pressure ratios of the pure liquid isotopes ^{20}Ne and ^{22}Ne according to different authors.

▽ Keesom and Haantjes [34] (smoothed values)

△ Boato et al. [35]

○ Bigeleisen and Roth [29]

□ Furukawa [10] (smoothed values)

The curve has been used in the present calculations.

The low values of Keesom and Haantjes were attributed by Bigeleisen and Roth to errors in the determination of isotopic abundances. The data of Bigeleisen and Roth and of Furukawa differ systematically by about 0.0003.

For the present calculations, the data of Furukawa have been chosen between 24.5 K and 27 K and above 27 K an extrapolation of these has been used which is about 0.0003 lower than the data of Bigeleisen and Roth (see fig. 2.12).

For the actual calculation of the vapour pressures of ^{20}Ne and ^{22}Ne, the equations

$$p^0_{20} = p + (p^0_{20} - p^0_{22})\, x_{22} \tag{2.6}$$

$$p^0_{22} = p - (p^0_{20} - p^0_{22})\, x_{20} \tag{2.7}$$

have been used, in which $x_{20} = 1 - x_{22}$ is the effective mole fraction of ^{20}Ne in liquid neon of normal isotopic composition and is taken equal to 0.9105 (see also Appendix 1 to this Chapter); p was taken from eq. (2.4) (table 2.7) and, for the range from 24.55 K to 27 K, $p^0_{20}-p^0_{22}$ was directly accessible from Furukawa's vapour-pressure equations for ^{20}Ne and ^{22}Ne (table 3 in ref. 10). For the range from 27 K to 30 K, p according to eq. (2.4) was used together with the data for $\ln p^0_{20}/p^0_{22}$ from fig. 2.12 (full line). Equations fitted to the calculated data for $p(^{20}Ne)$ and $p(^{22}Ne)$ versus T are given in table 2.14.

Table 2.14

Vapour-pressure equations for the liquid isotopes ^{20}Ne and ^{22}Ne between 24.5 K and 30 K on IPTS-68

$$\ln(p/p_0) = A + B/T_{68} + CT_{68} + DT^2_{68}$$

^{20}Ne		^{22}Ne	
A =	10.113948	A =	11.021406
B =	-240.21528 K	B =	-250.93278 K
C =	-6.690364×10^{-2} K^{-1}	C =	-9.553914×10^{-2} K^{-1}
D =	7.70630×10^{-4} K^{-2}	D =	1.077626×10^{-3} K^{-2}
p_0 =	101325 Pa	p_0 =	101325 Pa

The accuracy of the relations depends partly upon errors in $p^0_{20}-p^0_{22}$. These are probably nowhere larger than the equivalent of 2 mK; the maximum spread of data, excluding those of Keesom and Haantjes, is the equivalent of 5 mK. Of these errors about 10% enters into p^0_{20} and 90% in p^0_{22}. Consequently, the vapour-pressure equation for ^{20}Ne is estimated to be nearly as accurate as that for normal neon: about 0.9 mK at the triple point and at 30 K and 0.2 mK near 27 K (in terms of T_{68}). The equation for ^{22}Ne is estimated to be accurate within ± 2.5 mK between 24.5 K and 30 K.

The normal boiling points according to the equations in table 2.14 are T_{68} = 27.0908 K for ^{20}Ne and T_{68} = 27.2180 K for ^{22}Ne. These may be compared with the data of Furukawa [10]: T_{NBS-55} = 27.084 K for ^{20}Ne and T_{NBS-55} = 27.211 K for ^{22}Ne, both with an uncertainty of ± 0.001 K. Excellent agreement is found, when the scale difference according to ref. 14, $T_{68}-T_{NBS-55}$ = 7.1 mK, is applied.

Triple-point temperatures of ^{20}Ne and ^{22}Ne were calculated from the value 24.5618 K for normal neon and the linear dependence of T_{triple} on the isotopic composition, assuming the triple-point temperatures of the isotopes to differ by 147 mK (viz. Furukawa [10]). The triple-point pressures were then calculated from the vapour-pressure equations in table 2.14. For ^{20}Ne: $T_{68\ triple}$ = 24.5486 K, p_{triple} = 43336 Pa, and for ^{22}Ne: $T_{68\ triple}$ = 24.6956 K, p_{triple} = 43664 Pa. These values may be compared to those given by Furukawa [10]: for ^{20}Ne: T_{NBS-55} = 24.540 K, p = 43326 Pa, for ^{22}Ne: T_{NBS-55} = 24.687 K, p = 43654 Pa (the uncertainty in the temperatures was quoted as ± 0.001 K, that in the vapour pressures as ± 13 Pa). The temperatures, recalculated to IPTS-68 ($T_{68}-T_{NBS-55}$ = 8.0 mK), are 0.6 mK lower than the present values; the vapour pressures are roughly 12 Pa (equivalent to 0.75 mK) lower than the present values.

9.3 *Solid range from 19 K to 24.5 K*

Vapour-pressure ratios of solid ^{20}Ne and ^{22}Ne were determined by Keesom and Haantjes [34] and Bigeleisen and Roth [29] (see fig. 2.13); the latter data are 0.005_0 higher at 20 K, equivalent to 7.5 mK, and 0.001_6 (3.8 mK) at 24 K.

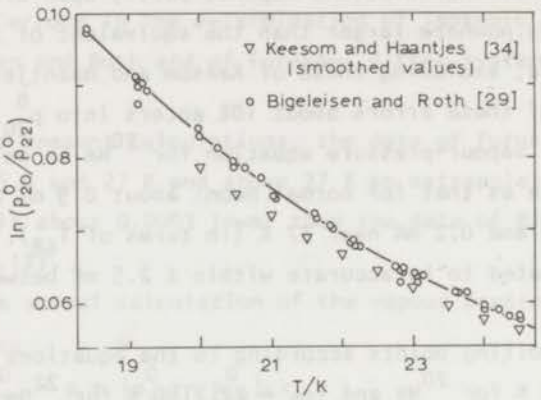

Fig. 2.13. Vapour-pressure ratios of the pure solid isotopes ^{20}Ne and ^{22}Ne according to different authors. The curve has been used in the present calculations.

Smoothed data of $\ln(p^0_{20}/p^0_{22})$ of Bigeleisen and Roth (full line in fig. 2.13) were used, together with the vapour-pressure equation of solid normal neon (eq. (2.5)), to determine p^0_{20} and p^0_{22} between 19 K and 24 K. The equations, fitted to these data and to the triple-point temperatures and pressures given in section 9.2, are given in table 2.15.

Table 2.15

Vapour-pressure equations for the solid isotopes ^{20}Ne and ^{22}Ne between 19 K and 24.5 K on IPTS-68

$$\ln(p/p_0) = A + B/T_{68} + CT_{68} + DT^2_{68}$$

^{20}Ne		^{22}Ne	
A =	10.651787	A =	6.247145
B =	-263.62328 K	B =	-235.14094 K
C =	-6.323236×10^{-2} K^{-1}	C =	1.4635494×10^{-1} K^{-1}
D =	1.310885×10^{-3} K^{-2}	D =	-1.937704×10^{-3} K^{-2}
p_0 =	101325 Pa	p_0 =	101325 Pa

The vapour-pressure equation for solid ^{20}Ne is probably accurate within ± 1.5 mK above 20 K, that for solid ^{22}Ne within ± 4 mK. At 19 K the accuracies are estimated to be 2.5 mK and 5 mK for ^{20}Ne and ^{22}Ne respectively.

10 Correlations of the experimental vapour-pressure equations with other thermophysical properties of neon

10.1 *Introduction*

Correlations of thermophysical and pVT data for pure substances, such as neon, appear in the literature regularly. They are generally made to provide 'best values' for various data, to be used for practical or scientific purposes. Since new vapour-pressure equations for liquid and solid neon, expressed on a well-defined temperature scale, were obtained in the present work, it seemed worthwhile to check their consistency with other thermophysical properties and to investigate whether certain quantities, for which no experimental data exists, could be calculated more accurately than before.

In the following sections the consistency of the experimental vapour-pressure equations of solid and liquid neon with the various data on the heat capacities of the condensed phases is investigated. The calculations yield new values for the vapour pressure of neon down to 0 K and for the heats of sublimation and vaporization of neon between 0 K and 30 K, for which quantities no experimental data exists, and values for the second virial coefficient of the gas.

10.2 *Thermodynamic equations*

In this section the thermodynamic vapour-pressure equations which are used for the computations will be given and their usage will be indicated. Remarks about their derivations and interrelations are given in Appendix 2 to this Chapter.

The vapour pressure of the solid and liquid phases of a mono-atomic substance such as neon is related to thermal and pVT data of the solid, liquid and vapour phase by the following relation [36]:

$$\ln p = i - \frac{L_{0K}}{RT} + \frac{5}{2} \ln T - \frac{1}{RT} \int_0^T S_{S,L}\,dT + \frac{1}{RT} \int_0^p V_{S,L}\,dp + \varepsilon \qquad (2.8)$$

where $i \equiv \ln(2\pi m)^{3/2} k^{5/2} h^{-3}$

and, when the virial equation of state

$$pV_G = RT(1 + B/V_G + C/V_G^2) \qquad (2.9)$$

is used for the gas,

$$\varepsilon \equiv \ln(pV_G/RT) - 2B/V_G - \frac{3}{2}C/V_G^2 \quad . \tag{2.10}$$

L_{0K} is the molar heat of vaporization (or sublimation) of the condensed substance at 0 K; $S_{S,L}$ and $V_{S,L}$ are the molar entropy and volume of the solid (index S) or liquid (index L) phase; m is the mass of an atom; the other symbols have their usual meaning. The quantities $S_{S,L}$, $V_{S,L}$, V_G and p are all to be taken at saturation (and the integrals along the solid-vapour and liquid-vapour equilibrium lines).

$S_{S,L}$ can be calculated from experimental data on the heat capacities of the solid and liquid phases and the heat of melting (L_f) by the relation

$$S_{S,L} = \int_0^{T_f} \frac{C_S}{T}\,dT + \frac{L_f}{T_f} + \int_{T_f}^{T} \frac{C_L}{T}\,dT \tag{2.11}$$

If all necessary data is known, the vapour pressure can be calculated from eq. (2.8). If L_{0K} is not known, i.e. if extrapolation of low-temperature heat-of-vaporization data to T = 0 K (or calculation of L_{0K} from eq. (2.34) in Appendix 2 to this Chapter) is not feasible, eq. (2.8) can still be used provided that the vapour pressure at at least one temperature is known. (L_{0K} can then be obtained by solving eq. (2.8) for this particular vapour pressure and temperature).

In sections 10.4.1 and 10.4.3 an equation is used which only requires knowledge of thermal quantities in the temperature range where the vapour pressure has to be calculated (contrary to eq. (2.8) in which heat capacities down to 0 K have to be used). This equation is [37]:

$$\ln\frac{p}{p_0} = \left(\frac{L_{T_0}}{RT_0} - \frac{5}{2} - \eta_0\right)\left(1 - \frac{T_0}{T}\right) + \frac{5}{2}\ln\frac{T}{T_0} -$$

$$- \frac{1}{R}\int_{T_0}^{T}\frac{C_{S,L}}{T}\,dT + \frac{1}{RT}\int_{T_0}^{T} C_{S,L}\,dT + \frac{1}{RT}\int_{p_0}^{p} V_{S,L}\,dp +$$

$$+ \varepsilon - \varepsilon_0 \tag{2.12}$$

where, when eq. (2.9) is used,

$$\eta \equiv (B - TdB/dT)/V_G + (C - \tfrac{1}{2}dC/dT)/V_G^2 \ . \qquad (2.13)$$

The quantities with index 0 are taken at a reference temperature T_0; L is the molar heat of vaporization or sublimation.

Eq. (2.12) has been used to compute vapour pressures of the liquid phase in section 10.4.1 and vapour pressures of the solid phase in section 10.4.3.

10.3 *Thermal and pVT data used in the computations*

10.3.1 *Heat capacity of liquid neon*

Experimental values of the molar heat capacity at saturation C_L of liquid neon of normal isotopic composition are given in fig. 2.14. Clusius [26] attributes his early low data [25] to a high content of helium in the neon. Data for normal neon were interpolated from smoothed values for ^{20}Ne and ^{22}Ne of Clusius et al. [28]. The smoothed values given by Brouwer, Van den Meydenberg and Beenakker [38], whose data show a maximum spread of ± 1%, are in agreement with the data of Clusius [26,28]; they lie between the data of Fagerström and Hollis Hallett [39] and of Gladun [40].

The calculations were made with values for C_L based on the data of Brouwer et al. and also with C_L based on Gladun's results: both sets of data were represented by expressions $C_L/J\ mol^{-1}K^{-1} = A_0 + A_1T$. For the

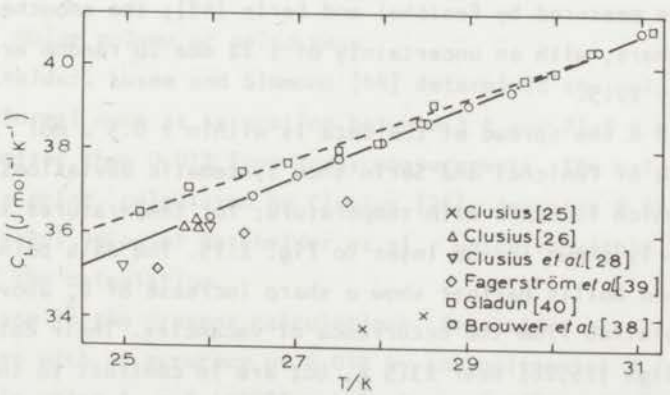

Fig. 2.14. Heat capacity at saturation pressure of liquid neon of normal isotopic composition.

data of Brouwer et al., coefficients A_0 = 13.89 and A_1 = 0.869 K^{-1} (RMS error in C_L 0.09%) were used (full drawn line in fig. 2.14), for the data of Gladun, A_0 = 18.29 and A_1 = 0.723 K^{-1} (RMS error 0.42%) (dashed line).

10.3.2 *Molar volume of liquid neon*

Kamerlingh Onnes and Crommelin [21] measured the molar volume of saturated liquid normal neon V_L at the triple point and the normal boiling point. Since then, only Clusius [25] has redetermined the value of V_L at the triple point. Mathias et al. [41] gave data at several temperatures above 25 K. Recently, Gladun [40] and Gibbons [42] reported values of V_L. The maximum spread in all data is less than 0.4%.

For the present calculations, V_L was represented between 24.5 K and 30 K by the expression $V_L/cm^3mol^{-1} = A_0 + A_1T$, where A_0 = 9.880 and A_1 = 0.2540 K^{-1}. This equation is probably accurate within 0.3% at all temperatures.

10.3.3 *Heat capacity of solid neon*

The earliest data on the molar heat capacity of saturated solid normal neon C_S were given by Clusius [25,26] (see fig. 2.15). From Clusius et al.'s [28] smoothed data for ^{20}Ne and ^{22}Ne, values for normal neon were determined by linear interpolation. Data of Fagerström and Hollis Hallett were derived from a small graph [39]. Values of C_S down to 1.5 K were measured by Fenichel and Serin [43]; the smoothed values of these authors, with an uncertainty of ± 2% due to random errors, are given in fig. 2.15.

Below 18 K the spread of the data is within ± 0.5 J $mol^{-1}K^{-1}$. Above 15 K the data of Fenichel and Serin show systematic deviations from the other data which increase with temperature; for temperatures above 19 K this is clearly shown in the inset to fig. 2.15. The data points of Fagerström and Hollis Hallett show a sharp increase of C_S above 23 K, which is explained from the occurrence of vacancies. Their data confirm data of Clusius [25,26] near 23.5 K, but are in contrast to the extrapolated values at 24 K and 24.5 K given by Clusius et al. (points between brackets in fig. 2.15).

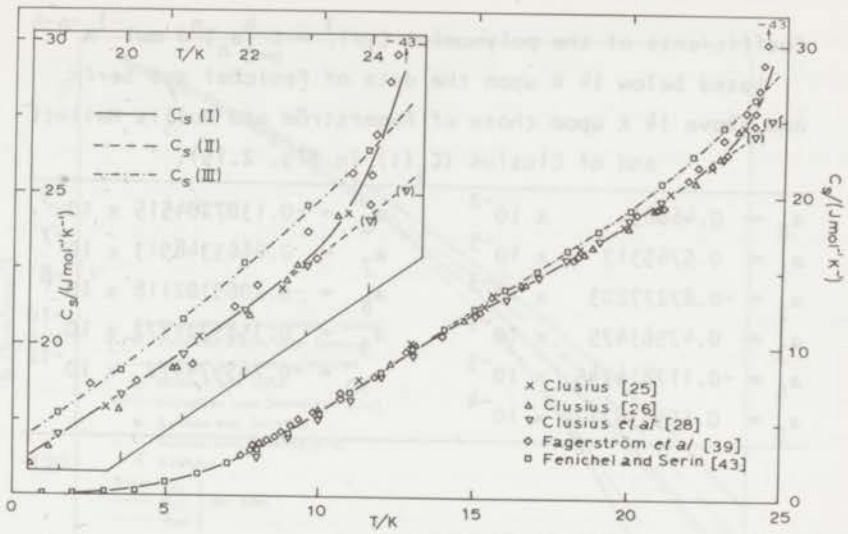

Fig. 2.15. Heat capacity at saturation pressure of solid neon of normal isotopic composition.

For the present calculations, the smoothed (viz. fig. 2.15) data of the different authors between 0 K and 24.5 K were represented by equations of the form $C_S/T^3 = \sum_{n=0}^{k} a_n T^n$, where k varied from 7 to 10, with an accuracy of 1% at the lower and 0.5% at the higher temperatures. The three representations are indicated as $C_S(I)$, $C_S(II)$ and $C_S(III)$ in fig. 2.15; the coefficients for $C_S(I)$ are given in table 2.16.

10.3.4 *Molar volume of solid neon*

Batchelder, Losee and Simmons [44] determined the molar volume V_S of solid normal neon at saturation between 3 K and 23.5 K with an accuracy of better than 0.01% from X-ray measurements. The value of V_S at the triple point, calculated by Clusius [26], deviates 0.6% from the (extrapolated) value of Batchelder et al., which is within the uncertainty of the calculation.

For use in the present calculations, Batchelder et al.'s data were represented with an accuracy of 0.01% by the polynomial $V_S/\mathrm{cm^3 mol^{-1}} = \sum_{n=0}^{4} A_n T^n$, in which $A_0 = 0.133886 \times 10^2$, $A_1 = -0.1585 \times 10^{-3}\mathrm{K}^{-1}$, $A_2 = -0.3189 \times 10^{-3}\mathrm{K}^{-2}$, $A_3 = 0.7729 \times 10^{-4}\mathrm{K}^{-3}$ and $A_4 = -0.7572 \times 10^{-6}\mathrm{K}^{-4}$.

Table 2.16

Coefficients of the polynomial $C_S/T^3 = \sum_{n=0}^{k} a_n T^n$ J mol^{-1}K^{-n-4} based below 14 K upon the data of Fenichel and Serin and above 14 K upon those of Fagerström and Hollis Hallett and of Clusius (C_S(l) in fig. 2.15).

$a_0 = 0.46883 \times 10^{-2}$	$a_6 = -0.1307204515 \times 10^{-5}$
$a_1 = 0.5765313 \times 10^{-3}$	$a_7 = 0.6663348913 \times 10^{-7}$
$a_2 = -0.87277203 \times 10^{-3}$	$a_8 = -0.2069102118 \times 10^{-8}$
$a_3 = 0.47963475 \times 10^{-3}$	$a_9 = 0.3585721372 \times 10^{-10}$
$a_4 = -0.117814745 \times 10^{-3}$	$a_{10} = -0.265974472 \times 10^{-12}$
$a_5 = 0.1595387170 \times 10^{-4}$	

10.3.5 *Virial coefficients of neon gas*

Crommelin, Palacios Martinez and Kamerlingh Onnes [45] determined virial coefficients of neon down to 55 K with a gas thermometer. The arithmetic means of their results (with a spread of 20%) for the second virial coefficient B below 100 K are shown in fig. 2.16.

Cath and Kamerlingh Onnes [46] determined B down to 53 K by differential gas thermometry (i.e. comparison with He and H_2 gas) assuming for $B_{0\ °C}$ the value given by Kamerlingh Onnes and Crommelin [21]. The results were extended to 27 K by Keesom and Van Lammeren [47]; these authors measured the velocity of sound in neon gas at 27 K, and obtained information on B from the relation [48]: $(\partial W^2/\partial p)_{p=0} RT/(2W^2_{p=0}) = B + (T/\lambda)dB/dT + (T^2/2\lambda(\lambda + 1))d^2B/dT^2$, in which W is the velocity of sound and $\lambda = (C_V)_{p=0}/R$.

Holborn and Otto [49,50] determined B down to 63 K. Sullivan and Sonntag [51] fitted to their data of B between 120 K and 70 K a Lennard-Jones (6-12) intermolecular potential function with the parameters σ = 2.782 Å and ε/k = 34.82 K. From this function and these parameters, Ziegler, Brown and Garber [52] calculated values of B down to 15 K; quantum corrections were applied. These calculated B values are indicated as Sullivan and Sonntag (L-J) in fig. 2.16.

Gibbons [42] determined values of B between 70 and 44 K.

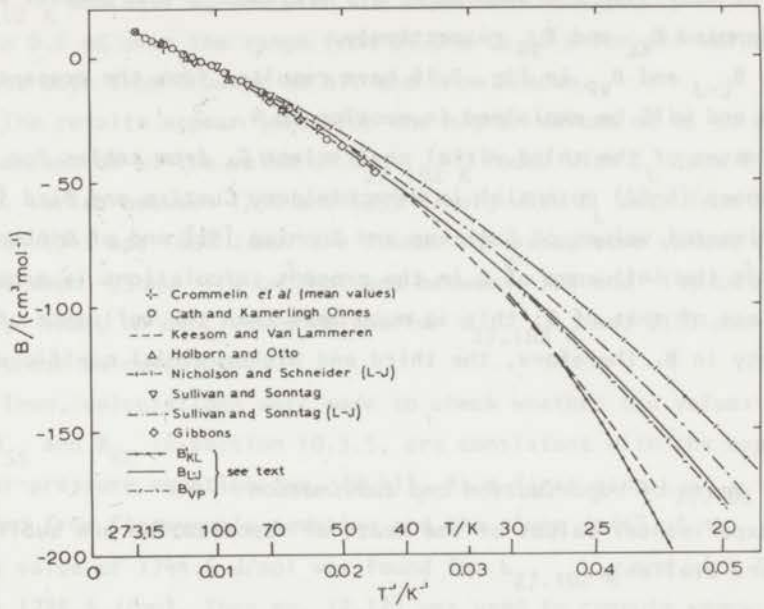

Fig. 2.16. Second virial coefficient of neon gas according to different authors and as calculated from the present vapour-pressure data.

Nicholson and Schneider [53] fitted to their data between 700 °C and 0 °C, and to those of Holborn and Otto [49] and Crommelin et al. [45] between 0 °C and 123 K, a L-J (6-12) potential. The values of B, calculated with this potential by Ziegler et al. [52], are too high between 100 K and 40 K (see fig. 2.16, Nicholson and Schneider (L-J)). (N.B. In ref. 53 some values of B, derived from ref. 45, are incorrect by about 0.4 cm^3/mol.)

The differences between data sets are roughly temperature independent between 100 K and 50 K, the differences between the recent data being just as large as between the older data ($\simeq$ 2 cm^3/mol). The experimental data of Crommelin et al. [45] and Sullivan and Sonntag [51] are equal within 4%. At the normal boiling point of neon the relation of Keesom and Van Lammeren [47] and the values Sullivan and Sonntag (L-J) [52] differ nearly 20%. Fig. 3 of ref. 47 suggests a possible error in $\partial W/\partial p$ of

about 7%, corresponding to an error in B of 10%. The data from ref. 47 and ref. 52 (Sullivan and Sonntag (L-J)) are used in the present analysis, and are denoted B_{KL} and B_{SS} respectively.

B'_{KL}, B_{L-J} and B_{VP} in fig. 2.16 have resulted from the present computations and will be explained in section 10.4.

Estimates of the third virial coefficient C, from tables for the Lennard-Jones (6-12) potential in Hirschfelder, Curtiss and Bird [54], and experimental values of Sullivan and Sonntag [51] and of Gibbons [42], showed that the influence of C in the present calculations is probably 0.5% or less of that of B; this is much less than the influence of the uncertainty in B. Therefore, the third and higher virial coefficients are ignored.

10.3.6 *Heats of vaporization and sublimation*

No experimental values of the heats of vaporization and sublimation of neon are available.

10.4 *Calculations*

10.4.1 *Preliminary calculations for liquid neon*

At first, attempts were made to calculate simultaneously the heat of vaporization L at the normal boiling point (27.102 K) and the second virial coefficient B(T) between 24.5 K and 30 K, by substituting p and T according to the experimental vapour-pressure equation (eq. (2.4)) between 24.5 K and 30 K into eq. (2.12) and using values of $C_L(T)$ and $V_L(T)$ as given in sections 10.3.1 and 10.3.2. To this end B was expressed as

$$B(T) = \sum_{n=0}^{k} A_n T^{-n} \qquad (2.14)$$

with $1 \leq k \leq 4$. Then, p and T according to eq. (2.4) were substituted in eq. (2.12) at T = 27.102 K and at (k + 2) evenly spread temperatures between 24.5 K and 30 K, and $L_{27.102\ K}$ and the coefficients A_n were computed in an iterative process. Calculations were made for C_L according to Brouwer et al. and according to Gladun. Subsequent checks showed that

the thermodynamic equation (eq. (2.12)) with the computed values for $L_{27.102\ K}$ and B(T) agrees with the experimental vapour-pressure equation within 0.1 mK over the range from 24.5 K to 30 K for all values of k for C_L data both from Brouwer et al. and from Gladun.

The results appear (even for the higher values of k) to be not fully independent of k: the value of $L_{27.102\ K}$ found with C_L data from Brouwer et al. varies between 1750 and 1733 J/mol; with C_L data from Gladun values between 1741 and 1698 J/mol are found. The associated values of $B_{27.102\ K}$ lie between -93 and -112 cm^3/mol and between -103 and -149 cm^3/mol respectively. Thus, no conclusive values for $L_{27.102\ K}$ and B(T) can be obtained from these calculations.

Then, calculations were made to check whether the values for B, denoted B_{SS} and B_{KL} in section 10.3.5, are consistent with the experimental vapour-pressure equation (eq. (2.4)). As a first step, $L_{27.102\ K}$ was calculated from Clapeyron's equation and the slope dp/dT of eq. (2.4): with B_{SS} a value of 1744.6 J/mol was found for $L_{27.102\ K}$ and with B_{KL} the value 1725.5 J/mol. Then eq. (2.12) was used to compute vapour-pressure equations. Differences between the thus obtained vapour-pressure equations, for different combinations of B_{SS}, B_{KL}, C_L (Brouwer et al.) and C_L (Gladun), and the experimental equation are shown in fig. 2.17.

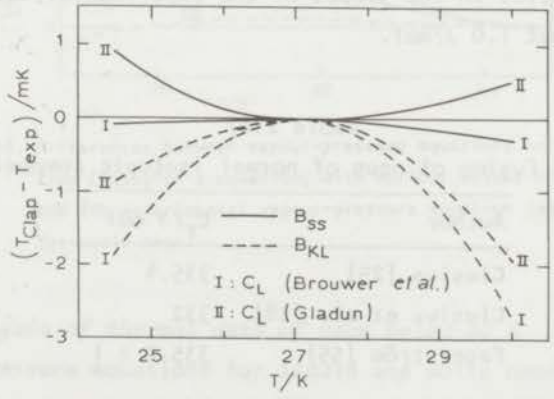

Fig. 2.17. Differences between vapour-pressure equations calculated from Clapeyron's equation, with various values for B and C_L, and the experimental vapour-pressure equation (eq. (2.4)) for liquid neon.

For B_{SS} the agreement is excellent with C_L (Brouwer et al.), but for B_{KL} no full agreement is found with plausible data of C_L. Therefore, new values for B(T) have been calculated, using the value of B_{KL} at 27.102 K, which are consistent with the experimental vapour-pressure equation. These values for B, for C_L according to Brouwer et al., will be denoted B'_{KL} in later calculations; they are shown in fig. 2.16.

10.4.2 *Heat of fusion*

The heat of fusion L_f is related to the difference of the slopes of the vapour-pressure equations for the liquid and solid phases at the triple point. Experimental values for L_f of neon are available, and it was checked whether these agree with the slopes of the experimental vapour-pressure equations.

Application of Clapeyron's equation at the triple point (with temperature T_0) yields

$$L_f = T_0[(\frac{dp}{dT})_S - (\frac{dp}{dT})_L](V_G - V_S)' + T_0(\frac{dp}{dT})_L(V_L - V_S) \qquad (2.15)$$

The second term on the right-hand side is independent of B and relatively small (1.0 J/mol).

Values for L_f calculated from eq. (2.15), with the slopes of eqs. (2.4) and (2.5) and B_{SS} or B'_{KL}, are given in table 2.17; the uncertainty due to uncertainties in the slopes of the experimental vapour-pressure equations is about 1.0 J/mol.

Table 2.17

Heat of fusion of neon of normal isotopic composition

Author	L_f/J mol^{-1}
Clusius [25]	335.4
Clusius et al. [28]	332
Fagerström [55]	335.2 ± 1
Calculated with B_{SS}	337.3
Calculated with B'_{KL}	334.8

The experimental values of L_f for normal neon of Clusius [25] and Fagerström [55], and a value calculated from the data of Clusius et al. [28] for ^{20}Ne and ^{22}Ne, are also given in the table.

10.4.3 *Preliminary calculations for solid neon*

Thermodynamic vapour-pressure equations were calculated for solid neon between 19 K and 24.56 K from eq. (2.12). Calculations were made with B_{SS} and B'_{KL} and with $C_S(I)$, $C_S(II)$ and $C_S(III)$. As reference temperature the (experimental) triple point was taken, and $L_{24.5618\ K}$ was chosen in such a way that the slopes of the calculated vapour-pressure equations agree with that of the experimental equation.

In fig. 2.18 the calculated vapour-pressure equations are compared with the experimental equation (eq. (2.5)).

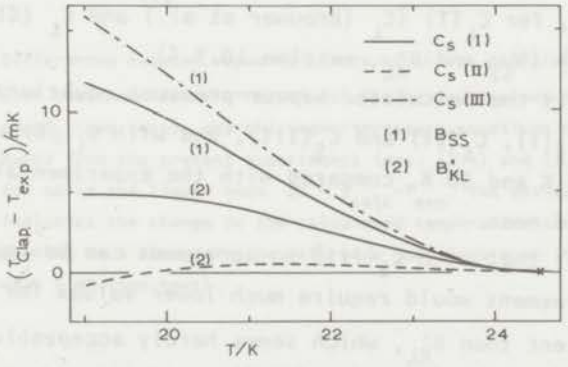

Fig. 2.18. Differences between vapour-pressure equations calculated from Clapeyron's equation, with various values of B and C_S, and the experimental vapour-pressure equation (eq. (2.5)) for solid neon.

10.4.4 *Analysis of thermal data of neon below 30 K*

Vapour-pressure equations for liquid and solid neon were calculated with eq. (2.8) using for $C_S(T)$, $V_S(T)$, L_f, $C_L(T)$, $V_L(T)$ and $B(T)$, between 0 K and T, data given in the preceding sections. L_{0K} was obtained from the same equation by substituting for T = 20.28 K the value p = 4573.60

Pa, taken from the experimental equation for solid neon (eq. (2.5)). The choice of 20.28 K as the "reference temperature" is rather arbitrary; it was influenced by the consideration that 20.28 K is a fixed point on IPTS-68, which, moreover, has recently been redetermined on the thermodynamic temperature scale (see later).

The mass m, in the expression for the chemical constant i, was taken equal to $\sum_i m_i^{x_i}$, where m_i is the mass of an atom of isotope i and x_i its mole fraction in normal neon (composition assumed to be: 90.92% ^{20}Ne, 0.26% ^{21}Ne and 8.82% ^{22}Ne, see also table 2.1); the value of i is $12.3669 + \ln(Pa/K^{5/2})$.

In the calculations the solid-liquid transition (triple point) was taken at a pressure of 43371 Pa (325.31 torr) (see table 2.5). For the heat of fusion the value 334.2 J/mol, as a fair average of the experimental values (see table 2.17), was used. $V_S(T)$ and $V_L(T)$ were taken according to sections 10.3.4 and 10.3.2. The calculations were made with combinations of the various data for $C_S(T)$ ($C_S(I)$, $C_S(II)$ and $C_S(III)$, section 10.3.3), for $C_L(T)$ (C_L (Brouwer et al.) and C_L (Gladun), section 10.3.1) and B(T) (B_{SS} and B'_{KL}, section 10.3.5).

In fig. 2.19 the calculated vapour-pressure equations, with B_{SS} and B'_{KL}, each for $C_S(I)$, $C_S(II)$ and $C_S(III)$, and with C_L (Brouwer et al.), are, between 19 K and 30 K, compared with the experimental equations for solid and liquid neon.

It appears, that with $C_S(III)$ no agreement can be found with either B_{SS} or B'_{KL}; agreement would require much lower values for the second virial coefficient than B'_{KL}, which seems hardly acceptable (see fig. 2.16).

When $C_S(I)$ is used, the deviations of the calculated temperatures from the experimental temperatures are opposite in sign for B_{SS} and B'_{KL} (see fig. 2.19). This suggests that reasonable agreement could be found with intermediate values of the second virial coefficient.

To test this, new values for B have been calculated with a Lennard-Jones (6-12) potential in which ε/k and b_0 are obtained from $B_{30\ K} = -86.66$ cm^3/mol and $B_{0°C} = 10.96$ cm^3/mol. The value for $B_{30\ K}$ is the average of B_{SS} and B'_{KL} at 30 K, and the value for $B_{0°C}$ has been derived from ref. 53. The table for reduced values of the second virial coef-

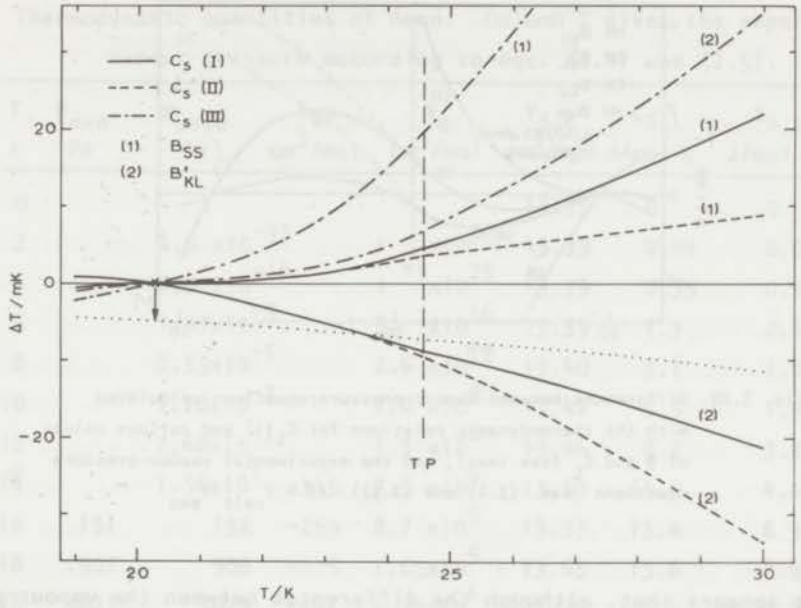

Fig. 2.19. Differences between vapour-pressure equations calculated with the thermodynamic relations, for various values of B and C_s (see text), and the vapour-pressure equations deduced from the present experiments (eqs. (2.4) and (2.5)) for solid and liquid neon. $\Delta T = T_{calc} - T_{exp}$. The dotted curve indicates the change in the calculated temperature corresponding to a change in the reference temperature at 20.28 K with 5 mK (see text).

ficient for the Lennard-Jones (6-12) potential, given by Hirschfelder et al. [54], have been taken into account. The obtained values for the parameters ε/k and b_0 are: ε/k = 35.90 K and b_0 = 27.56 cm^3/mol. The obtained values for B are denoted B_{L-J} and are shown in fig. 2.16. B_{L-J} is in better agreement with the experimental data of Gibbons [42] than B_{SS} and B according to Nicholson and Schneider.

The vapour-pressure equations for solid and liquid neon calculated with B_{L-J} and C_S(I) are shown in fig. 2.20. (As in fig. 2.19 the base line in fig. 2.20 represents the experimental vapour-pressure equations.)

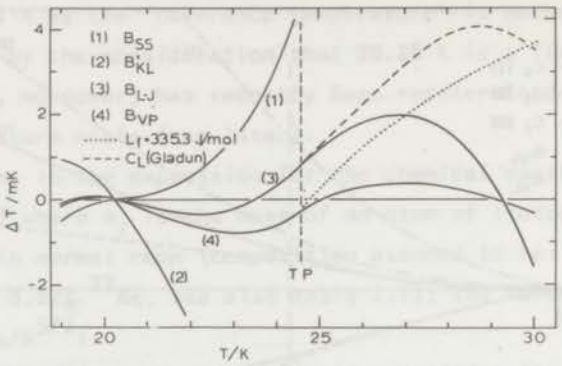

Fig. 2.20. Differences between vapour-pressure equations calculated with the thermodynamic relations for $C_s(l)$ and various values of B and C_L (see text), and the experimental vapour-pressure equations (eqs. (2.4) and (2.5)). $\Delta T = T_{calc} - T_{exp}$.

It appears that, although the differences between the vapour-pressure equation calculated with B_{L-J} and $C_s(l)$ and the experimental equations are less than 2 mK, the temperature dependence of these differences is rather pronounced. The shape of the ΔT-curves is not much improved if C_L (Gladun) is used in the calculations instead of C_L (Brouwer) (see fig. 2.20).

It was tried whether better agreement between calculated and experimental vapour pressures, in particular ΔT-curves with less curvature than line (3) in fig. 2.20, could be obtained through slight changes of B. Curve (4) in fig. 2.20, calculated with B_{VP} in fig. 2.16, is an example of such an attempt.

In table 2.18 values for different quantities which occur in the calculations are given. As input data has been used p = 4573.60 Pa at T = 20.28 K, $C_s(l)$, L_f = 334.2 J/mol, C_L (Brouwer et al.), B_{VP} and V_s and V_L as given in sections 10.3.4 and 10.3.2. Vapour pressures p_{calc} have been calculated with eq. (2.8). Also values for the heats of sublimation and vaporization, calculated with eq. (2.34) in Appendix 2, are given.

In all thermodynamic calculations presented so far in this section, 20.28 K has been used as a reference temperature. Recent gas thermometer

Table 2.18

Thermodynamic quantities of neon. Column 2 gives the experimental vapour pressure according to eqs. (2.4) and (2.5).

T K	P_{exp} Pa	P_{calc} Pa	B_{VP} cm^3/mol	V_G cm^3/mol	$V_{S,L}$ cm^3/mol	$C_{S,L}$ J/mol K^{-1}	$S_{S,L}$ J/mol K^{-1}	$L_{S,L}$ J/mol
0					13.39	0	0	1870
2		1.9×10^{-43}		1×10^{50}	13.39	0.04	0.01	1912
4		2.9×10^{-18}		1×10^{25}	13.39	0.35	0.11	1953
6		1.07×10^{-9}		5×10^{16}	13.39	1.3	0.41	1993
8		2.55×10^{-5}		2.6×10^{12}	13.40	3.1	1.03	2030
10		1.20×10^{-2}		7.0×10^{9}	13.42	5.5	1.97	2063
12		7.68×10^{-1}		1.3×10^{8}	13.46	8.2	3.20	2091
14		1.56×10^{1}	-315	7.5×10^{6}	13.50	11.0	4.67	2113
16	151	152	-259	8.7×10^{5}	13.57	13.4	6.30	2131
18	907	908	-215	1.65×10^{5}	13.65	15.6	8.01	2143
20	3823	3823	-181	4.33×10^{4}	13.75	18.4	9.79	2149
22	12483	12488	-155	1.45×10^{4}	13.88	21.1	11.7	2147
24	33723	33732	-133	5.78×10^{3}	14.02	26.1	13.7	2135
26	71594	71589	-116	2.90×10^{3}	16.51	36.5	30.0	1764
28	131740	131730	-101	1.66×10^{3}	17.02	38.2	32.7	1714
30	223339	223354	- 90	1.02×10^{3}	17.52	40.0	35.4	1653

The accuracy of the input data B_{VP}, $V_{S,L}$ and $C_{S,L}$, and also of the derived quantities $S_{S,L}$ and V_G, can be estimated from the discussions in the text. The accuracy of P_{calc} below 19 K is estimated to vary from 20% at 2 K to 4% at 10 K and to 0.5% at 18 K. The accuracy of the values of $L_{S,L}$ is estimated to be 3 J/mol at 0 K, 5 J/mol at 20 K and 15 J/mol at 30 K.

experiments [56] have yielded temperatures at 20.28 K which are about 5 mK below IPTS-68; in fig. 2.19 the change in the calculated vapour-pressure equations (expressed as the temperature change) is indicated when the reference temperature is lowered by this amount. According to magnetic thermometer data, the change in IPTS-68 should be approximately constant between 20 K and 30 K, which means that the experimental

vapour-pressure equations would shift by a constant amount of 5 mK. As a consequence, the difference $T_{calc}-T_{exp}$ would be, of course, unchanged at 20.28 K, but would decrease by 6.5 mK at 30 K. This would bring the calculated relation with B_{SS} and $C_S(II)$ within 2.5 mK in agreement with the experimental vapour-pressure equation.

10.4.5 *Concluding remarks*

Figs. 2.19 and 2.20 show the consistencies (or inconsistencies) between the present vapour-pressure equations for solid and liquid neon and values for the heat capacities of the solid and the liquid, $C_S(T)$ and $C_L(T)$, the heat of fusion, L_f, and the second virial coefficient of the gas B(T).

Fig. 2.17 shows the consistencies (or inconsistencies) between the vapour-pressure equation of liquid neon and values for $C_L(T)$ and B(T).

Fig. 2.18 shows the consistencies (or inconsistencies) between the vapour-pressure equation of solid neon and values for $C_S(T)$ and B(T).

Figs. 2.17 and 2.18 are more restrictive in significance than figs. 2.19 and 2.20; in the first two cases agreement for the temperatures and derivatives of the vapour-pressure equations at the reference temperatures is postulated, whereas in figs. 2.19 and 2.20 this agreement is only assumed for the temperature value at 20.28 K.

Which data are consistent and which are not, can best be judged directly from the figures. However, the following tentative conclusions may be given.

With values for $C_S(T)$, $C_L(T)$, L_f and B(T) which are not outside the limits of the experimental errors in these quantities, vapour-pressure equations for solid and liquid neon have been calculated which are within ± 1 mK in agreement with the experimental vapour-pressure equations.

Since the experimental equations are expressed on IPTS-68 and, naturally, the calculated equations on the thermodynamic temperature scale, it means that no inconsistencies between IPTS-68 and the thermodynamic temperature is found within the limits of ± 1 mK.

Because measurements of vapour pressures and temperatures can be made with high accuracy, the vapour-pressure equation has been used as a check on the consistency of experimental C_S, C_L, L_f and B data,

and for the calculation of the heat of vaporization (see table 2.18).

It has been found that the solid heat capacity C_s(III) (see fig. 2.15) is almost certainly in error; in fact, the calculations show a preference for C_s(II) (obtained from a simple extrapolation by Clusius et al.) above C_s(I). In view of the large differences even between recent measurements, new data on the solid heat capacity would be desirable.

If the present value of the reference temperature (boiling point of para-hydrogen, 20.28 K) is right, B values are between those of Sullivan and Sonntag and those of Keesom and Van Lammeren (but somewhat closer to those of Sullivan et al.); if the value of the reference temperature is lowered by 5 mK or better by 8 mK, virial coefficients of Sullivan et al. are in agreement with the experimental vapour-pressure equations.

The latter remark shows that more precise information could be obtained if the temperature scale between 20 K and 30 K was accurate to, say, ± 0.1 mK. This looks like an unfulfilled wish for the coming next decades.

Appendix 1 Vapour pressures and triple points of mixtures of isotopes

1 *The liquid-vapour equilibrium*

1.1 *Vapour pressures of liquid mixtures*

A mixture of isotopes, such as natural neon, is on theoretical basis considered to be ideal, which means that for the chemical potential of each component the following relation holds [57]

$$\mu_\alpha(p,T,x_\alpha) = \mu_\alpha^0(p,T) + RT \ln x_\alpha \qquad (2.16)$$

where μ_α is the chemical potential of component α, x the mole fraction and μ^0 the chemical potential of the pure component; R is the molar gas constant.

An expression for the vapour pressure of a binary liquid mixture is found in the usual way by equating the chemical potentials in gas and

liquid phases for each component. The chemical potentials can be written as

$$\mu_{1L}(p,x_{1L}) = \mu^0_{1L}(p^0_1) + RT \ln x_{1L} + V_{1L}(p - p^0_1) \tag{2.17}$$

$$\mu_{1G}(p,x_{1G}) = \mu^0_{1G}(p^0_1) + RT \ln x_{1G} + RT \ln(p/p^0_1) + B_1(p - p^0_1) \tag{2.18}$$

where the number 1 refers to the component and the indices L and G to the liquid and gas phase; p is the vapour pressure of the mixture and p^0 the vapour pressure of the pure component, V_L is the molar volume in the liquid phase which is assumed to be independent of the pressure and B is the second virial coefficient of the gas. (The temperature is considered to be constant.)

Since $\mu_{1L}(p,x_{1L}) = \mu_{1G}(p,x_{1G})$ and $\mu^0_{1L}(p^0_1) = \mu^0_{1G}(p^0_1)$, it follows that

$$x_{1G}p = x_{1L}p^0_1 \exp \frac{(p - p^0_1)(V_{1L} - B_1)}{RT} \tag{2.19A}$$

and, in the same way,

$$x_{2G}p = x_{2L}p^0_2 \exp \frac{(p - p^0_2)(V_{2L} - B_2)}{RT} \tag{2.19B}$$

Neglecting powers of p beyond the first one obtains:

$$\begin{aligned} x_{1G}p &= x_{1L}p^0_1 + x_{1L}p^0_1 \frac{(p - p^0_1)(V_{1L} - B_1)}{RT} \\ x_{2G}p &= x_{2L}p^0_2 + x_{2L}p^0_2 \frac{(p - p^0_2)(V_{2L} - B_2)}{RT} \end{aligned} \tag{2.20}$$

For a perfect gas and when the small influence of V_L is neglected, eq. (2.20) yields Raoult's law for the single components:

$$\begin{aligned} x_{1G}p &= x_{1L}p^0_1 \\ x_{2G}p &= x_{2L}p^0_2 \end{aligned} \tag{2.21}$$

from which, because $x_{1G} + x_{2G} = 1$, Raoult's law for the mixture follows:

$$p = x_{1L}p_1^0 + x_{2L}p_2^0 . \qquad (2.22)$$

Eq. (2.22) may be generalized to multi-component mixtures.

If V_L and B are retained in eqs. (2.20), it follows that, neglecting powers of $(V_L - B)$ beyond the first, that

$$p = x_{1L}p_1^0 + x_{2L}p_2^0 - x_{1L}x_{2L}(p_1^0 - p_2^0)\frac{p_1^0(V_{1L} - B_1) - p_2^0(V_{2L} - B_2)}{RT} \qquad (2.23)$$

Since for the saturated vapour B is always negative, an ideal liquid mixture in equilibrium with an ideal but imperfect gas mixture shows negative deviations from Raoult's law, unless B_1 and B_2 are widely different.

The deviations from Raoult's law for the single components follow directly from eqs. (2.20) and (2.21):

$$\begin{aligned} \delta_1 &= x_{1L}p_1^0(p - p_1^0)(V_{1L} - B_1)/(RT) \\ \delta_2 &= x_{2L}p_2^0(p - p_2^0)(V_{2L} - B_2)/(RT) \end{aligned} \qquad (2.24)$$

and the deviation from Raoult's law for the mixture is given by

$$\delta_{12} = - x_{1L}x_{2L}(p_1^0 - p_2^0)[p_1^0(V_{1L} - B_1) - p_2^0(V_{2L} - B_2)]/(RT) \qquad (2.25)$$

The equations can be extended to the case of normal neon which is a mixture of ^{20}Ne, ^{21}Ne and ^{22}Ne (see table 2.1). In this case

$$p = x_{20L}p_{20}^0 + x_{21L}p_{21}^0 + x_{22L}p_{22}^0 \qquad (2.26)$$

No experimental values for p_{21}^0 exist, but calculations of Keesom and Haantjes [34] have shown that $p_{21}^0 - p_{22}^0 = 0.45(p_{20}^0 - p_{22}^0)$. Since ^{21}Ne is only a minor component in normal neon, the approximation

$$p_{21}^0 = 0.5(p_{20}^0 + p_{22}^0) \qquad (2.27)$$

may be used; the error due to this approximation is smaller than the equivalent of 0.02 mK. Then eq. (2.26) can be written as

$$p = x_{20L}^{eff} p_{20}^{0} + x_{22L}^{eff} p_{22}^{0} \qquad (2.28)$$

in which $x_{20L}^{eff} = x_{20L} + 0.5\, x_{21L}$ and $x_{22L}^{eff} = x_{22L} + 0.5\, x_{21L}$, while $x_{20L}^{eff} + x_{22L}^{eff} = 1$. Thus the three-component mixture may be considered as a binary mixture of ^{20}Ne and ^{22}Ne with effective mole fractions x_{20}^{eff} and x_{22}^{eff}.

For this "binary mixture" the deviations from Raoult's law for the single components as calculated from eq. (2.24) are at 27 K

$$\delta_{20}^{eff} \approx - \delta_{22}^{eff} \approx - 14 \text{ Pa}(-0.11 \text{ torr}) .$$

The deviation from Raoult's law for the mixture, calculated from eq. (2.25), is at 27 K only - 0.6 Pa (-0.004_5 torr) which is equivalent to 0.02 mK.

Experimentally, Keesom and Haantjes [34] found no larger deviation from Raoult's law for the mixture than 0.3% of $p_{20}^{0} - p_{22}^{0}$, which corresponds to 11.5 Pa (equivalent to 0.38 mK) at 27 K; the differences which these authors found did not exceed their experimental error.

Furukawa [10] calculated from observed vapour-pressure equations for ^{20}Ne and ^{22}Ne between the triple point and the normal boiling point the equation for normal neon, assuming the validity of Raoult's law, and found agreement with the experimental equation within ± 0.5 mK, i.e. within the combined precision of the measurements.

1.2 *Difference in concentrations of isotopes in liquid and vapour phases*

The mole fractions of the isotopes in the liquid and vapour phases differ slightly. The difference for a mixture of two isotopes can be obtained readily by eliminating p from eq. (2.21). One obtains

$$\frac{x_{1G}}{1 - x_{1G}} = \frac{p_1^0 x_{1L}}{p_2^0 (1 - x_{1L})} \qquad (2.29)$$

or

$$x_{1L} - x_{1G} = \frac{(p_2^0 - p_1^0) x_{1L} (1 - x_{1L})}{p_2^0 - (p_2^0 - p_1^0) x_{1L}} \qquad (2.30)$$

Eq. (2.30), which was given earlier by Van Dijk [58], yields for the difference $x_{22L} - x_{22G}$ in normal neon 0.0037 near the triple point and 0.0031 at the normal boiling point. This means that, e.g., at the normal boiling

point the dew point of normal neon (nearly 100% of the sample in the vapour phase) is 0.4 mK higher than the boiling point (nearly 100% of the sample in the liquid phase).

2 *The solid-vapour equilibrium*

The equations for the liquid-vapour equilibrium hold with the suitable substitutions also for the equilibrium between the solid and the vapour phase.

3 *The solid-liquid-vapour equilibrium*

3.1 *Pressure and temperature of the triple point*

The triple-point temperature and pressure of a mixture of two isotopes and the differences in mole fractions of the isotopes in the solid, liquid and vapour phase at the triple point can be obtained by applying the equations given in the preceding sections to the three-phase equilibrium. For this case

$$\mu_{1S}(p,T,x_{1S}) = \mu^0_{1S}(p^0_1,T^0_1) + RT \ln x_{1S} - S_{1S}(T-T^0_1) + V_{1S}(p-p^0_1) \qquad (2.31)$$

$$\mu_{1L}(p,T,x_{1L}) = \mu^0_{1L}(p^0_1,T^0_1) + RT \ln x_{1L} - S_{1L}(T-T^0_1) + V_{1L}(p-p^0_1) \qquad (2.32)$$

$$\mu_{1G}(p,T,x_{1G}) = \mu^0_{1G}(p^0_1,T^0_1) + RT \ln x_{1G} - S_{1G}(T-T^0_1) + RT \ln(p/p^0_1) + B_1(p-p^0_1) \qquad (2.33)$$

The notation is similar to that in section 1; the index S refers to the solid, p and T denote the triple-point temperature and pressure of the mixture and p^0 and T^0 those of the pure component; S is the molar entropy, which is assumed to be temperature-independent in the interval from T^0 to T.

The equilibrium conditions are:

$$\mu_{1S}(p,T,x_{1S}) = \mu_{1L}(p,T,x_{1L}) = \mu_{1G}(p,T,x_{1G})$$

$$\mu^0_{1S}(p^0_1,T^0_1) = \mu^0_{1L}(p^0_1,T^0_1) = \mu^0_{1G}(p^0_1,T^0_1)$$

By substituting these in eqs. (2.31 - 2.33) one obtains for the two components in the mixture, in total, four independent equations. If p^0_1, T^0_1, p^0_2, T^0_2 and e.g., x_{1S} are known, p, T, x_{1L} and x_{1G} may be calculated.

The calculation has been carried through for a mixture of ^{20}Ne and ^{22}Ne using values for the triple-point temperatures and pressures of the pure isotopes given by Furukawa [10]. As a result it is found that p and T vary nearly linearly (between p_1^0 and p_2^0 and T_1^0 and T_2^0 respectively) with the mole fractions of the components in the solid phase or in the liquid phase. The deviations from linearity are for p and T smaller than one half of a percent of the differences between p and T of the mixture and of the pure components. In particular, for normal neon, $x_{20}^{eff} = 0.9105$, $x_{22}^{eff} = 0.0895$, linear interpolation between the triple-point pressures and temperatures yields values for p_{triple} and T_{triple} which are accurate within 0.2 Pa (0.001 torr) and 0.07 mK respectively.

3.2 *Differences between mole fractions of isotopes in the three phases*

The calculation yields for neon

$$(x_{1L} - x_{1S})/x_{1S} = - 0.0089$$
$$(x_{1G} - x_{1L})/x_{1L} = - 0.0415$$

from which follows for the natural composition

$$x_{1L} - x_{1S} = - 0.00079$$
$$x_{1G} - x_{1L} = - 0.0038$$

where x_1 and $1 - x_1$ are the effective mole fractions of ^{22}Ne and ^{20}Ne respectively.

This means that if, in a vapour-pressure bulb, the solid neon sample melts at its triple point, the mole fraction of ^{20}Ne in the liquid varies from 0.9113 in the limit of 100% solid to 0.9105 for 100% liquid (the amount of neon in the vapour phase is neglected). This change of concentration causes that the triple-point temperature increases with 0.11 mK and that the triple-point pressure increases with 0.3 Pa (0.002 torr) during melting.

Appendix 2 Remarks on thermodynamic equations

Eq. (2.8) in section 10.2 is a generalization of the equation for the vapour pressure of the liquid phase of a mono-atomic substance derived by Van Dijk et al. (see ref. 36) from the equality of the Gibbs free energies of the coexisting phases.

When the heat of sublimation at 0 K is obtained from eq. (2.8) (by substituting values for p and T at at least one temperature, knowing all other quantities which occur in the equation), then the heat of sublimation and vaporization at other temperatures can be deduced from the equation

$$L(T) = L_{0K} + \frac{5}{2} RT - \int_0^T C_{S,L}\,dT - \int_0^p V_{S,L}\,dp - \sum_i^{(0\to T)} Q_i + RT\eta \qquad (2.34)$$

where $C_{S,L}$ is the molar heat capacity at saturation of the condensed phase and $\sum_i^{(T_1\to T_2)} Q_i$ is the sum of latent heats of transition (and heat of fusion) in the temperature range from T_1 to T_2; η is defined by eq. (2.13).

If an experimental value for the heat of vaporization or sublimation at some temperature T is available, then L_{0K} can be calculated from eq. (2.34).

It will now be shown, that eq. (2.12), section 10.2, for the vapour pressure of the solid or the liquid phase can be derived from eqs. (2.8) and (2.34).

L_{0K}, obtained from eq. (2.34), may be substituted in eq. (2.8), which yields

$$\ln p = i - \frac{L_{T_0}}{RT} + \frac{5}{2}\frac{T_0}{T} + \frac{5}{2}\ln T - \frac{1}{RT}\int_0^{T_0} C_{S,L}\,dT - \frac{\sum_i^{(0\to T_0)} Q_i}{RT} -$$

$$- \frac{1}{RT}\int_0^T S_{S,L}\,dT + \frac{1}{RT}\int_{p_0}^p V_{S,L}\,dp + \varepsilon + \frac{T_0}{T}\eta_0 \qquad (2.35)$$

By substraction from eq. (2.35) of the corresponding expression for $p = p_0$, one obtains

$$\ln \frac{p}{p_0} = \left(\frac{L_{T_0}}{RT_0} - \frac{5}{2} - \eta_0\right)\left(1 - \frac{T_0}{T}\right) + \frac{5}{2} \ln \frac{T}{T_0} - \frac{1}{RT} \int_0^{T_0} C_{S,L}\,dT +$$

$$+ \frac{1}{RT_0} \int_0^{T_0} C_{S,L}\,dT - \frac{1}{RT} \int_0^{T} S_{S,L}\,dT + \frac{1}{RT_0} \int_0^{T_0} S_{S,L}\,dT +$$

$$+ \frac{1}{RT} \int_{p_0}^{p} V_{S,L}\,dp + \sum_i^{(0 \to T_0)} Q_i \left(\frac{1}{RT_0} - \frac{1}{RT}\right) + \varepsilon - \varepsilon_0 \,. \qquad (2.36)$$

Partial integration yields

$$\int_{T_1}^{T_2} S_{S,L}\,dT = S(T_2)T_2 - S(T_1)T_1 - \sum_i^{(T_1 \to T_2)} Q_i - \int_{T_1}^{T_2} C_{S,L}\,dT \,.$$

Thus

$$-\frac{1}{RT} \int_0^{T} S_{S,L}\,dT = -\frac{S_{S,L}(T)}{R} + \frac{1}{RT} \sum_i^{(0 \to T)} Q_i + \frac{1}{RT} \int_0^{T} C_{S,L}\,dT$$

and

$$\frac{1}{RT_0} \int_0^{T_0} S_{S,L}\,dT = \frac{S_{S,L}(T_0)}{R} - \frac{1}{RT_0} \sum_i^{(0 \to T_0)} Q_i - \frac{1}{RT_0} \int_0^{T_0} C_{S,L}\,dT \,.$$

Further

$$-\frac{1}{R}\left[S_{S,L}(T) - S_{S,L}(T_0)\right] = -\frac{1}{R}\left[\int_{T_0}^{T} \frac{C_{S,L}}{T}\,dT + \sum_i^{(T_0 \to T)} \frac{Q_i}{T_i}\right] \,.$$

Eq. (2.36) now reduces to

$$\ln \frac{p}{p_0} = \left(\frac{L_{T_0}}{RT_0} - \frac{5}{2} - \eta_0\right)\left(1 - \frac{T_0}{T}\right) + \frac{5}{2} \ln \frac{T}{T_0} - \frac{1}{R} \int_{T_0}^{T} \frac{C_{S,L}}{T}\,dT + \frac{1}{RT} \int_{T_0}^{T} C_{S,L}\,dT +$$

$$+ \frac{1}{RT} \int_{p_0}^{p} V_{S,L}\,dp + \frac{1}{R} \sum_i^{(T_0 \to T)} Q_i \left(\frac{1}{T} - \frac{1}{T_i}\right) + \varepsilon - \varepsilon_0 \qquad (2.37)$$

which is a more general form of eq. (2.12).

Another, easier, way to derive eq. (2.37) is integration of Clapeyron's equation

$$\frac{dp}{dT} = \frac{L(T)}{T(V_G - V_{S,L})} \qquad (2.38)$$

with substitution of

$$L(T) = L_{T_0} + \frac{5}{2} R(T - T_0) - \int_{T_0}^{T} C_{S,L} dT - \int_{p_0}^{p} V_{S,L} dp - \sum_{i}^{(T_0 \to T)} Q_i + R(Tn - T_0 n_0) \qquad (2.39)$$

Eq. (2.39) can be derived immediately from eq. (2.34).

Ter Harmsel [37] has given the derivation of eq. (2.37) from eq. (2.38), for the case where no heats of transition are involved, i.e. of eq. (2.12).

References

1. The International Practical Temperature Scale of 1968, Metrologia 5, 35 (1969).
2. C. van Rijn, Mrs. M.C. Nieuwenhuys-Smit, J.E. van Dijk, J.L. Tiggelman and M. Durieux, Temperature, It's Measurement and Control in Science and Industry (Instrument Society of America, Pittsburgh, 1972) Vol. 4.
3. J.S. Blakemore, Temperature, It's Measurement and Control in Science and Industry (Instrument Society of America, Pittsburgh, 1972) Vol. 4.
4. M. Durieux, Ph.D. Thesis, Leiden (1960).
5. P.G. Cath, Commun. Phys. Lab., Leiden, No. 152d (1918).
6. P. Eberhardt, O. Eugster and K. Marti, Z. Naturforsch. 20A, 623 (1965).
7. J.R. Walton and A.E. Cameron, Z.Naturforsch. 21A, 115 (1966).
8. A.O. Nier, Phys. Rev. 79, 450 (1950).
9. E.R. Grilly, Cryogenics 2, 226 (1962).
10. G.T. Furukawa, Metrologia 8, 11 (1972).
11. J.P. Compton, Metrologia 6, 103 (1970).
12. G.T. Furukawa, private communication to C.R. Barber.
13. R.E. Bedford, H. Preston-Thomas, M. Durieux and R. Muijlwijk, Metrologia 5, 45 (1969).
14. R.E. Bedford, M. Durieux, R. Muijlwijk and C.R. Barber, Metrologia 5, 47 (1969).
15. G.T. Furukawa, W.G. Saba, D.M. Sweger and H.H. Plumb, Metrologia 6, 35 (1970).

16. J.P. Compton, Ninth Session of the Advisory Committee of Thermometry of the C.I.P.M., Sèvres, France, doc. CCT/71-46.
17. J. Ancsin and M.J. Phillips, Metrologia 5, 77 (1969).
18. J. Ancsin, Metrologia 6, 53 (1970).
19. E. Löchtermann, Cryogenics 3, 44 (1963).
20. H. Kamerlingh Onnes, Commun. Phys. Lab., Leiden, No. 112 (1909).
21. H. Kamerlingh Onnes and C.A. Crommelin, Commun. Phys. Lab., Leiden, No. 147d (1915).
22. C.A. Crommelin and R.A. Gibson, Commun. K.O. Lab., Leiden, 185b (1927).
23. J.E. Verschaffelt, Commun. K.O. Lab., Leiden, Suppl. 64d (1928).
24. P.G. Cath and H. Kamerlingh Onnes, Commun. Phys. Lab., Leiden, No. 152b (1918).
25. K. Clusius, Z. phys. Chem. 4B, 1 (1929).
26. K. Clusius, Z. phys. Chem. 31B, 459 (1936).
27. F. Henning and J. Otto, Phys. Z. 37, 633 (1936).
28. K. Clusius, P. Flubacher, U. Piesbergen, K. Schleich and A. Sperandio, Z. Naturforsch. 15a, 1 (1960).
29. J. Bigeleisen and E. Roth, J. Chem. Phys. 35, 68 (1961).
30. C.A. Crommelin, Commun. K.O. Lab., Leiden, Suppl. 60 (1924).
31. J. Haantjes, Ph.D. Thesis, Leiden (1936).
32. T.C. Cetas, Ph.D. Thesis, Iowa State Univ. of Science and Technology, Ames, Iowa (1970).
33. W.H. Keesom and J. Haantjes, Physica 2, 460 (1935); Commun. K.O. Lab., Leiden, No. 235c.
34. W.H. Keesom and J. Haantjes, Physica 2, 986 (1935); Commun. K.O. Lab., Leiden, No. 239c.
35. G. Boato, G. Casanova and M.E. Vallauri, Il Nuovo Cimento 16, 505 (1960); G. Boato, G. Casanova, G. Scoles and M.E. Vallauri, Il Nuovo Cimento 20, 87 (1961).
36. H. van Dijk and M. Durieux, Physica 24, 1 (1958); Commun. K.O. Lab., Leiden, Suppl. No. 113c.
37. H. ter Harmsel, Ph.D. Thesis, Leiden (1966).
38. J.P. Brouwer, C.J.N. van den Meydenberg and J.J.M. Beenakker, Physica 50, 93 (1970); Commun. K.O. Lab., Leiden, No. 380a.

39. C.H. Fagerström and A.C. Hollis Hallett, Proc. Ninth Int. Conf. low Temp. Phys., Columbus, Ohio, 1964. (Plenum Press Inc., N.Y.) B-1092 (1965).
40. C. Gladun, Cryogenics 7, 78 (1967); see also Cryogenics 6, 27 (1966).
41. E. Mathias, C.A. Crommelin and H. Kamerlingh Onnes, Commun. Phys. Lab., Leiden, No. 162b (1922).
42. R.M. Gibbons, Cryogenics 9, 251 (1969).
43. H. Fenichel and B. Serin, Phys. Rev. 142, 490 (1966).
44. D.N. Batchelder, D.L. Losee and R.O. Simmons, Phys. Rev. 162, 767 (1967).
45. C.A. Crommelin, J. Palacios Martinez and H. Kamerlingh Onnes, Commun. Phys. Lab., Leiden, No. 154a (1919).
46. P.G. Cath and H. Kamerlingh Onnes, Commun. Phys. Lab., Leiden, No. 156a (1922).
47. W.H. Keesom and J.A. van Lammeren, Physica 1, 1161 (1934); Commun. K.O. Lab., Leiden, No. 234c.
48. W.H. Keesom, A. van Itterbeek and J.A. van Lammeren, Commun. Phys. Lab., Leiden, No. 216d (1931); W.H. Keesom and J.A. van Lammeren, Commun. K.O. Lab., Leiden, No. 221c (1932).
49. L. Holborn and J. Otto, Z. Physik 33, 1 (1925).
50. L. Holborn and J. Otto, Z. Physik 38, 359 (1926).
51. J.A. Sullivan and R.E. Sonntag, Advances in Cryog. Eng. 12, 706 (1967).
52. W.T. Ziegler, G.N. Brown and J.D. Garber, Techn. Report No. 1, project No. A1194, Eng. Exp. Station, Georgia Inst. of Techn., Atlanta, Georgia (1970).
53. G.A. Nicholson and W.G. Schneider, Can. J. Chem. 33, 589 (1955).
54. J.O. Hirschfelder, C.F. Curtiss and R. Byron Bird, Molecular Theory of gases and liquids, John Wiley and Sons Inc., New York (1954).
55. C.H. Fagerström, Ph.D. Thesis, Toronto Univ., Ontario, Canada (1965).
56. K.H. Berry, Metrologia 8, 125 (1972).
57. J.S. Rowlinson, Liquids and liquid mixtures, (Butterworth, London, 2nd ed., 1969).
58. H. van Dijk, Ph.D. Thesis, Leiden (1935).

CHAPTER 3

VAPOUR PRESSURES OF OXYGEN

1 Introduction

The vapour-pressure temperature relation of liquid oxygen has been determined between the triple point (54.361 K) and 99 K. Temperatures were measured on the International Practical Temperature Scale of 1968 (IPTS-68) [1] with two platinum thermometers.

The dependence of the accuracy and reproducibility of realizations of the triple point and the normal boiling point upon the experimental conditions, which is of importance for the use of these points as fixed points in thermometry, has been investigated.

The measured vapour pressures have been correlated with other thermophysical properties of oxygen.

2 Experimental method

2.1 *Apparatus and procedure of measurement*

The apparatus used in the experiments is described in section 2.1 of Chapter 2.

In the dewar, in which the apparatus was placed, as coolants liquid oxygen was used for temperatures above 70 K and liquid or solid nitrogen at the lower temperatures (the triple point of nitrogen is 63.148 K).

The procedure of the measurements was similar to that for the experiments with neon described in Chapter 2.

2.2 *Corrections to measured pressures*

Corrections for the thermal expansion of the manometer fluids and the invar scale, and for the local acceleration of gravity have been applied as described in Chapter 2.

2.2.1 Aerostatic pressure head

The correction was calculated as described in Chapter 2. The correction applied for the gas in the section of the capillary between the vapour-pressure bulb and the top of the dewar, varied from 0.7 mK at the triple point to 2.1 mK at 100 K. The level of the oxygen bath, or nitrogen bath, was always between 5 cm and 7 cm above the top of the vacuum can. For one series at the normal boiling point (series 36.2) exchange gas was used in the vacuum jacket, which caused a different temperature distribution along the capillary; the estimated correction was 1.8 mK in this case (bath level 5.5 cm above the top of the vacuum can). The maximum uncertainty in these corrections is probably less than 25%.

2.2.2 Isotopic composition

The isotopic composition of the oxygen has been determined mass spectrometrically at the FOM-Instituut voor Atoom- en Molecuulfysica in Amsterdam. From the relative abundances of molecules O_2 with relative molecular masses between 32 and 36, the abundances of the isotopes given in table 3.1 have been calculated. The data found for oxygen from the two

Table 3.1

Isotopic composition of oxygen

Isotope	natural abundance	abundance in Air Prod. sample	abundance in Matheson's sample
O^{16}	99.759%	99.748$_5$%	99.748$_5$%
O^{17}	0.037%	0.041$_5$%	0.041 %
O^{18}	0.204%	0.210 %	0.210$_5$%

suppliers differ slightly from the assumed natural abundance [2]. The correction for this difference would be less than the equivalent of 0.01 mK.

2.2.3 Thermomolecular pressure effect

If of a gas-filled closed tube the ends are at different temperatures, the pressure will in the steady state be higher at the warmer end than at the colder end when the mean free path of the molecules is of the same

order of magnitude as the tube diameter. This pressure difference depends upon species of gas, pressure, temperatures, tube diameter and tube surface.

The data of Weber, Keesom and Schmidt [3] with glass tubes are confirmed by others [4,5,6,7] who used pyrex glass and by Roberts and Sydoriak [8] for inconel tubes. Other data with inconel [7] and stainless-steel [9,10] tubes give systematically about 25% larger values for the pressure differences.

McConville et al. [9] gave equations for the steady-state thermomolecular pressure effect in which the interactions between the gas molecules and the tube wall are expressed in the momentum accommodation coefficient f; for fully diffuse reflection f = 1 and for fully specular reflection f = 0. For f = 0.89, found for glass by Millikan [11], consistency is found with the experimental data on glass [3-7]. The data on stainless steel [9] are consistent with f > 1, implying rough surfaces with back scattering. Values of f for polished metal surfaces are lower than those for unpolished surfaces and higher than for glass.

Prolonged exposure of a metal surface to gas significantly reduces the value of f (Hurlbut [12]) and thus reduces the pressure differences, which can explain [13] the difference between the data of Roberts and Sydoriak [8] and of McConville et al. [9].

The thermomolecular pressure effect in the present experiments could not be measured separately, nor was the value of f for the stainless-steel capillary known. However, the conditions were comparable to those in the experiments of Roberts and Sydoriak. Because it was found that Roberts and Sydoriak's results on ^{3}He and ^{4}He agree with those for glass tubes as explained above, data of Bennett and Tompkins [6] for oxygen and glass tubes have been used for the present experiments. These data agree within 1% with those calculated, using reduced parameters, from values given by Weber et al. [3] for He, H_2, Ne and Ar.

The corrections applied to measured pressures and the temperature equivalents are given in fig. 3.1. It may be mentioned that with data for clean stainless-steel tubes the correction, expressed in its temperature equivalent, would be 4 mK higher at 54 K, which would enlarge the difference between the experimental vapour-pressure equation and the calculated

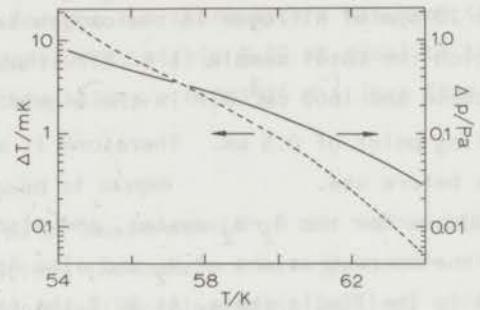

Fig. 3.1. Thermomolecular-pressure effect for vapour-pressure measurements of liquid oxygen for a tube diameter of 1.6 mm calculated from data of Bennett and Tompkins. The warm end of the tube is supposed to be at 300 K, the cold end at the temperature of the vapour-liquid equilibrium. The full curve indicates the thermomolecular-pressure effect, the dashed curve the temperature equivalent of the pressure effect.

equation (see section 7) with 4 mK at 54 K.

2.3 *Oxygen samples*

Samples were taken from research-grade oxygen supplied in metal cylinders by Air Products and Chemicals Inc. (U.K.) and Matheson Gas Products (U.S.A.). The impurities in these gases are given in table 3.2.

Table 3.2

Impurities in oxygen samples according to manufacturers' analyses

Impurity	Air Products and Chemicals	Matheson Gas Products	vapour pressure at 90 K
N_2	14 ppm	< 20 ppm	3.3 atm
Ar	< 5 ppm	< 20 ppm	1.3 atm
CO	< 1 ppm	-	2.2 atm
Hydrocarbons	< 1 ppm	< 20 ppm	0.1 atm
Kr	-	< 15 ppm	0.03atm
NO	< 0.1 ppm	< 5 ppm	10^{-3}atm
Xe	-	< 5 ppm	10^{-4}atm

It follows from phase diagrams for the O_2-N_2 system given by Ruhemann [14] that 20 ppm of nitrogen in the oxygen sample causes, in a typical case in which the total sample is 2ℓ NTP of which 400 cm^3 NTP is in the vapour phase and 1600 cm^3 NTP in the liquid phase, a change in the normal boiling point of 0.5 mK. Therefore it was tried to purify the gas samples before use.

The phase diagrams for the O_2-N_2 system, and also for the O_2-Ar system, show that the concentrations of N_2 and also Ar are higher in the vapour phase than in the liquid phase. At 90 K the ratio of the mole fraction in the vapour phase x_G and the mole fraction in the liquid phase x_L is about 7 for N_2 and about 1.4 for Ar. This means, of course, that pumping off the vapour will tend to purify the sample. The process is more efficient at lower temperatures, e.g. at 77 K the ratio x_G/x_L for N_2 is about 33.

The actual purification was performed by condensing the oxygen into a separate glass bulb in a liquid oxygen bath. The pressure of this bath was reduced to a few torr (with corresponding temperature of about 60 K), whereupon the sample was pumped for about 15 minutes. This process should reduce the amount of volatile impurities without appreciable loss of pure oxygen. After this, the oxygen was condensed into the vapour-pressure bulb. Checks of the purity by pumping off vapour showed no detectable changes of the normal boiling point (see table 3.3).

3 Temperature measurements on IPTS-68

Temperatures were measured with the two platinum thermometers B2 and T4.

In the present experiments, B2 and T4 were calibrated at the triple point (see section 5) and the normal boiling point (see section 4) of oxygen. The calibrations at the triple point and the normal boiling point of water are described in Chapter 4. From the accuracy estimates of the fixed-point calibrations it can be calculated, that the uncertainties in the calibration of the thermometers do not exceed 1.3 mK in the range between 54 K and 100 K. A more detailed account of the calibration uncertainties in this range is given in table 3.9 in section 6.4.

For all final calculations of the experimental results, the average of the T_{68} values for the two thermometers has been taken. This average is, between 54 K and 100 K, within 0.05 mK equal to the average for seven platinum thermometers with $\alpha > 0.003926\ K^{-1}$ (see Chapter 4).

4 Normal boiling point of oxygen

Several series of measurements of the vapour pressure and the resistances of the platinum thermometers have been made within 10 mK from the temperature of the normal boiling point (NBP) of oxygen. The procedure of measurements was similar to that for the NBP of neon (Chapter 2). Two samples of oxygen from Air Products, samples A2 and A3, have been used and one from Matheson Gas Products, sample M. Results are given in table 3.3. Temperatures T_p have been obtained from the vapour pressures and the vapour-pressure equation of IPTS-68 (eq. (3.1)). T_{68} in table 3.3 is

Table 3.3

Experimental data at the normal boiling point of oxygen

series number	oxygen sample	$T_{68}-T_p$ (mK)	$T_{68}^{(T4)}-T_{68}^{(B2)}$ (mK)	liquid volume in cm^3	remarks
16	A2	-0.1	0.1	0.5	
17		-0.1	0.1_5	1.4	T_{bath}=75 K
18		0.0_5	0.0	1.4	T_{bath}=88 K
25		-0.2_5	0.0	1.27	
26		-0.2_5	0.0	0.92	280cm^3NTP pumped off
27		0.0_5	0.0	0.56	290cm^3NTP pumped off
31	A3	-0.2_5	0.0	1.50	
34.1	M	0.0	0.0	1.71	T decreases slightly
34.2		-0.1	0.1	1.71	
35		0.0_5	0.0	1.10	490cm^3NTP pumped off
36.1		0.2	0.1	0.48	500cm^3NTP pumped off
36.2		-0.0_5	0.0	0.48	O_2 gas in jacket (p=15 torr)

the mean of $T_{68}^{(B2)}$ and $T_{68}^{(T4)}$. (The average of all series has served as the calibration of the thermometers at the oxygen NBP.)

No clear influence upon the NBP of the repeated removal of part of the oxygen vapour, as a check of the purity, has been found.

For sample M the values for $T_{68}-T_p$ are on the average 0.15 mK higher than for the other samples. The differences do not exceed the precision in $T_{68}-T_p$, and thus no clear systematic deviations between the samples are present.

The results are not dependent upon the temperature of the oxygen bath, viz. the series 17 and 18.

The reproducibility for the samples from two different sources is, as can be seen from the table, ± 0.2 mK. Similar results were recently reported by Mochizuki, Sawada and Takahashi [15].

The absolute accuracy of the present realization of the NBP of oxygen is estimated to be ± 0.5 mK; this includes the uncertainty in the aerostatic head correction (see section 2.2.1).

5 Triple point of oxygen

5.1 *Introduction*

The triple point (TP) of oxygen, which is a defining fixed point of IPTS-68, has been measured. The dependence of the observed TP temperature upon experimental conditions is investigated.

The results are compared with those obtained for neon (Chapter 2). A survey of methods and results in recent determinations of triple points of neon, oxygen, nitrogen and argon for thermometric purposes is given.

5.2 *Experiment*

Solid nitrogen at a temperature of about 52 K was used as a coolant in the bath. The copper block, with about 1.8 cm^3 of condensed oxygen in the vapour-pressure bulb, and the shield were cooled a few kelvin below TP by admission of exchange gas into the vacuum can. Further, the procedure was the same as described for neon in Chapter 2, section 6.

During the TP passage a heating power between 0.5 and 1 mW was applied to the shield to keep it at a constant temperature T_S slightly above the block temperature T_B.

Because the temperature and vapour pressure are dependent upon the heat influx into the sample, actual measurements were made at very low heat input and controlled amounts of heat were applied to the block between measurements.

The heat influx into the block is for $T_S - T_B = 0.1$ K, with no heating current on the block, equal to 50 μW. This was determined from the heat capacity of the block with condensed oxygen and the observed rate of change of T_B for a given value of $T_S - T_B$ at a temperature above TP. The additional joule heating due to the platinum-thermometer current of 2 mA during measurements is about 16 μW. (Under these circumstances the full transition with 1.8 cm^3 of condensed oxygen would take 10 days.)

Two samples of oxygen from Air Products and one sample from Matheson Gas Products were used.

5.3 *Discussion of the results*

Temperatures measured with the thermometer B2 and vapour pressures, for different fractions of melted oxygen and for different heat inputs into the sample (different values of $T_S - T_B$), are given in table 3.4. The temperatures $T_{68}^{(B2)}$ and $T_{68}^{(T4)}$ are not corrected for self-heating of the thermometers. Normalization from a current of 2 mA to one of 1 mA can be made by subtracting 0.7 mK (cf. e.g. series 3.5 and 3.6). This implies a self-heating of the thermometers of 0.1 mK per μW power dissipation. The differences between the temperatures T_{68} given by the two thermometers B2 and T4 are in general not larger than 0.1 mK. In fig. 3.2 the average of T_{68} for the two thermometers, normalized to a current of 1 mA as described above, is plotted versus the fraction of melted oxygen for various values of $T_S - T_B$. Except for very small fractions of melted oxygen, the temperature depends on the heat influx into the sample. The real TP temperature was deduced from the data at low fractions of melted oxygen and from extrapolations of the data at higher fractions of melted oxygen to zero heat influx (taking into account the heat influx due to the platinum-thermometer current which is, for 2 mA, equivalent to 35 mK in $T_S - T_B$). This temperature, T_{triple}, is used for the IPTS-68 calibration of the two platinum thermometers.

In fig. 3.3 the overheating $T - T_{triple}$ due to heat influx into the

Table 3.4

Triple point transition data for oxygen

series number	oxygen sample	melted fraction	T_S-T_B (mK)	i (mA)	$T_{68}^{(B2)}$ (K)	$T_{68}^{(T4)}-T_{68}^{(B2)}$ (mK)
1.1	A1	3 %	300	2	54.3618	-0.1
1.2		18	300	2	54.3620	0.0
1.3		83	820	2	54.3710	-0.1
1.4		88	80	2	54.3646	-0.2
1.5		88	25	2	54.3638	0.0
2.1	A2	1.5	350	2	54.3617	-0.1
2.2		2.5	200	2	54.3617	0.0
2.3		3.5	100	2	54.3617	0.0
2.4		30	150	2	54.3620	0.0
2.5		30	40	2	54.3618_5	-0.0_5
2.6		60	400	2	54.3633	-0.1
2.7		70	220	2	54.3635	-0.1
2.8		70	75	2	54.3628_5	0.0_5
2.9		70	30	2	54.3623	0.0
3.1	A2	50	320	2	54.3625	0.0
3.2		50	180	2	54.3623	0.0
3.3		70	200	2	54.3629_5	-0.0_5
3.4		70	100	2	54.3625	-0.1
3.5		70	30	2	54.3622	-0.1
3.6		70	30	1	54.3616	-0.0_5
37.1	M	22	100	1	54.3611	0.1_5
37.2		46	110	1	54.3610	0.2
37.3		49	120	2	54.3620	0.0

sample is shown as a function of T_S-T_B for various fractions of melted oxygen. It can be seen from the figure that the overheating is very roughly proportional to the heat influx. Some of the scatter of the data may be caused by the assumption that the heat input is proportional to T_S-T_B; this is only true if the vacuum in the can is always the same, because part of the heat conduction from the shield to the block is through the remaining gas in the can. The overheating increases rapidly with an increasing fraction of melted oxygen as can be seen from fig. 3.4 which has been obtained from a rough interpolation of the experimental points in fig. 3.3.

The same crude model as used in the case of the neon TP, i.e. a spherical sample with a radius of 5 mm which is melting from the outside

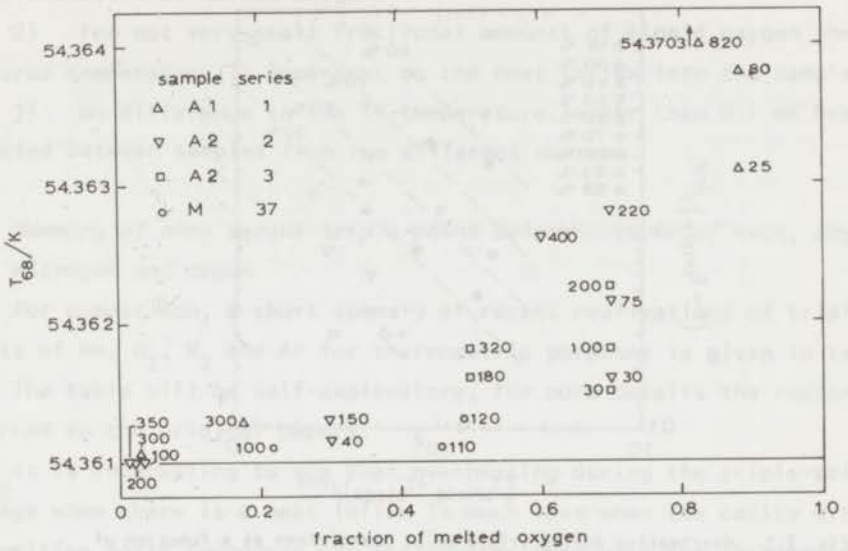

Fig. 3.2. The measured temperature at the triple point of oxygen versus the fractional amount of melted oxygen. The numbers near the points indicate the temperature differences in mK between the shield and the block (T_{shield}-T_{block}).

under the influence of a radial heat flow (see Chapter 2), was used to see whether such overheatings are plausible. The dashed lines in fig. 3.3 have been calculated from the model with 1.9 $mWcm^{-1}K^{-1}$ for the heat conductivity of liquid oxygen; it can be seen that the calculated effects are still a factor of 1.5 to 5 larger than the experimental data.

Vapour pressures have been measured during the TP passage; however, contrary to the case of the neon TP, the vapour pressure is so small (146.3 Pa), and the temperature derivative too (46 Pa/K), that a detailed comparison of measured vapour pressures and temperatures is not useful. The data are given in section 6 when dealing with the vapour-pressure equation of liquid oxygen.

5.4 *Conclusions*

1) The TP has been realized with different samples of oxygen within ± 0.1 mK; this accuracy is obtained for a small heat input and

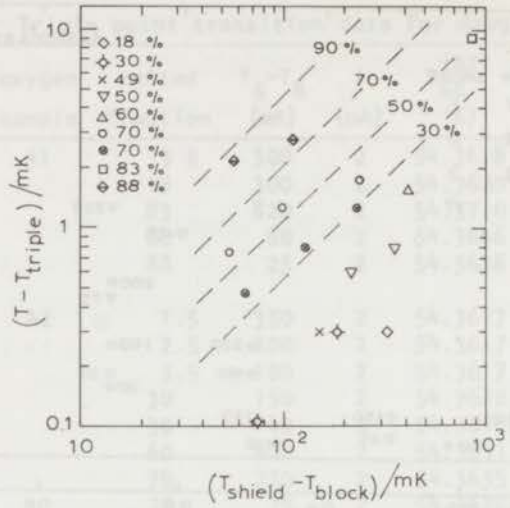

Fig. 3.3. Overheating during triple point transitions as a function of T_{shield}-T_{block} for various fractions of melted oxygen. The actual values of T_{shield}-T_{block} have been increased with 35 mK to account for the heat input due to the thermometer current. The dashed lines have been calculated from a crude model.

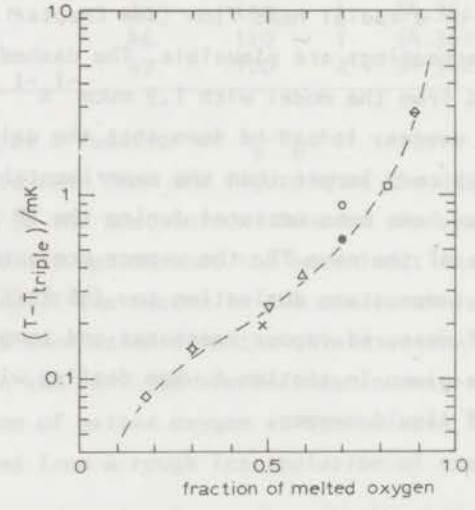

Fig. 3.4. Overheating as a function of the fractional amount of melted oxygen for a heat influx of 50 μW, determined by rough interpolation of the experimental points in fig. 3.3.

small fractions of melted oxygen.

2) For not very small fractional amounts of liquid oxygen the measured temperature is dependent on the heat influx into the sample.

3) No difference in the TP temperature larger than 0.1 mK has been detected between samples from two different sources.

5.5 *Summary of some recent triple-point determinations of neon, oxygen, nitrogen and argon*

For comparison, a short summary of recent realizations of triple points of Ne, O_2, N_2 and Ar for thermometric purposes is given in table 3.5. The table will be self-explanatory; for more details the reader is referred to the original papers.

It is interesting to see that overheating during the triple-point passage when there is a heat influx is much less when the cavity with the melting solid surrounds the thermometer than when the thermometers are placed around this cavity; very small and even negligible overheating is detected when the thermometer is placed directly inside the cavity. When the overheating is sufficiently small, continuous heating can be used, otherwise intermittent heating (method of adiabatic calorimetry) is necessary.

Although some authors reported difficulties in reaching a precision better than 1 or 2 mK, it seems to be proved that, for the four triple points, reproducibilities of ± 0.1 or ± 0.2 mK can be realized experimentally. In this respect the suggestion to replace the O_2 normal boiling point (90.188 K) by the Ar triple point (83.800 K) as a fixed point of IPTS-68 is much to be recommended.

The very high overheating effect in the present apparatus, even compared to other ones of type B, could be caused by the presence of iron-oxyde catalyst packed in nylon stocking in the vapour-pressure bulb.

6 The vapour-pressure equation of liquid oxygen below 100 K

6.1 *Introduction*

Vapour pressures of liquid oxygen have been measured at 20 temperatures between the triple point (54.361 K) and 99 K. From the data and, at the lower temperatures, from thermodynamic arguments a vapour-pressure

Table 3.5

Realization of Ne, O_2, N_2 and Ar triple points by different authors

Author	sub-stance	appara-tus	sample	reproducibility	overheating [a]	comments
Soejima et al.[16](1964)	O_2	A* [b]	several samples; lab. produced $KMnO_4$-heated O_2	$\leq \pm$ 0.1 mK	$<$ 0.3 mK [†]	continuous heating; no heat shield
Moussa et al.[17](1966)	N_2	A*	several samples; one source	$\pm$ 0.4 mK or better	-	continuous heating; no heat shield
Muijlwijk et al.[18](1966)	O_2	A*	-	$\pm$ 1 mK	-	no details given
Muijlwijk [19] (1968)	O_2	B [c]	-	$\pm$ 2 mK	-	no details given
Ancsin et al.[20](1969)	Ar	A	five samples two sources	$\pm$ 0.25 mK	10 mK [†]	intermittent heating
Furukawa et al.[21](1970)	Ne	A	-	$\leq \pm$ 1 mK	-	no details given
Compton[22](1970)	Ne	B	-	$\pm$ 2 mK	-	no horizontal plateaux in heating curve could be detected
Ancsin[23](1970)	O_2	A	several samples; three sources	$\pm$ 1 mK	2.5 mK [†]	intermittent heating
Thomas et al.[24](1971)	O_2	B	several samples; one source	$\pm$ 0.3 mK	20 mK [†]	intermittent heating
Kemp et al.[25](1971)	O_2	A	two samples; one source	$\pm$ 0.3 mK	$<$ 1 mK [†]	continuous heating possible
Present work	Ne	B	two samples; two sources	$\pm$ 0.1 mK	1800 mK	intermittent heating
	O_2	B	three samples; two sources	$\pm$ 0.1 mK	400 mK	intermittent heating

equation is derived. The results are compared with previous data.

6.2 *Experimental results*

The experimental procedure was similar to that described for the normal boiling point. The outer dewar was filled with liquid oxygen or, for the lower temperatures, with liquid or solid nitrogen under reduced pressure. Vapour pressures have been determined with the mercury manometer for pressures above 6.4 kPa and with the oil manometer for pressures below 6.4 kPa. Temperatures have been measured with the two platinum thermometers B2 and T4.

The data are given in table 3.6 and fig. 3.5; for a convenient representation of the results they have been compared with the vapour-pressure equation in IPTS-68 (eq. (26) of ref. 1):

$$^{10}\log(p/p_0) = A + B/T_p + C\,{}^{10}\log(T_p/T_0) + DT_p + ET_p^2$$

where $A = 5.961546$, $B = -467.45576$ K, $C = -1.664512$, $D = -0.01321301$ K^{-1}, $E = 50.8041 \times 10^{-6}$ K^{-2}, $T_0 = 90.188$ K, $p_0 = 101325$ Pa (3.1)

The pressures have been corrected as described before. The correction for the aerostatic pressure head in the section of the capillary between the vapour-pressure bulb and the top of the dewar varies from 0.04 Pa (equivalent to 1 mK) at 54.361 K to 18 Pa (1.7 mK) at 90.188 K and 41 Pa (1.9 mK) at 100 K. The applied correction for the thermomole-

Footnotes to Table 3.5.

a At 50% liquid - 50% solid for a heat influx of 100 mW.

b A refers to an apparatus in which the cavity with the melting solid surrounds the platinum-thermometer cavity; the asterisk means that the thermometer is in direct contact with the melt.

c B refers to an apparatus in which the melting solid is in a central cavity (in a copper block) and the thermometers are placed outside the cavity (as in the present apparatus).

† These figures were not directly given by the authors, but could be estimated from the data in their papers. When entries are left open, no data could be deduced from the authors' papers.

Table 3.6

Experimental vapour-pressure vs. temperature data for liquid oxygen

series number	sample	T_{68}/K [a]	$(T_{68}-T_p)$/mK [b]	ΔT_{68}/mK [c]
1	A1	54.361	6±0.3	-0.1
2	A2	54.361	-17- - 3 [d]	0.0
3		54.361	12±2	-0.0_5
4		57.06	6.5_5	-0.2
5		60.02	2.0_5	-0.3
6		62.99	- 0.9	-0.6
7		66.47	$- 2.8_5$	0.1
8		70.14	- 5.6 (oil) - 3.0 (Hg)	0.0
9		73.75	- 3.3	0.0
10		76.94	$- 2.8_5$	0.1
11		80.02	$- 2.2_5$	0.1
12		82.08	- 1.3	-0.1_5
13		84.73	- 1.2	0.4
14		86.41	- 1.0	-0.2
15		88.40	- 0.6	-0.1_5
19		91.47	0.6_5	0.0
20		92.89	0.3	-0.1
21		95.01	$- 0.2_5$	-0.1
22		97.07	- 0.7	0.2
23		99.12	0.7	0.0
24		99.14	0.5_5	0.1
28	A3	57.08	5.7	0.1_5
29		70.18	$- 4.5_5$(oil) $- 3.5_5$(Hg)	0.5
30		80.06	- 1.9	0.3
32		97.66	0.4	-0.2_5
33		99.11	0.5	0.0
37	M	54.361	13±1.5	0.1

[a] In this column values of the series temperatures are given which are rounded off to two digits behind the decimal point; this is sufficient because of the small temperature dependence of $T_{68}-T_p$.

[b] T_{68} is the average of the temperatures $T_{68}^{(T4)}$ and $T_{68}^{(B2)}$; T_p is derived from the vapour pressure by using eq. (3.1).

[c] $\Delta T_{68} = T_{68}^{(T4)} - T_{68}^{(B2)}$

[d] The pressure during this series was not constant; therefore, this point is omitted in fig. 3.5.

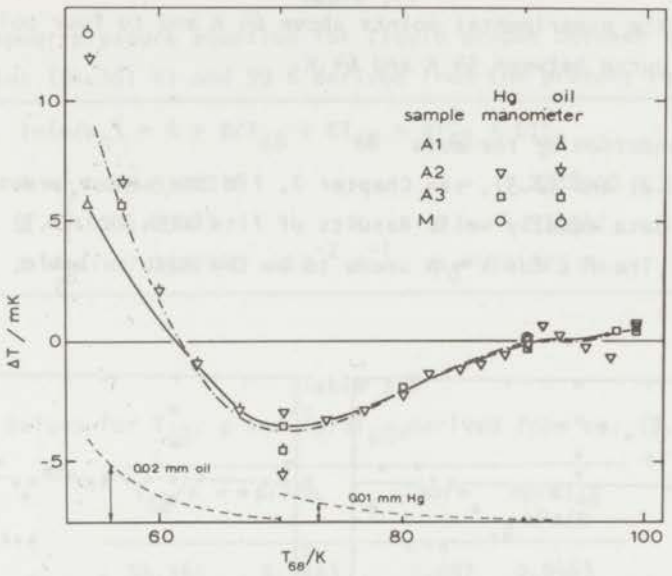

Fig. 3.5. Deviations of experimental vapour-pressure temperature data for liquid oxygen from eq. (3.1). The full curve represents eq. (3.2). The dash-dotted curve represents at the lower temperatures the fit to the experimental points.

cular pressure effect is 0.79 Pa (17 mK) at 54.361 K, 0.38 Pa (4.2 mK) at 57 K, 0.16 Pa (0.9 mK) at 60 K, 0.04 Pa (0.1 mK) at 63 K and smaller than the equivalent of 0.1 mK at higher temperatures (see fig. 3.1).

An evaluation of the possible systematic errors will be given later (section 6.4). At the lower temperatures the accuracy of the pressure measurements is such that rather large errors in T_p may arise. This can explain the larger spread near 54 K.

Thermodynamic analyses (section 7) showed that a vapour-pressure equation fitted to the experimental data (dash-dotted line in fig. 3.5) is below 64 K inconsistent with other thermal data for oxygen. This inconsistency was assumed to be partly caused by errors in the present experimental data. As a somewhat arbitrary choice between the results of the thermodynamic calculations and the experimental data, the full curve in fig. 3.5 was chosen below 64 K. Actually, the full-drawn curve in the

range from 54.361 K to 99 K was obtained by fitting an equation (see next section) to the experimental points above 64 K and to four points from a provisional curve between 54 K and 64 K.

6.3 *Representation of the data*

Eqs. (2.2) and (2.3), see Chapter 2, fit the vapour-pressure vs. temperature data equally well. Results of fits with eq. (2.3) are given in fig. 3.6. The fit for k = 4 seems to be the most suitable, because

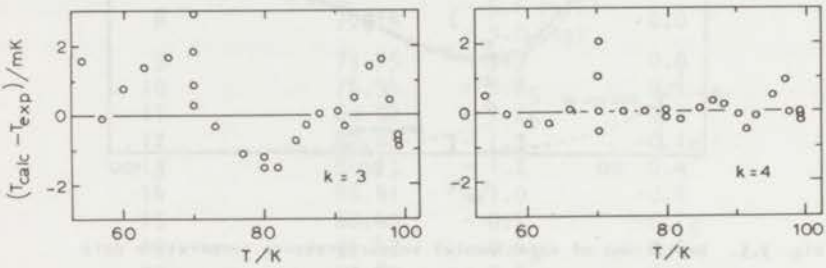

Fig. 3.6. Differences between the experimental data for liquid oxygen in table 3.4 and fits with eq. (2.3) for k = 3 and k = 4. The points below 64 K are no experimental points but have been chosen as described in the text.

systematic deviations which exceed the uncertainties in the data, such as for k = 3, do not occur. A fit with k = 5 is not significantly better than one with k = 4 and shows signs of overfitting: the coefficients deviate widely from those which are predicted by Clapeyron's equation and thermal data, this in contrast to those for k = 3 and k = 4. The equation chosen as the final representation of the data is given in table 3.7. For convenience a list of values for T, p and dp/dT, calculated from the equation, is given in table 3.8.

Eq. (3.2) in table 3.7 yields for the triple point, 54.361 K, a vapour pressure of 146.26 Pa (1.0971 torr). The estimated accuracy of this value is ± 0.32 Pa. Data for the vapour pressure at the triple point has also been given by other authors. The early measurements by Dewar [26] yielded the value 149 Pa, Justi [27] found 160 Pa. More recently,

Table 3.7

The vapour-pressure equation for liquid oxygen between the triple point (54.361 K) and 99 K derived from the present results

$$\ln(p/p_0) = A + B/T_{68} + CT_{68} + DT_{68}^2 + ET_{68}^3$$

$A = 15.9331216$ $\qquad D = 3.2788302 \times 10^{-4}\ K^{-2}$ (3.2)

$B = -1056.29083\ K$ $\qquad E = -4.974942 \times 10^{-7}\ K^{-3}$

$C = -\ 7.2327040 \times 10^{-2}\ K^{-1}$ $\qquad p_0 = 101325$ Pa

Table 3.8

Values for T_{68}, p and dp/dT_{68} derived from eq. (3.2)

T_{68}/K	p/kPa	p/torr	dp/dT_{68} kPa/K
54.361	0.1463	1.097	0.0463
55	0.1786	1.339	0.0551
60	0.7261	5.446	0.1852
65	2.336	17.52	0.4998
70	6.263	46.98	1.139
75	14.55	109.1	2.273
80	30.13	226.0	4.086
85	56.83	426.3	6.754
90	99.35	745.2	10.43
99.188	101.3	760	10.59
95	163.1	1223	15.25
100	254.0	1905	21.32

Hoge [28] reported as most reliable value 152 Pa (this author also measured 149 Pa and 150.5 Pa). Muijlwijk et al. [18] gave the value 146.32 Pa, deduced from two determinations, the difference between which was 0.13 Pa [19]. This value is in excellent agreement with the present result. In a later single measurement Muijlwijk found 146.8 Pa [19]; he gave as final value for the vapour pressure at the triple point 146.5 Pa (± 0.3 Pa). The latter value was used in the derivation of the IPTS-equation (eq. (3.1)).

6.4 *Accuracy of the experimental vapour-pressure equation*

Table 3.9

Accuracy estimate of the vapour-pressure equation for liquid oxygen, 54.361 K - 99 K. Accuracy figures are expressed in mK

1	2	3	4	5	6	7	8	9
T_{68} K	δT_{68} (90.188 K)	δT_{68} (other fixed points)	δT_p (aero-static)	δT_p (thermo-molecular)	δT_p (oil density)	δT (spread)	δT (total)	δT (IPTS-68 spread)
54.361	0.0	0.1	0.2	4	0.3	±3	7	0.0
57	0.0_3	0.2	0.2	1.8	0.3	±2	4	±0.2
60	0.2_5	0.4	0.2_5	0.2	0.4	±1	1.5	±0.4
63	0.3_5	0.5	0.3	-	0.5	±0.5	1	±0.6
70	0.5_5	0.7	0.3	-	0.6	±0.2	0.7	±0.7
80	0.6_5	0.6_5	0.3_5	-	-	±0.2	0.5	±0.5
90.188	0.6	0.2_5	0.4	-	-	±0.2	0.0	0.0
99	0.5	0.8	0.5	-	-	±0.2	0.7	±0.2

In table 3.9 an evaluation of the accuracy of the experimental vapour-pressure equation (eq. (3.2)) is given. The table is set up in a similar way as described for neon in section 7.4 of Chapter 2 (see the description there). Errors affecting the measured T_{68}-values are given in columns 2 and 3 (see also Chapter 4). Temperature equivalents of errors affecting the measured vapour pressures are given in columns 4, 5 and 6 (for columns 4 and 5 see section 2.2; column 6 gives the temperature equivalents of an uncertainty of 0.01% in the density of the Octoil-S in the manometer: such an uncertainty may be present in the density data which has been used, see section 2.2). The spread of the p-T_{68} data is given in column 7 and the estimated accuracy of eq. (3.2) in column 8. (The last column gives the spread in T_{68}-values for seven platinum thermometers with $\alpha > 0.003926\ K^{-1}$ as determined in Chapter 4. The average for these seven thermometers differs at all temperatures between 54 K and 100 K 0.05 mK or less from the average of T_{68} for the two thermometers T4 and B2.)

6.5 *Comparison with previous data*

A survey of data published before 1940 has been given by Muijlwijk [19]. A comparison of recent data with the present equation is shown in fig. 3.7. All data have been recalculated to IPTS-68. Hoge's results

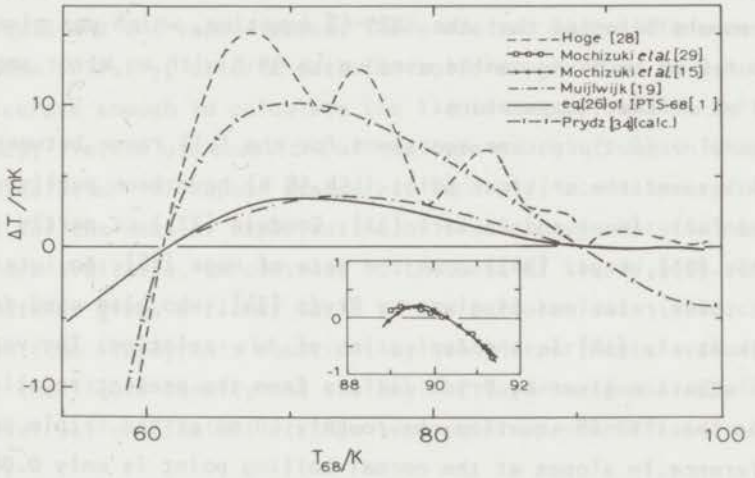

Fig. 3.7. Deviations of data of previous authors from the present vapour-pressure equation (eq. (3.2)) for liquid oxygen. The base line represents eq. (3.2).

[28], taken from his table 2, are accurate to 0.1 to 0.2 torr in the vapour pressure, which can explain the deviations from the present data. The differences with the relations of Mochizuki et al. [29,15] for the range from 89 K to 91.5 K, recalculated from the extrapolated IPTS-48 which these authors used, are below 90.8 K smaller than 0.2 mK; near 91.5 K the differences in slopes are about 0.8 mK/K.

The results of Muijlwijk (eq. V-2 of ref. 19), recalculated from the CCT-64 scale which was used by this author, are also shown in fig. 3.7. The recalculation has been made using table III-C of ref. 19 for the conversion from the CCT-64 scale to the NBS-55 scale and ref. 30 for the conversion from NBS-55 to IPTS-68. The scatter in the data of Muijlwijk makes that even for a fixed value of the normal boiling point uncertainties of a few millikelvin near 70 K remain; this can explain the dif-

ferences with the present equation. The vapour-pressure equation for liquid oxygen in IPTS-68 (this is eq. (3.1)) has been derived in 1968 from Muijlwijk's eq. V-2 [19] by recalculation from the CCT-64 scale to IPTS-68. Because at that time slightly different data were used for the scale conversion, the IPTS-68 equation in fig. 3.5 differs slightly from the presently recalculated equation of Muijlwijk.

It should be noted that the IPTS-68 equation, which was given for temperatures up to 94 K, can be used up to 99 K with an error smaller than 0.5 mK at that temperature.

Several vapour-pressure equations for the full range between the triple point and the critical point (154.58 K) have been published which are based fully (Hust and Stewart [31], Goodwin [32]) or partly (Brower and Thodos [33], Prydz [34]) upon the data of Hoge [28]. An intercomparison of these relations is given by Prydz [34], who also used data of Muijlwijk et al. [18] in the derivation of his relation. The vapour-pressure equation given by Prydz differs from the present relation, and also from the IPTS-68 equation, by roughly 40 mK at the triple point; the difference in slopes at the normal boiling point is only 0.08%. (The large difference at the triple point can be explained by Prydz's method of taking the least-square average of various experimental data for the triple-point pressure without taking into account the wide variation in accuracy of the data of different authors.)

6.6 *Conclusions*

Eq. (3.2) represents the present vapour-pressure temperature data for liquid oxygen between 54.361 K and 99 K. At the lower temperatures, where vapour pressures are small, thermodynamic arguments have been used in the derivation.

Eq. (3.2) is exact by definition at 90.188 K; its accuracy is estimated to be about 0.7 mK at 99 K, 0.5 mK at 80 K, 0.7 mK at 70 K, 1.5 mK at 60 K and 7 mK at 54.361 K. The accuracy in terms of thermodynamic temperatures is dealt with in section 7.

A liquid-oxygen vapour-pressure thermometer can be useful in cases where the platinum thermometer is less suitable. The sensitivity between 99 K and 80 K is better than 4 Pa/mK (0.03 torr/mK) but goes down towards lower temperatures.

7 Correlation of the experimental vapour-pressure equation with other thermophysical properties of oxygen

7.1 *Introduction*

Similar calculations as described for neon in Chapter 2 were made for oxygen to check the consistency of the vapour-pressure equation deduced from the present measurements with other thermal and pVT data for the liquid and the vapour phase. There are two main differences compared with neon. Firstly, caloric data for solid oxygen down to 0 K are by far not accurate enough to calculate the liquid entropy with a sufficient accuracy, i.e. to use equations of the type as eq. (2.8) in Chapter 2 for the calculation of vapour pressures. Secondly, accurate experimental values for the heat of vaporization of liquid oxygen at the normal boiling point are available, in contrast to the case of liquid neon. The latter circumstance gives a firmer basis to the calculations. (This can easily be seen from Clapeyron's equation: by using experimental values for p, dp/dT, the liquid density and the heat of vaporization at 90.188 K, the second virial coefficient at this temperature can immediately be calculated.)

The calculations to be described in the next sections were made with the equation

$$\ln \frac{p}{p_0} = \left(\frac{L_{T_0}}{RT_0} - 1 - \eta_0\right)\left(1 - \frac{T_0}{T}\right) + \ln \frac{T}{T_0} - \int_{T_0}^{T} \frac{C_L - C_{V_i}}{RT}\, dT + \\ + \frac{1}{RT}\int_{T_0}^{T} (C_L - C_{V_i})\, dT + \frac{1}{RT}\int_{P_0}^{P} V_L\, dp + \varepsilon - \varepsilon_0 \qquad (3.3)$$

which was derived in this form by Van Dijk [35]. The equation differs from eq. (2.12) only in that there is a contribution from internal degrees of freedom in the oxygen molecule to the heat capacity of the vapour.

7.2 *Data used in the computations*

7.2.1 *Heat of vaporization at 90.188 K*

Muijlwijk [19] has given a survey of the experimental values of the heat of vaporization of oxygen at the normal boiling point. The spread in the data is about ± 0.1%. The average value given by Muijlwijk, 6821.8

J/mol, is probably accurate within 0.05% and is used in the present calculations.

7.2.2 *Heat capacity of liquid oxygen at saturation*

The available data on the molar heat capacity of liquid oxygen at saturation, C_L, is shown in fig. 3.8. The earliest measurements were made

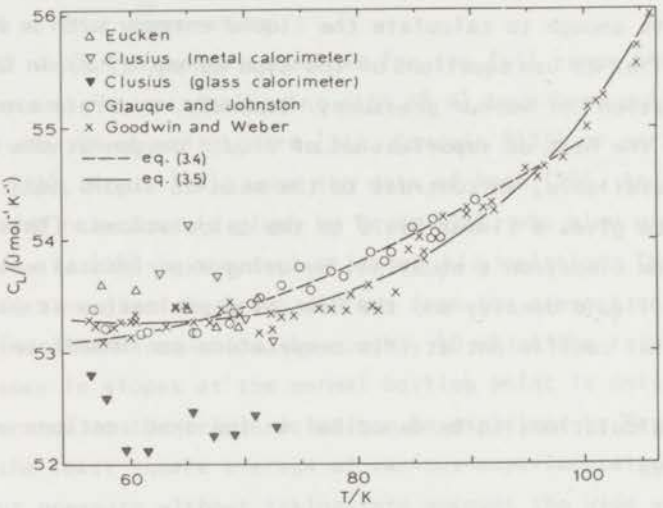

Fig. 3.8. Heat capacity at saturation pressure of liquid oxygen.

by Eucken [36]. The results of Clusius [37] with a glass calorimeter are evidently too low, in contrast to those obtained with a metal apparatus. Muijlwijk [19] represented the data of Giauque and Johnston [38] between 56 K and 90 K, which shows a very small scatter, by the formula

$$C_L/R = \sum_{n=1}^{3} A_n T^{n-2} \qquad (3.4)$$

where A_1 = 30.15 K, A_2 = 5.280 and A_3 = 0.01019 K^{-1}, and R = 8.3143 J/mol K. Muijlwijk used this representation for calculations up to 100 K.

Recently, Goodwin and Weber [39] calculated values of C_L from experimental data of the heat capacity at constant volume at temperatures between the triple point (T_t = 54.3507 K, assumed) and the critical point

(T_c = 154.77 K, assumed). They represented C_L by the formula

$$C_L/J\,mol^{-1}K^{-1} = [A + B\frac{1 - T/T_c}{1 - T_t/T_c} + C(\frac{T}{T_c})^{12}]/(\frac{1 - T/T_c}{1 - T_t/T_c})^{\frac{1}{2}} \quad (3.5)$$

where A = 25.60277, B = 27.71001 and C = -2.48274.

The present calculations were made with C_L according to eq. (3.4) and according to eq. (3.5).

7.2.3 *Heat capacity of oxygen in the ideal gas state*

Values of the molar heat capacity of oxygen gas in the ideal gas state at constant volume (C_{V_i}) have been given by Woolley [40]. The data in the range from 50 K to 100 K is represented by the formula $C_{V_i}/R = \sum_{n=1}^{3} A_n T^{n-2}$, where A_1 = 0.35 K, A_2 = 2.4958 and $A_3 = 3 \times 10^{-5} K^{-1}$*. Errors in C_{V_i} are probably smaller than 0.1% and are insignificant for the present calculations.

7.2.4 *Molar volume of liquid oxygen at saturation*

A survey of densities of liquid oxygen at saturation between 77 K and 155 K, reported by twenty authors, is given by Goldman and Scrase [41]. The total spread of the vast majority of these data is within 0.7%.

In the present calculations, for the molar volume of the liquid at saturation V_L a formula, derived by Muijlwijk, has been used. This formula is $V_L/m^3mol^{-1} = \sum_{n=0}^{2} A_n T^n$, where $A_0 = 2.3290 \times 10^{-5}$, $A_1 = -1.24 \times 10^{-8} K^{-1}$ and $A_2 = 7.25 \times 10^{-10} K^{-2}$. It is based on data of Mathias and Kamerlingh Onnes [42] and of Van Itterbeek and Verbeke [43] between 60 K and 100 K. The spread between these data is nowhere larger than 0.4%. Between 80 K and 100 K, the formula differs nowhere more than 0.4% from the mean of the majority of the available data [41].

The total influence of the term with V_L in the thermodynamic vapour-pressure equation is smaller than the equivalent of 25 mK at temperatures below 95 K and increases to 50 mK at 99 K. This implies, that the maximum uncertainty in the thermodynamic equation due to the uncertainty in V_L is 0.2 mK, which is negligible.

---

* The coefficient A_3 given by Muijlwijk [19] evidently contains a typographical error.

7.2.5 *The virial coefficients of oxygen gas*

Data for the second virial coefficient B according to several authors are shown in fig. 3.9. Only Cath and Kamerlingh Onnes [44] have

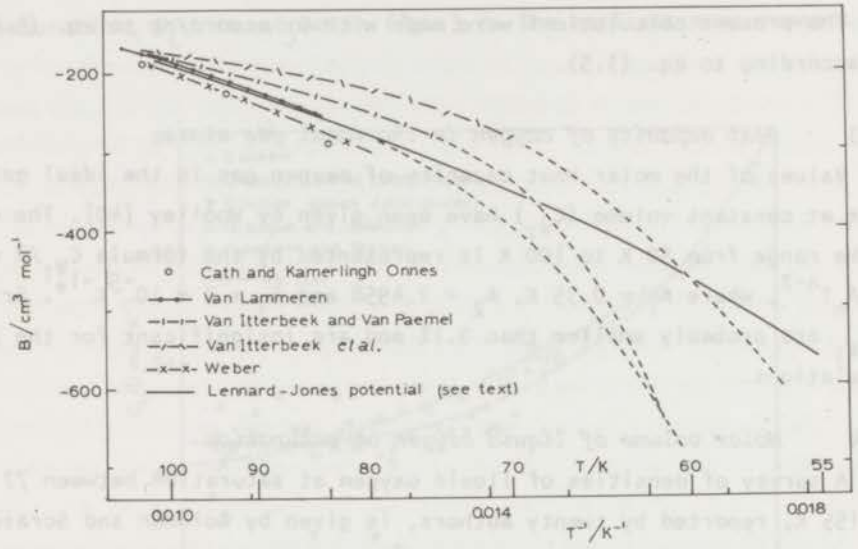

Fig. 3.9. Second virial coefficient of oxygen gas according to different authors (extrapolations are shown as dashed lines) and as calculated from a Lennard-Jones (6-12) potential (see text).

determined values of B below 100 K with a gas thermometer. Van Lammeren [45], Van Itterbeek and Van Paemel [46] and Van Itterbeek et al. [47] derived from their data on the velocity of sound in oxygen gas below 100 K, and from values of B above 120 K from Nijhoff and Keesom [48], formulae for B below 100 K. Recently, Weber [49] calculated values of B, with an estimated uncertainty of roughly 10% below 100 K, from pVT data.

From Clapeyron's equation a value of B at 90.188 K can be calculated with dp/dT according to the experimental vapour-pressure equation (eq. (3.2)), $L_{90.188\,K}$ = 6821.8 J/mol and V_L according to the equation in section 7.2.4, it follows that $B_{90.188\,K}$ = -224.4 cm^3/mol. Due to uncertainties of 0.05% in dp/dT and in L at 90.188 K this value for B is uncertain

by about 3%. (The neglect of higher virial coefficients introduces a relatively small uncertainty, see below.) The value for B at 90.188 K given by Van Lammeren [45] (B_{vL}) differs 1.4% from the value given above, the values of the other authors 7% or more (see fig. 3.9).

Calculation of B(T) from a Lennard-Jones (6-12) potential, in which the parameters ε/k and b_0 are determined by fitting the calculated B-values to experimental data (see ref. 50) were made, e.g., by Mullins, Ziegler and Kirk [51]. In the present work parameters ε/k and b_0 were derived from the conditions $B_{90.188\ K} = -224.4$ cm^3/mol and $B_{0°C} = -21.6$ cm^3/mol. This value for $B_{0°C}$ was chosen from data in refs. 52 to 55. The resulting values for the (effective classical) parameters are ε/k = 114.20 K and b_0 = 58.72 cm^3/mol. These values may be compared with those given by Hirschfelder et al. [50] (ε/k = 118 K, b_0 = 52.26 cm^3/mol), by Woolley and Benedict [56] (ε/k = 116 K, b_0 = 54.7 cm^3/mol) and by Mullins et al. (ε/k = 112 K, b_0 = 60.84 cm^3/mol). The parameter values given by Hirschfelder et al. and Woolley et al. are less satisfactory, since they yield values for $B_{90.188\ K}$ which are, respectively, 6% and 4.4% higher than the calculated value -224.4 cm^3/mol; those given by Mullins et al. yield -224.6 cm^3/mol for $B_{90.188\ K}$ and -20.9 cm^3/mol for $B_{0°C}$, the latter value being somewhat outside the spread of the data in refs. 52 to 55.

Tests showed that values of B at liquid-oxygen temperatures calculated with ε/k = 114.20 K and b_0 = 58.72 cm^3/mol do not differ significantly from those calculated with the parameters as given by Mullins et al. (In general, it appeared that for sets of ε/k and b_0 values which satisfy the condition $B_{90.188\ K} = -224.4$ cm^3/mol the calculated values of B at liquid-oxygen temperatures are about the same for variations of ε/k up to 6%.) Therefore, the parameters given by Mullins et al. could be chosen for the present calculations of B; the obtained values are indicated B_{L-J} and shown in fig. 3.9.

The influence of the third virial coefficient C on the calculated molar volume of the saturated vapour is, at temperatures below 100 K, probably less than 1% of that of B: Weber [49] estimates the term C/V_G to be less than 0.7% of B; calculations of C with a Lennard-Jones potential

yield that C/V_G is smaller than 0.2% of B (V_G is the molar volume of the saturated vapour). In the present calculations C and higher virial coefficients are neglected.

7.3 *Results of computations*

In figs. 3.10 and 3.11 vapour-pressure equations calculated from eq. (3.3) are compared with the experimental vapour-pressure equation. ($T_{Clap.}$ denotes the temperature according to eq. (3.3), which can be considered as an integrated form of Clapeyron's equation.)

For $L_{90.188\ K}$ the value 6821.8 J/mol (and, in one case, 6824.8 J/mol) has been used and V_L has been taken according to section 7.2.4; calculations were made with C_L (eq. (3.4)) and C_L (eq. (3.5)) and with B_{VL} and B_{L-J} (see section 7.2.5).

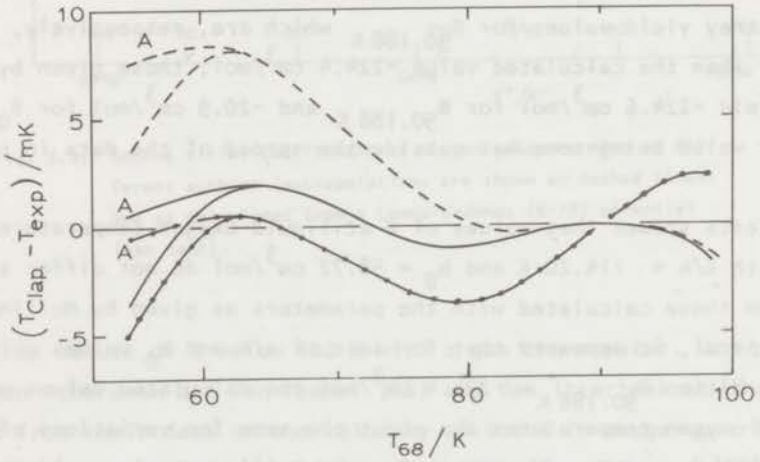

Fig. 3.10. Differences between the provisional experimental vapour-pressure equation and vapour-pressure equations calculated from Clapeyron's relation. For curves A, T_{exp} indicates the revised experimental equation. As input data for the calculations B values given by Van Lammeren and different values for L(90.188 K) and C_L(T) have been used.

—•—•— C_L: eq. (3.4) L(90.188 K) = 6821.8 J/mol

– – – – C_L: eq. (3.4) L(90.188 K) = 6824.8 J/mol

——— C_L: eq. (3.5) L(90.188 K) = 6824.8 J/mol

With B_{vL} and $L_{90.188\ K}$ = 6821.8 J/mol, the slopes of the calculated equation and the experimental equation differ 0.044% at 90.188 K; agreement can be obtained by changing $L_{90.188\ K}$ with 0.044% (see fig. 3.10).

Both for B_{vL} and B_{L-J} the agreement between the calculated and the experimental equation is (above 64 K) better with C_L(eq. (3.5)) than with C_L(eq. (3.4)).

For T < 64 K systematic deviations of the calculated equation from the experimental equation (dash-dotted line in fig. 3.5) are found which are similar for B_{vL} and B_{L-J} and for C_L(eq. (3.5)) and C_L(eq. (3.4)). It seems impossible to change B(T) in such a way that these deviations are reduced considerably.

It has been investigated whether reasonable values for C_L could be found with which agreement could be obtained. The relation between δC_L and the resulting change $\delta \ln p$ is, according to eq. (3.3), given by the relation

$$\delta C_L = -\frac{d}{dT}\left(RT^2 \frac{d}{dT}\delta \ln p\right) \qquad (3.6)$$

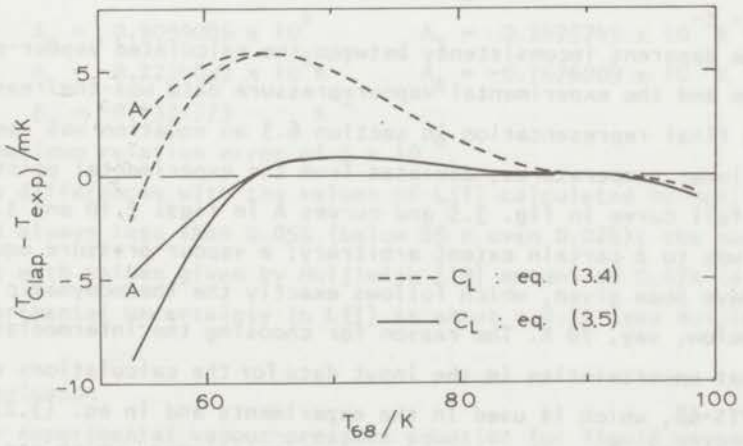

Fig. 3.11. Differences between the provisional experimental vapour-pressure equation and vapour-pressure equations calculated from Clapeyron's relation. For curves A, T_{exp} indicates the revised experimental equation. As input data for the calculations B values computed from a Lennard-Jones (6-12) potential have been used.

The change $\delta C_L(T)$ with respect to C_L (eq. (3.5)), that would be necessary to obtain full agreement between the calculated vapour-pressure equation (with B_{L-J}) and the experimental equation, is shown in fig. 3.12. It can be deduced from the figure that at the lower temperatures quite unreasonable values for C_L have to be assumed to get agreement between calculated and experimental vapour-pressure equations.

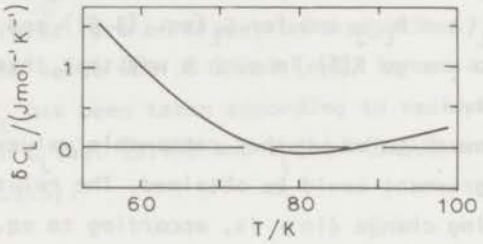

Fig. 3.12. Change of $C_L(T)$ which would be required to obtain agreement between the provisional experimental vapour-pressure equation and a vapour-pressure equation calculated from Clapeyron's relation. Comparison with fig. 3.8 (full curve) shows that such a change of C_L is highly unlikely.

The apparent inconsistency between the calculated vapour-pressure equation and the experimental vapour-pressure data was the reason that for the final representation in section 6.3 an equation was used which, at the lower temperatures, deviates from the experimental points (eq. (3.2), full curve in fig. 3.5 and curves A in figs. 3.10 and 3.11). The choice was to a certain extent arbitrary; a vapour-pressure equation could have been given, which follows exactly the thermodynamic calculations below, say, 70 K. The reason for choosing the intermediate curve A was, that uncertainties in the input data for the calculations exist, and that IPTS-68, which is used in the experiments and in eq. (3.2), may differ slightly from the thermodynamic temperatures, which are used in the calculations.

The calculations have shown a better agreement between the calculated and the experimental vapour-pressure equations for B_{L-J} than for B_{vL} (see figs. 3.10 and 3.11). In this sense the B_{L-J}-values should be preferred

over B_{vL}. This preference for B_{L-J} was substantiated by calculations of B(T)-values between 64 K and 99 K from eq. (3.3) with vapour pressures according to eq. (3.2). These calculations yield values for B which are within 2% equal to B_{L-J}. There is no evidence from experimental data on the second virial coefficient to prefer either B_{vL} or B_{L-J}. (As pointed out earlier by Muijlwijk [19], experimental values for the quantity S (see section 10.3.5, Chapter 2) in acoustic determinations of the virial coefficients [45,46,47] disagree slightly with B_{L-J}; however, these differences can easily be accounted for by the uncertainties in the experimental data for S.)

7.4 *Heat of vaporization of oxygen*

The latent heat of vaporization of liquid oxygen between the triple point and 99 K was calculated from eq. (2.39) in Appendix 2 to Chapter 2. $L_{90.188\,K}$ was taken equal to 6821.8 J/mol, $C_L(T)$ was calculated from eq. (3.5) and for the second virial coefficient B_{L-J}, derived from the Lennard-Jones (6-12) potential, was chosen. The results of the calculation were expressed in the formula $L(T)/J\ mol^{-1} = \sum_{n=0}^{4} A_n T^n$, in which

$$A_0 = 0.9099085 \times 10^{4} \qquad A_3 = 0.2675745 \times 10^{-2} K^{-3}$$
$$A_1 = -0.2234803 \times 10^{2} K^{-1} \qquad A_4 = -0.1676009 \times 10^{-4} K^{-4}$$
$$A_2 = -0.1371773\ K^{-2}$$

with a maximum relative error of 5×10^{-6}.

The differences with the values of L(T) calculated by Mullins et al. [51] are always less than 0.05% (below 85 K even 0.02%); the maximum differences with values given by Muijlwijk [19] amount to 0.07% (at 99 K). The experimental uncertainty in L(T) is about ± 0.1% (see Muijlwijk [19]).

7.5 *Conclusion*

The experimental vapour-pressure equatior for liquid oxygen is between 64 K and 99 K within 1 mK in agreement with vapour pressures calculated from a thermodynamic equation, in which as input data are used experimental values for the heat of vaporization at 90.188 K, the heat capacity and density of liquid oxygen and the second virial coefficient of oxygen gas. The thermodynamic calculations have been used to define the vapour-pressure

equation below 64 K, where the experimental data are less accurate.

The calculations have shown that values for the second virial coefficient calculated with a suitable Lennard-Jones (6-12) potential are better consistent with the experimental vapour-pressure equation than values obtained from (extrapolations of) formulae for the second virial coefficient derived from acoustic data.

Values for the heat capacity of liquid oxygen based upon data of Goodwin and Weber are better consistent with the present vapour-pressure data than earlier heat-capacity data. It follows from the calculations, that the data of Goodwin and Weber probably represent the heat capacity of liquid oxygen below 95 K within 0.2%.

References

1. International Practical Temperature Scale of 1968, Metrologia 5, 35 (1969).
2. Handbook of Chem. and Phys., Ed. R.C. Weast, 48th ed. (1967-1968), Chemical Rubber Co., Ohio, p. B-7.
3. S. Weber, W.H. Keesom and G. Schmidt, Commun. Kamerlingh Onnes Lab., Leiden, No. 246a (1936).
4. A. van Itterbeek and E. de Grande, Physica 13, 289 (1947).
5. S. Chu Liang, J. Appl. Phys. 22, 148 (1951).
6. M.J. Bennett and F.C. Tompkins, Trans. Far. Soc. 53, 185 (1957).
7. J.M. Los and R.R. Fergusson, Trans. Far. Soc. 48, 730 (1952).
8. T.R. Roberts and S.G. Sydoriak, Phys. Rev. 102, 304 (1956).
9. G.T. McConville, R.A. Watkins and W.L. Taylor, Proc. of the 10th Int. Conf. on Low Temp. Physics, Vol. 1, 248-252 (Moscow, U.S.S.R., 1966).
10. A. Freddi and I. Modena, Cryogenics 8, 18 (1968).
11. R.A. Millikan, Phys. Rev. 21, 217 (1923).
12. F.C. Hurlbut, Phys. of Fluids 3, 217 (1960).
13. G.T. McConville, Temperature, It's Measurements and Control in Science and Industry (Instrument Society of America, Pittsburgh, 1972) Vol. 4.

14. M. Ruhemann, The separation of gases, 2nd ed., Clarendon Press, Oxford (1949).

15. T. Mochizuki, S. Sawada,and M. Takahashi, Jap. J. of Appl. Phys. 8, 488 (1969).

16. T. Soejima, M. Takahashi and S. Sawada, Comité Consultatif de Thermométrie, 7^{e} session (1964), doc. 15, Annexe 2, T 29.

17. M.R. Moussa, R. Muijlwijk and H. van Dijk, Physica 32, 900 (1966); Commun. Kamerlingh Onnes Lab., Leiden, No. 346b.

18. R. Muijlwijk, M.R. Moussa and H. van Dijk, Physica 32, 805 (1966); Commun. Kamerlingh Onnes Lab., Leiden, No. 346c.

19. R. Muijlwijk, Ph.D. Thesis, Leiden (1968).

20. J. Ancsin and M.J. Phillips, Metrologia 5, 77 (1969).

21. G.T. Furukawa, W.G. Saba, D.M. Sweger and H.H. Plumb, Metrologia 6, 35 (1970).

22. J.P. Compton, Metrologia 6, 69 (1970); 6, 103 (1970).

23. J. Ancsin, Metrologia 6, 53 (1970).

24. W. Thomas and W. Blanke, Temperature, It's Measurement and Control in Science and Industry (Instrument Society of America, Pittsburgh, 1972), Vol. 4.

25. W.R.G. Kemp and C.P. Pickup, Temperature, Vol. 4.

26. J. Dewar, Proc. Roy. Soc. London (A) 85, 589 (1911).

27. E. Justi, Ann. Physik 10, 983 (1931).

28. H.J. Hoge, J. Res. Natl. Bur. Stands. 44, 321 (1950).

29. T. Mochizuki, S. Sawada and M. Takahashi, Comité International des Poids et Mesures, Comité Consultatif de Thermométrie, 7^{e} session, doc. 14, Annexe 3, T 34 (1964).

30. R.E. Bedford, M. Durieux, R. Muijlwijk and C.R. Barber, Metrologia 5, 47 (1969).

31. J.G. Hust and R.B. Stewart, Internal NBS Laboratory Report (1965); reported by R.B. Stewart, Ph.D. Thesis, Iowa State Univ. (1966).

32. R.D. Goodwin, J. Res. Natl. Bur. Stands. 73A, 487 (1969).

33. G.T. Brower and G. Thodos, J. Chem. and Eng. Data 13, 262 (1968).

34. R. Prydz, Metrologia 8, 1 (1972).

35. H. van Dijk, Physica 32, 945 (1966); Commun. Kamerlingh Onnes Lab., Leiden, No. 346a.
36. A. Eucken, Verhandl. Deut. Physik. Ges. 18, 4 (1916).
37. K. Clusius, Z. physik. Chem. B3, 41 (1929).
38. W.F. Giauque and H.L. Johnston, J. Amer. Chem. Soc. 51, 2300 (1929).
39. R.D. Goodwin and L.A. Weber, J. Res. Natl. Bur. Stands. 73A, 1 (1969).
40. H.W. Woolley, J. Res. Natl. Bur. Stands. 40, 163 (1948).
41. K. Goldman and N.G. Scrase, Physica 44, 555 (1969).
42. E. Mathias and H. Kamerlingh Onnes, Commun. Phys. Lab., Leiden, No. 117 (1911).
43. A. van Itterbeek and O. Verbeke, Cryogenics 1, 77 (1960).
44. P.G. Cath and H. Kamerlingh Onnes, Commun. Phys. Lab., Leiden, No. 156a (1922).
45. J.A. van Lammeren, Ph.D. Thesis, Leiden (1935).
46. A. van Itterbeek and O. van Paemel, Physica 5, 593, (1938).
47. A. van Itterbeek, J. Nihoul, G. Forrez and L. van Gerven, Bull. Inst. Intern. du Froid, Annexe 1956-2, 215-225.
48. P. Nijhoff and W.H. Keesom, Commun. Phys. Lab., Leiden, No. 179b (1925).
49. L.A. Weber, J. Res. Natl. Bur. Stands. 74A, 93 (1970).
50. J.O. Hirschfelder, C.F. Curtiss and R.B. Bird, Molecular Theory of Gases and Liquids, J. Wiley and Sons Inc., New York (1954).
51. J.C. Mullins, W.T. Ziegler and B.S. Kirk, Techn. Report No. 2, Project No. A-593, Engineering Exp. Station, Georgia Inst. of Technology; Adv. cryog. Engineering 8, 126 (1963).
52. H. Kamerlingh Onnes and H.H. Francis Hyndman, Commun. Phys. Lab., Leiden, No. 78 (1902).
53. L. Holborn and J. Otto, Z. Physik 10, 367 (1922).
54. H.A. Kuypers and H. Kamerlingh Onnes, Commun. Phys. Lab., Leiden, No. 165a (1923).
55. A. Michels, H.W. Schamp and W. de Graaff, Physica 20, 1209 (1954).
56. H.W. Woolley and W.S. Benedict, NACA Techn. Note TM 3272 (1956).

CHAPTER 4

INTERCOMPARISON OF PLATINUM THERMOMETERS BETWEEN 13.81 K AND 373.15 K

1 Introduction

As a result of the experiments described in Chapters 2 and 3, and also of earlier experiments in this laboratory at liquid-hydrogen temperatures, the calibration of two platinum thermometers on the International Practical Temperature Scale of 1968 (IPTS-68) [1] was obtained. In this Chapter an experiment is described, in which seven platinum thermometers were compared with these two thermometers at 25 temperatures between 13.81 K and 373.15 K, including the temperatures of the eight defining fixed points of IPTS-68 for measurements below 0 °C. The thermometers were also intercompared at temperatures between 2 K and 13.81 K and calibrated at these temperatures against a magnetic temperature scale; these measurements will be described in Chapter 5.

In section 2, the thermometers which have been used are listed and the calibration of the two reference thermometers (B2 and T4) is reviewed.

In section 3, the apparatus used for the intercomparisons of the thermometers is shown and the experimental method is outlined.

The experimental results, presented as differences between the reduced resistances $W(T) = R(T)/R_{0\ °C}$, are given in section 4.

In section 5, the deviation functions $\Delta W(T_{68})$, defined in IPTS-68, are shown for the various thermometers.

In section 6, differences between IPTS-68 realizations for the nine thermometers are discussed. The suggestion to use Matthiessen's rule for the higher range is criticized.

Discontinuities in the second derivative d^2W/dT^2, which occur due to the calibration procedure, are given in section 7.

Finally, in section 8, the accuracy of extrapolations of IPTS-68 below its lower limit of 13.81 K is discussed.

2 The platinum thermometers

The nine platinum thermometers which have been used are listed in table 4.1. Only nos. 1 to 7 satisfy the condition of IPTS-68 that $W_{100\ °C}$ should be not less than 1.39250; for thermometer 188677, $W_{100\ °C}$ is just

Table 4.1

Data of platinum thermometers used in this investigation

no	thermometer	source	$W_{100\ °C}$
1	213866	Tinsley, London	1.392699
2	T4	P.R.M.I., Moscow	1.392691
3	213860	Tinsley, London	1.392668
4	145	K.O.L.	1.392647
5	153	K.O.L.	1.392635
6	164956 (B2)	Tinsley, London	1.392626
7	143	K.O.L.	1.392612
8	188677	Tinsley, London	1.392478
9	A2	P.S.U., Penn., U.S.A.	1.392097

below this value, and for thermometer A2, $W_{100\ °C}$ is much lower.

The thermometers 164956, also referred to as B2, and T4 were calibrated at liquid neon and oxygen fixed points; this is described in Chapters 2 and 3. B2 was also calibrated at the hydrogen fixed points by Van Rijn in this laboratory; the calibration of T4 at these temperatures was obtained by intercomparison with B2.

The resistances of all thermometers were measured at the triple point and the normal boiling point of water. Some difficulties were encountered in the calibrations at these fixed points: inconsistencies, up to 2 mK and 4 mK at the triple point and the boiling point of water, respectively, showed up between the direct calibrations and the intercomparisons of the thermometers at about 0 °C and 100 °C to be described later in this Chapter. Therefore, the fixed-point calibrations of one thermometer, B2, at the triple point and the boiling point of water were assumed to be correct and the resistances of the other thermometers at these temperatures were derived from the intercomparisons. The possible systematic errors in the absolute values of the resistances, equivalent to 1 mK and 3 mK at the triple point and the boiling point respectively, do not affect the conclu-

sions which will be drawn later in this Chapter concerning the differences between thermometers and the reproducibility of IPTS-68.

3 Experimental method

The apparatus for the intercomparison of platinum and germanium thermometers at temperatures between 2 K and 100 °C (this Chapter and Chapter 5) is sketched in fig. 4.1. In a copper block O with a mass of 2.1 kg there are ten holes M to accommodate platinum thermometers and ten holes P for germanium thermometers. The block is suspended by three thin-walled stainless-steel capillaries L from the top of the copper thermal shield I which surrounds the block. The shield is suspended by three thin-walled stainless-steel capillaries G from the top plate of the vacuum can K, which is sealed with an indium O-ring (D). B is the pumping line (I.D. 9 mm). Au-0.03 at.%Fe versus chromel thermocouples are used to measure temperature differences between the bath, top and bottom of the block and top, middle and bottom of the shield. The Au-Fe and chromel wires are soldered to copper wires which pass through B, the junctions being thermally anchored to the copper extension E of tube B. A calibrated germanium thermometer, mounted on top of the shield, is used to measure the shield temperature.

The wiring, comprising the fixation of about 70 wires, is essentially the same as described in Chapter 2, but there are a few changes. The lead wires from the germanium thermometers are twisted around the copper posts Q before they are glued with GE 7031 to the block and the shield. Notches in perspex ring segments H serve to guide the leads. At the top of the vacuum can, the leads are soldered to copper extension wires which enter the can through eight stainless-steel tubes A. The junctions are thermally anchored to the copper posts F.

A provision has been made for later insertion of a vapour-pressure thermometer through the tube C and the central tube J in the shield into the hole N in the block; in the present experiments the tube C is closed at the top.

The device at the lower end of the vacuum can is a mechanical heat switch. Inside a bellows a spring holds a copper rod. This rod has a conical top that fits, through a hole in the bottom of the shield, into a loose conically shaped copper disk which is thermally anchored to the

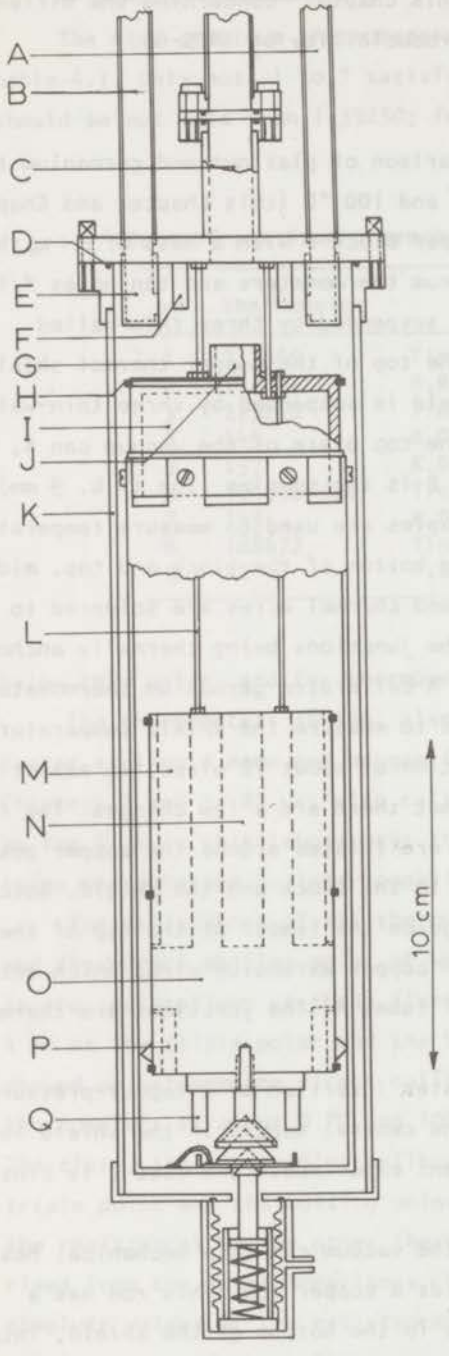

shield by means of twisted copper wires. This disk fits into a conical copper extension of the block. When the bellows is pressurized, heat contact is made between can, shield and block. The dimensions are such that, for a pressure difference of one atmosphere, the copper rod exerts a force of 3 kN upon the copper pieces.

The heat switch can be used to accelerate cooling of block and shield; however, it still takes about two days to cool to liquid-hydrogen temperatures. Usually exchange gas is used to cool the block and shield.

The block, the top of the shield and the switch are gold-plated to prevent oxidation when the apparatus is open to the air.

The procedure of measurement is different from that described in Chapter 2 only in that no pressure measurements are made and that the shield temperature is kept constant automatically.

Fig. 4.1.
Apparatus for intercomparison of platinum and germanium thermometers.

To this end the off-balance of the voltage from the shield germanium thermometer and an auxiliary potentiometer, set to a preset value, is fed into a Keithley model 140 d.c. amplifier and thereafter into a second amplifier, which provides a current through the shield heater which is proportional to the off-balance signal. The shield temperature can be kept constant in this way within ± 0.5 mK, under favourable conditions even within ± 0.1 mK. At temperatures above 130 K, the differential thermocouples are sometimes used instead of the shield germanium thermometer.

It may be mentioned that the system, of which the temperature has to be kept constant, is very well isolated from the surroundings. This makes that the heater currents are small, which facilitates the temperature control; a disadvantage is that cooling of the system with a reasonable speed must be done with exchange gas.

The apparatus is placed in a dewar which is filled with liquid helium for measurements below 20 K, with liquid hydrogen for measurements between 20 K and 60 K and with liquid oxygen for measurements up to 250 K. For the measurements near 273.15 K the apparatus is placed in ice and for measurements up till 98 °C in a water-bath thermostat. Before making the measurements above room temperature, the germanium thermometers were removed from the apparatus to avoid the possibility of changing their calibration by excessive heating.

The current through the platinum thermometers was varied from 5 mA at 13.81 K to 3 mA at 20.28 K and to 1 mA at 54.361 K and at higher temperatures. Tests at 20 K, 54 K and 70 K showed for the thermometers a self-heating rate of about 0.1 mK/μW; this corresponds for the currents used with a self-heating of 0.1 mK, 0.2 mK and 0.4 mK respectively at these temperatures. No reductions to zero-current have been made.

The sensitivity of the voltage measurements was, under favourable conditions, 5 nV, which is equivalent to 0.15 mK at 13.81 K and to 0.1 mK at 17 K and at higher temperatures. For the measurements at the higher temperatures, where a large relative accuracy in the measurements is required, care was taken to use high dial settings of the calibrated Van Dijk potentiometer (see Chapter 2), which makes the influence of errors in the calibration of the potentiometer smaller than 1 in 10^6.

The finally obtained accuracy in the intercomparison of the

thermometers can best be judged from the scatter of the points around the smooth curves in figs. 4.5 to 4.8, which is ± 0.3 mK from 373 K to 300 K, ± 0.2 mK from 300 K to 125 K, ± 0.1 mK from 125 K to 16 K and ± 0.2 mK below 16 K.

The estimated accuracy for the fixed-point calibrations of thermometers B2 and T4 was given earlier (see section 2 and Chapters 2 and 3).

Table 4.2

Experimental results of intercomparisons of nine platinum thermometers between 13.81 K and 373.15 K. Differences are given between the reduced resistances of the various thermometers and the reduced resistance of thermometer B2. (The last column is explained in the text.)

T_{68}/K	$10^6(W^{(x)}_{exp} - W^{(B2)}_{exp})$								$10^6 \Delta W^{(B2)}(T_{68})$
	213866	T4	213860	145	153	143	188677	A2	
13.81	-149.7	-152.4	-120.5	20.2	- 9.8	82.7	302.9	895.5	- 4.70
14.53	-151.8	-153.5	-121.1	19.3	-10.2	82.5	312.4	905.8	- 3.82
15.29	-153.8	-154.2	-121.4	18.1	-10.5	82.3	322.9	916.9	- 3.06
16.16	-156.0	-154.6	-121.7	16.6	-11.0	81.9	334.6	928.7	- 2.58
17.02	-157.8	-154.5	-121.6	15.3	-11.1	81.5	335.0	938.7	- 2.35
17.78	-159.2	-154.0	-121.3	14.0	-11.1	80.9	353.6	946.6	- 2.19
18.57	-160.6	-153.3	-120.8	12.5	-11.0	80.2	362.1	954.6	- 1.91
19.37	-161.7	-152.3	-120.2	10.9	-10.6	79.6	369.8	961.5	- 1.44
20.28	-162.7	-151.0	-119.4	9.2	-10.3	78.9	377.9	968.8	- 0.62
22.00	-164.5	-148.2	-117.7	6.3	- 9.2	77.4	309.9	980.2	1.1
23.74	-165.6	-145.0	-115.8	3.5	- 7.6	76.1	401.0	989.5	1.9
25.40	-166.4	-142.0	-113.8	1.2	- 5.8	74.9	408.5	997.5	1.9
27.10	-166.8	-139.3	-112.1	- 1.0	- 4.0	73.7	414.0	1004.4	1.3
33.11	-166.5	-131.7	-106.7	- 6.3	2.5	71.1	420.7	1022.8	- 4.3
40.05	-163.1	-125.9	-101.5	- 9.2	8.4	69.7	414.4	1033.3	-12.5
47.00	-158.5	-122.3	- 97.3	-10.8	11.7	67.5	401.0	1032.6	-14.8
54.361	-152.6	-118.8	- 91.9	-11.4	12.9	67.0	384.7	1022.8	- 2.0
62.98	-146.4	-116.2	- 88.5	-13.9	12.6	62.8	364.2	1000.1	21.1
72.40	-140.3	-111.9	- 85.1	-14.0	11.6	60.0	341.5	969.4	35.2
80.95	-135.6	-110.2	- 82.6	-15.4	11.0	56.9	322.1	936.5	38.3
90.20	-131.8	-107.2	- 81.0	-17.2	8.4	52.7	302.3	897.8	30.9
116.2	-113.9	- 95.6	- 69.3	-21.3	- 0.2	38.0	258.3	786.1	2.7
143.5	- 94.9	- 80.7	- 58.0	-23.2	- 6.1	26.1	210.7	659.9	-13.3
174.9	- 71.5	- 63.4	- 43.3	-22.7	-12.4	10.4	157.5	504.1	-19.6
225.4	- 36.4	- 28.7	- 22.3	- 7.1	- 1.7	11.0	75.9	251.1	-13.3
273.15	0	0	0	0	0	0	0	0	0
302.4	18.8	17.0	10.9	3.7	- 1.7	- 5.7	- 47.0	- 154.7	
338.4	46.8	39.1	25.5	13.0	4.6	-12.0	-102.8	- 344.8	
373.1	73.0	63.9	42.0	21.0	9.0	-14.0	-148.3	- 528.8	29.3

4 Intercomparison of reduced resistances

From the measured resistances of the thermometers, values for $W(T) = R(T)/R_{0\ °C}$ were derived. The results are given in table 4.2. For convenience, the data for individual thermometers are not given, but only differences with respect to thermometer B2, $W_{exp}^{(x)} - W_{exp}^{(B2)}$. The temperatures in the first column of the table are approximate temperatures derived from the calibration of B2. The last column gives the values of the deviation function $\Delta W(T_{68})$ of IPTS-68 (see section 5 and the Appendix to this thesis) for B2. The data are plotted in fig. 4.2.

The dashed curves in fig. 4.2 indicate $\Delta W^{(x)}(T_{68}) - \Delta W^{(B2)}(T_{68})$, the differences between the IPTS-68 deviation functions of the thermometers (with $\Delta W(T_{68})$ for B2 as the reference). The fact that the experimental points do not follow exactly the dashed lines, means, of course, that the different thermometers yield slightly different values for T_{68}; this will be discussed in detail in section 6.

In fig. 4.3 differences between the reduced resistances of four thermometers are given, with the KOL thermometer 153 as a reference.

It can be seen from the figures, that the differences between the reduced resistances above 90 K are linearly or nearly linearly dependent on T for the three KOL thermometers as a group and also for the Tinsley thermometers and the Russian thermometer T4. The results for thermometer 188677, which shows a slightly anomalous behaviour, and for A2, which has a very low α-coefficient ($\alpha = (R_{100\ °C} - R_{0\ °C})/100\ R_{0\ °C}\ °C^{-1}$), will be discussed in section 5.

5 The deviation functions $\Delta W(T_{68})$ for the thermometers

It is described in the Appendix that in IPTS-68 so-called deviation functions $\Delta W(T_{68})$ are defined. At the fixed-point temperatures, $\Delta W(T_{68})$ is obtained from the relation

$$\Delta W(T_{68}) = W(T_{68}) - W_{CCT\text{-}68}(T_{68})$$

where $W_{CCT\text{-}68}(T_{68})$ is a reference function, representing the reduced resistance of a (hypothetical) reference thermometer. At intermediate temperatures, $\Delta W(T_{68})$ is obtained from simple interpolation formulae (see the

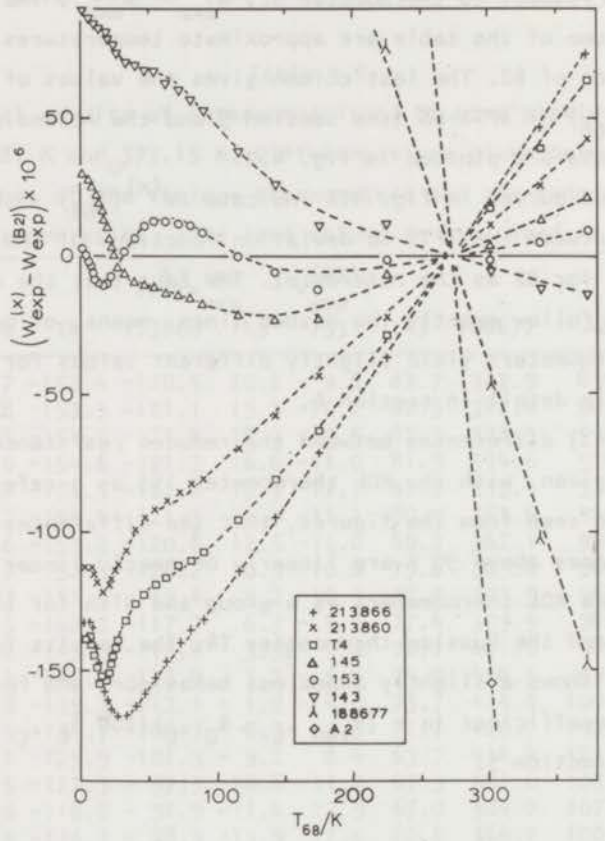

Fig. 4.2. Differences between experimental reduced resistances of the platinum thermometers. Thermometer B2 has been chosen as the reference. The points below 13.81 K have been taken from Chapter 5.
The dashed curves indicate the differences between the IPTS-68 deviation functions $\Delta W(T_{68})$ for the thermometers.

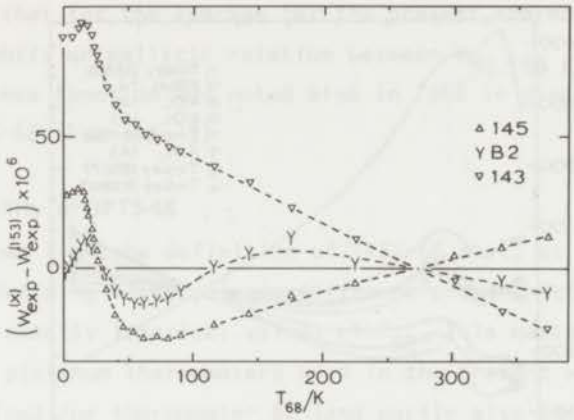

Fig. 4.3. This figure shows the same data as fig. 4.2 but with thermometer 153 as the reference.

Appendix).

The deviation functions for the thermometers have been plotted in fig. 4.4. Thermometer A2 has been omitted from the figure because of its large value of $\Delta W(T_{68})$ (with a maximum of 1026×10^{-6} near 40 K). The behaviour of thermometer 188677 is remarkably different from that of the other thermometers.

The shapes of the $\Delta W(T_{68})$ curves for the various thermometers show irregularities which are strikingly similar. If the values of the reference function $W_{CCT-68}(T_{68})$ were slightly changed at 373.15 K and 90.188 K, more regular $\Delta W(T_{68})$ curves would be obtained for most of the present thermometers. A good choice would be to raise the value of W_{CCT-68} (90.188 K) by about 29×10^{-6} and that of W_{CCT-68} (100 °C) by about 37×10^{-6}. (The value of 37×10^{-6} at 100 °C is uncertain by 12×10^{-6}, due to the uncertainty of 3 mK in the calibration of the thermometers at the steampoint, see section 2.) If these changes were applied, the deviation functions of the first seven thermometers in table 4.1 would not deviate from straight lines more than 12×10^{-6} (which is equivalent to 3 mK) in the range from 50 K to 373 K.

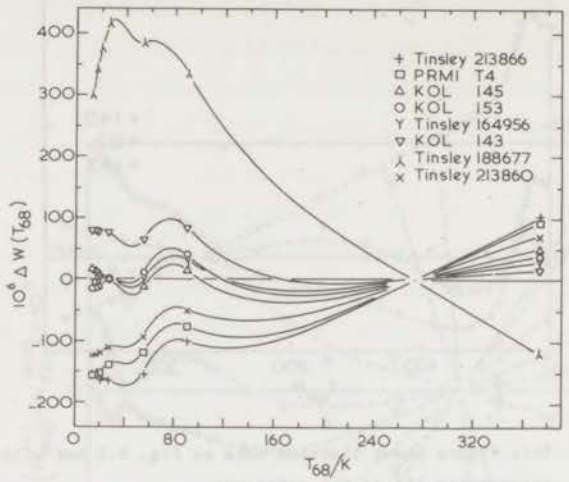

Fig. 4.4. The deviation functions $\Delta W(T_{68})$ for the various thermometers between 13.81 K and 373.15 K.
The values at the fixed points are indicated.

In connection with the irregularities in the $\Delta W(T_{68})$ functions, it should be mentioned that the relation between $W_{90.188\ K}$ and $W_{100\ °C}$ found for the present thermometers is somewhat different from that given by Berry [2] as an average for a large number of platinum thermometers. The assumed average curve in a $W_{90.188\ K}$ vs. $W_{100\ °C}$ graph, given by Berry, can be represented by the relation

$$W_{100\ °C} = -0.592\ W_{90.188\ K} + 1.536942$$

For the present thermometers (188677 excluded) the corresponding relation is

$$W_{100\ °C} = -0.592\ W_{90.188\ K} + 1.536942 + (36 \pm 13) \times 10^{-6}.$$

Thus, the mean of $W_{100\ °C}$ for the present thermometers is, with respect to $W_{90.188\ K}$, 36×10^{-6} higher than according to Berry's curve, or alternatively, $W_{90.188\ K}$ is 65×10^{-6} too low.

As a result, for Berry's average thermometer the 'irregularity' in the

deviation function $\Delta W(T_{68})$ between 90.188 K and 373.15 K would be about one third of that for the average for the present thermometers.

The slightly unrealistic relation between $W_{90.188\ K}$ and $W_{100\ °C}$ in the CCT-68 reference function was noted also in 1968 in discussions for establishing IPTS-68 (see ref. 3).

6 Reproducibility of IPTS-68

It follows from the definition of IPTS-68 that, at temperatures between the defining fixed points, different platinum thermometers will not indicate exactly identical values of T_{68}. This matter was investigated for the nine platinum thermometers used in the present work. Temperatures T_{68} were derived for thermometer B2 (and partly also for T4) from the fixed-point calibrations, and for the other thermometers from the calibration-by-intercomparison at the fixed-point temperatures.

The differences between T_{68} values for the various thermometers are shown in figs. 4.5 to 4.8. The base line is the mean of T_{68} for the first eight thermometers in table 4.1; it is denoted $\overline{T}_{68}$.

The two determinations which were performed at each temperature during a run are shown separately, which gives an impression of the precision with which the intercomparisons have been carried out. For clarity, curves have been drawn through the experimental points; below 90.188 K the curves could be drawn unambiguously, above 90.188 K their shapes are sometimes slightly arbitrary at the sub-millikelvin level.

6.1 *The range from 90.188 K to 273.15 K.*

In order to make it easier to determine the slopes of the curves in figs. 4.5 to 4.8 near 273.15 K, and also to check the reliability of the intercomparisons near 273.15 K and 373.15 K, two additional intercomparisons were made at 302 K and 338 K. For these points the temperatures were deduced from the reference function $W_{CCT\text{-}68}(T_{68})$ and the deviation functions $\Delta W(T_{68})$ for the range from 90.188 K to 273.15 K. (Thus, at these temperatures, ΔT does not represent the differences between the real T_{68} values for the thermometers.) The data points at 273.15 K marked with an arrow were determined in a separate series of measurements.

The thermometers with $W_{100\ °C} > 1.3926$ (i.e. the first seven

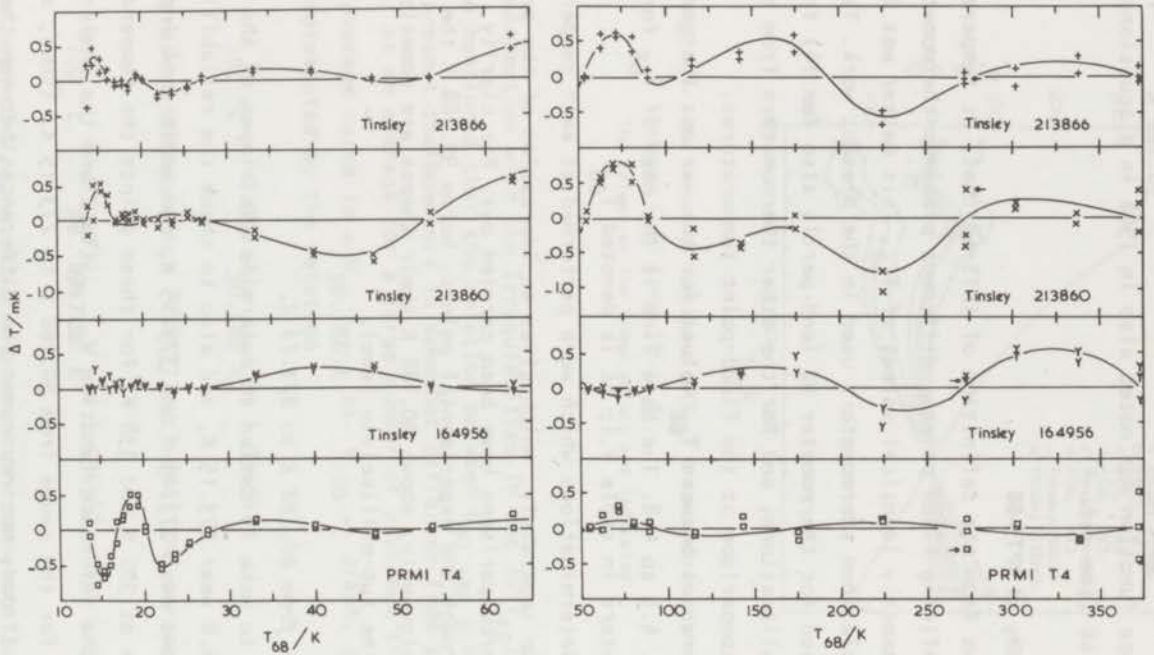

Fig. 4.5. Differences between T_{68} for various thermometers and $\overline{T_{68}}$ ($\overline{T_{68}}$ is the mean temperature of thermometers nos. 1 to 8, see table 4.1). $\Delta T = T_{68} - \overline{T_{68}}$.

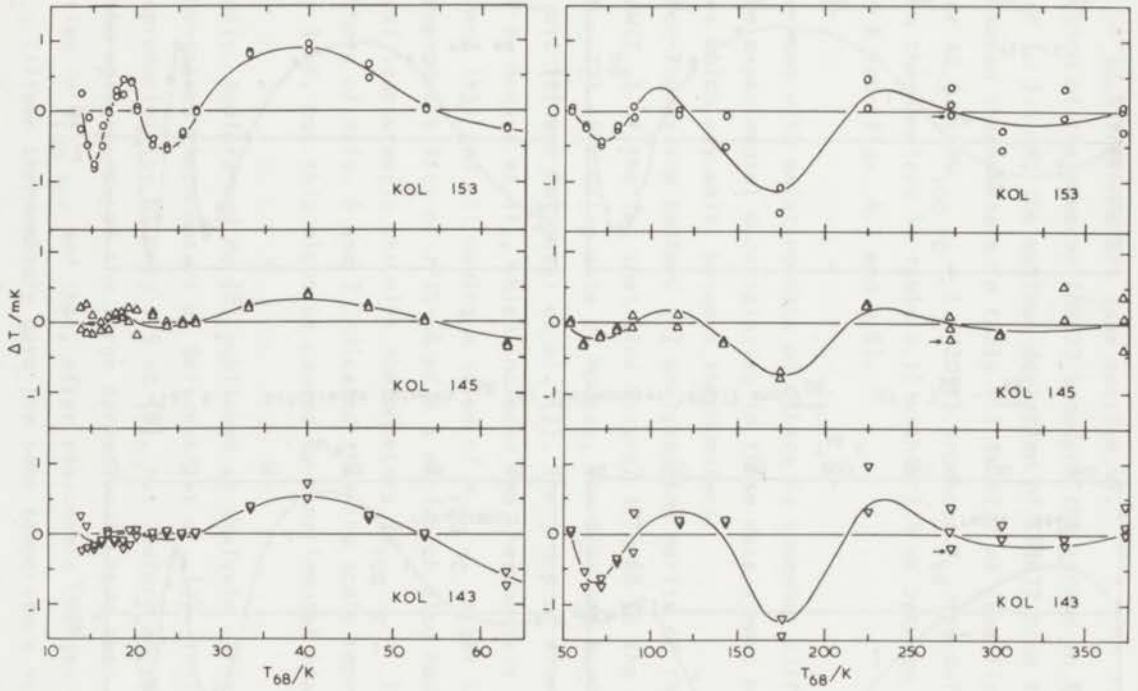

Fig. 4.6. Differences between T_{68} for various thermometers and $\overline{T_{68}}$.
$\Delta T = T_{68} - \overline{T_{68}}$.

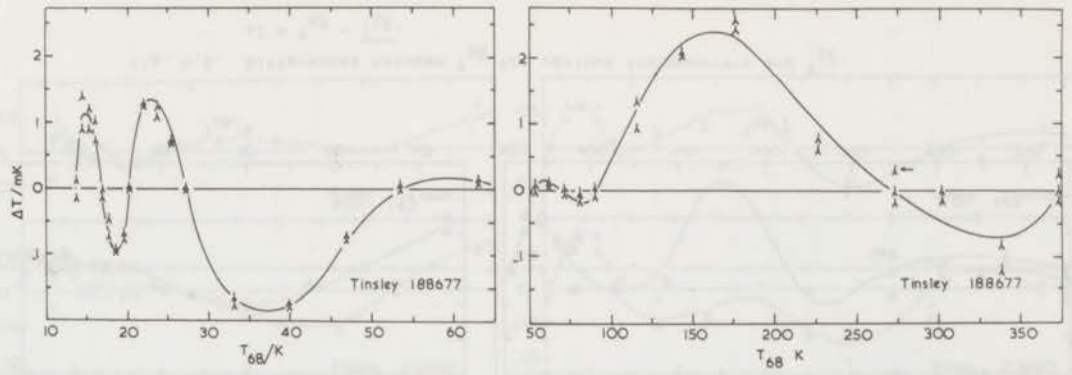

Fig. 4.7. Difference between T_{68} for thermometer 188677 and $\overline{T_{68}}$. $\Delta T = T_{68} - \overline{T_{68}}$.

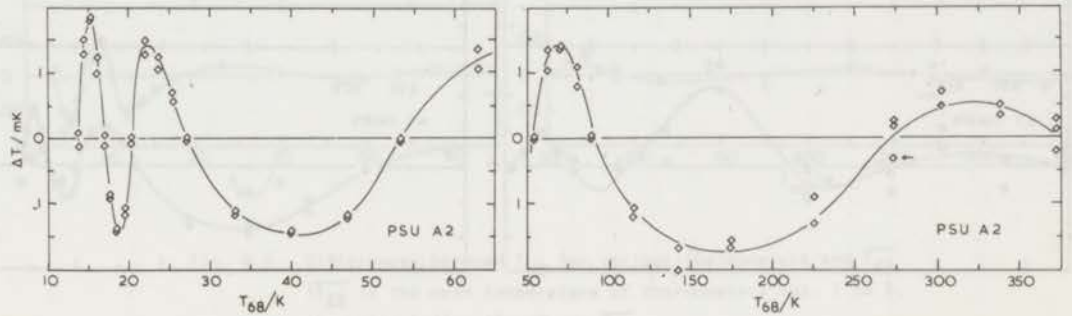

Fig. 4.8. Difference between T_{68} for thermometer A2 and $\overline{T_{68}}$. $\Delta T = T_{68} - \overline{T_{68}}$.

thermometers in table 4.1) give between 90.188 K and 273.15 K the same realization of IPTS-68 to within ± 0.8 mK (see fig. 4.5 and 4.6).

The curves for thermometers of the same origin have a similar shape. This could be expected from the observed similarities between reduced resistances of such thermometers (see section 4).

Inclusion of thermometer 188677 broadens the spread in T_{68} values from 1.6 mK to 3.5 mK; the maximum deviation of 188677 from the mean of the first seven thermometers in table 4.1 is +2.7 mK (see fig. 4.7). Thermometer A2 (with $W_{100\ °C} = 1.392097$) produces T_{68} (as defined by the first seven thermometers in table 4.1) within 1.4 mK between 90.188 K and 273.15 K (see figs. 4.7 and 4.8).

Comparison with existing data of others is somewhat difficult, because the experimental uncertainties in those data almost mask the small differences which may exist between thermometers.

Preston-Thomas and Bedford [4] analyzed the merits of the deviation function $\Delta W(T_{68})$ of the (at that time future) IPTS-68 in the range from 90.188 K to 273.15 K using data of Moussa, Van Dijk and Durieux [5], Orlova et al. [6] and Belyanski et al. [7]. The group of five thermometers used by Moussa et al., which included two thermometers of the present group (B2 and 143) and all having a value of $W_{100\ °C}$ larger than 1.3926, showed a reproducibility of IPTS-68 of ± 1 mK (which also had been the experimental inaccuracy); the nine thermometers ($W_{100\ °C} \geq 1.39245$) used by the authors of refs. 6 and 7 indicated that the scale reproducibility was only ± 3 mK, but this might be caused by experimental inaccuracy of the data.

Recently, Bedford and Ma [8] published an analysis of intercomparison data for seventeen thermometers of Belyanski et al. [9]. These data gave a scale reproducibility of only ± 5 mK [8], but Bedford and Ma demonstrated that the main source of the large spread could have been calibration uncertainties in $W_{100\ °C}$, and that, after reasonable changes of the values of $W_{100\ °C}$, fifteen thermometers gave the same temperature scale to within the experimental uncertainty of the intercomparison (i.e. ± 1 mK). Only two thermometers deviated +1.5 mK from this scale between 220 K and 280 K.

6.2 *The range from 54.361 K to 90.188 K*

From figs. 4.5 to 4.8 it appears that the variations between thermometers are less than ± 0.8 mK for all thermometers except A2. When A2 is included, these are ± 1.0 mK.

Preston-Thomas and Bedford [4] and Bedford and Ma [8] reported in this range variations of about ± 3 mK for forty-eight thermometers; this improved to ± 2 mK if three non-typical thermometers were excluded. According to figs. 10 and 12 of ref. 4 even an estimate of ± 1 mK seems to be justified (for the forty-five thermometers).

For two of the three thermometers excluded by Preston-Thomas and Bedford (Tinsley 164998, VD 127 and PRMI T2) the values of the constant C in the Callendar-Van Dusen equation, used in IPTS-48 between -182.97 °C and 0 °C, lies outside the range recommended in IPTS-48. (The recommended range was $(-4.35 \pm 0.05) \times 10^{-12} K^{-4}$, and the C-values for the two excluded thermometers are $-4.404 \times 10^{-12} K^{-4}$ and $-4.241 \times 10^{-12} K^{-4}$.) There was no valid reason for excluding T2, the only Russian thermometer in the test group.

For the present thermometers, the Callendar-Van Dusen constants C could not accurately be determined, because no experimental values for the constants B were available. When it is assumed, that the values of B lie within the limits recommended in IPTS-48, $(-5.857 \pm 0.010) \times 10^{-7} K^{-2}$, then the C-values of T4, the KOL thermometers (145, 153, 143) and Tinsley 188677 are slightly below the lower limit of the IPTS-48 criterion; these are $(-4.296, -4.290, -4.288, -4.287$ and $-4.284 \pm 0.009) \times 10^{-12} K^{-4}$ respectively. For the Tinsley thermometers 213866, 213860 and B2 and for A2, the values of C on IPTS-48 are $(-4.301, -4.304, -4.302$ and $-4.343 \pm 0.009) \times 10^{-12} K^{-4}$ respectively.

Muijlwijk, Durieux and Van Dijk [10] reported variations within ± 0.4 mK for eight thermometers. Four of these are included in the present experiments, Nos. 2, 4, 5 and 7 in table 4.1. For this group, Muijlwijk et al. found a maximum spread of 0.2 mK, contrary to the present results which show a maximum spread of 1.0 mK. The explanation for this is probably, that Muijlwijk et al. used values of $(d\Delta W/dT)_{90.188\ K}$ which had been derived from the experimental values of ΔW in the range from 54 K to 90 K (see

tables I and II of ref. 10) instead of from the deviation function for the range above 90.188 K.

Sharevskaya et al. [11] reported a reproducibility of IPTS-68 of ± 1 mK for fifteen PRMI thermometers. This result was found after smoothing the experimental data, which involved corrections up to ± 1 mK, and by using values of $(d\Delta W/dT)_{90.188\ K}$ calculated from functions through experimental data in the 90-273 K range. These facts prohibit a full comparison with the present results.

The tentative conclusion may be that, in the range from 54.361 K to 90.188 K, IPTS-68 is reproducible for different thermometers within ± 1 mK.

6.3 *The range from 20.28 K to 54.361 K*

The reproducibility of IPTS-68, according to the first seven thermometers in table 4.1, is ± 0.7 mK in the full range, and even ± 0.3 mK between 20.28 K and 27.102 K. The maximum deviation for 188677 from the mean for Nos. 1 to 7 is 2.0 mK, which is even larger than the maximum deviation for A2 (1.7 mK).

The results are in accordance with observations of Bedford and Ma [8] yielding a reproducibility of IPTS-68 of ± 1 mK for forty-six thermometers out of a group of forty-eight. Of the two other thermometers, one had an error in its calibration, while the other one was the earlier mentioned Tinsley 164998.

A reproducibility of ± 1 mK was also reported by Sharevskaya et al. [11] for fifteen PRMI thermometers.

6.4 *The range from 13.81 K to 20.28 K*

In the lower part of this range, the smaller sensitivity of the platinum thermometer begins to limit the attainable accuracy. In the present experiments, the uncertainty in the intercomparisons was about 0.2 mK near 13.81 K; this improved to about 0.1 mK towards 17 K and higher temperatures.

The reproducibility of IPTS-68 according to the first seven thermometers in table 4.1 appears to be ± 0.6 mK (see figs. 4.5 and 4.6); the results for 188677 differ from the mean of Nos. 1 to 7 by at maximum 1.2 mK, and for A2 by 1.9 mK (see figs. 4.7 and 4.8 respectively).

The present results are noticeably different from those reported by Bedford and Ma [8]; these authors found a reproducibility of IPTS-68, for forty-eight thermometers, of not better than ± 3 mK in this range. However, Preston-Thomas and Bedford [4], who used the same data in an earlier analysis, noticed that there was a considerable randomness in the distribution of the points and remarked, that calibration uncertainties were beginning to limit the accuracy of the intercomparisons.

According to Sharevskaya et al. [11], the reproducibility of IPTS-68, as measured with fifteen thermometers, is about ± 1 mK.

The evidence therefore is not conclusive and accurate intercomparisons of more thermometers are necessary to draw a definite conclusion, but it seems to be not unjustified to expect IPTS-68 to be reproducible to better than ± 2 mK, maybe even to within ± 1 mK, in the range from 13.81 K to 20.28 K.

6.5 *Selection criteria for platinum thermometers to be used in IPTS-68*

It is unlikely that the different behaviour of thermometer 188677 ($\alpha = 0.00392478\ K^{-1}$) with respect to the seven thermometers with $\alpha > 0.003926\ K^{-1}$ can be explained by its lower α value alone. Rejection of this thermometer for reason of the α coefficient being below the IPTS-68 criterion ($\alpha \geq 0.0039250\ K^{-1}$) does not seem to be reasonable.

However, it appears from fig. 4.4, and it is shown in more detail in Chapter 5, that thermometer 188677 exhibits unusually large deviations from Matthiessen's rule below 15 K, the deviations being even larger than for thermometer A2 (with $\alpha = 0.00392097\ K^{-1}$). This suggests that the magnitudes of these deviations could constitute a useful selection criterion for platinum thermometers. It would be possible to put this into a more quantitative form, e.g., it could be required that

$$W_{13.81\ K} - W_{0\ K} < 930 \times 10^{-6}$$

or, alternatively,

$$W_{20.28\ K} - W_{0\ K} < 4025 \times 10^{-6}\ .$$

Experiments with more thermometers would be necessary to check the usefulness of such a criterion.

6.6 *Applicability of Matthiessen's rule for the range from 90.188 K to 273.15 K*

Recently, Sharevskaya et al. [11] showed that, in the range from 90.188 K to 273.15 K, a group of fifteen PRMI thermometers yield the same temperatures within ± 1 mK, if an interpolation procedure based on Matthiessen's rule is used. The results with this procedure for the present thermometers will be given here.

When Matthiessen's rule holds, differences between reduced resistances of different thermometers at temperature T, $\Delta W(T)$, are related to the differences at a reference temperature (e.g. the normal boiling point of oxygen) by the equation

$$\Delta W(T) = \frac{1 - W(T)}{1 - W_{90.188\ K}} \Delta W_{90.188\ K} .$$

Results of calculations for the present thermometers are compared with experimental data in table 4.3. Matthiessen's rule appears to be valid

Table 4.3

Differences between reduced-resistance differences of platinum thermometers as determined experimentally and as calculated from Matthiessen's rule. Thermometer B2 (Tinsley 164956) has been taken as a reference, except for the last column where the reference function $W_{CCT-68}(T_{68})$ has been taken as a reference.

T/K	$10^6(\Delta W_{calc} - \Delta W_{exp})$								
	KOL 153	KOL 145	KOL 143	PRMI T4	Tinsley 213866	Tinsley 213860	Tinsley 188677	A2	B2
90.188	0	0	0	0	0	0	0	0	0
116	7.4	6.7	7.0	4.1	1.5	0.2	0.5	-20.4	23.7
143	12.0	11.2	10.9	5.4	2.4	1.2	1.4	-29.8	35.0
175	16.8	13.7	17.3	7.0	2.2	0.7	1.5	-31.9	35.9
225	3.8	2.7	2.5	1.2	2.7	1.6	1.4	-21.5	21.2
273.15	0	0	0	0	0	0	0	0	0

within 0.6 mK for the group of four Tinsley thermometers (among which the reference, B2) and within 1 mK for the group of three KOL thermometers (4×10^{-6} in W is equivalent to 1 mK). Deviations from Matthiessen's rule for thermometers of the two groups, however, are as large as the equivalent of 4.5 mK. For T4 intermediate values are found; A2 shows large differences with the other thermometers. These results show, that Matthiessen's rule is, in general, not suitable as basis for interpolation between 90 K and 273 K.

It should be noted, that a deviation function based on Matthiessen's rule differs systematically from the current deviation function for the range from 90.188 K to 273.15 K. For thermometer B2 the maximum difference is 9 mK (see last column of table 4.3).

7 Discontinuities in higher derivatives of IPTS-68 below 0 °C

The calibration procedure in IPTS-68 leads to discontinuities in the second and higher derivatives of $\Delta W(T_{68})$, and consequently of $W(T_{68})$, at the junctions of the temperature ranges in which different deviation functions are defined.

The magnitudes of discontinuities in $d^2W(T_{68})/dT_{68}^2$ for a group of about 40 thermometers were discussed by Bedford [12]. In a recent report [13], the question was raised whether IPTS-68 should be changed in the future in such a way as to remove the discontinuities, which could affect the slope of experimental heat capacity or thermopower vs. temperature curves.

In table 4.4 a summary is given of 'jumps' in $d^2W(T_{68})/dT_{68}^2$ for the first seven thermometers in table 4.1. It can be seen that the magnitudes of the discontinuities are very similar for the various thermometers.

The magnitudes of the discontinuities in $d^2W(T_{68})/dT_{68}^2$, reported by Bedford for about forty thermometers, are in the same direction, but are about a factor of two smaller than those found in the present work. The reason of the differences between Bedford's and the present results is not clear; a possible error in the realization of the steampoint of 3 mK (see section 2) would explain only 30% of the difference.

When the earlier mentioned changes in W_{CCT-68} would be applied (increase of W_{CCT-68} at 90.188 K with 29×10^{-6} and at 100 °C with 37×10^{-6}),

Table 4.4

Discontinuities in $d^2W(T_{68})/dT_{68}^2$ for the first seven thermometers in table 4.1.[a]

T_{68} K	$d^2W_{CCT-68}(T_{68})/dT_{68}^2$ K^{-2}	$10^8\delta$ K^{-2}	%	$10^8\delta_{90}$ K^{-2}	$10^8\delta_{373}$ K^{-2}	$10^8\delta_{corr}$ K^{-2}
90.188	-1.07×10^{-6}	-15.9 ± 1.6	14.9 ± 1.5	8.6	7.5	0.2
54.361	40.8×10^{-6}	56 ± 5	1.4 ± 0.1	-36.8	-18.5	1
20.28	100.5×10^{-6}	128 ± 47	1.3 ± 0.5	-72	-31	25

[a] δ gives the average discontinuous increase in $d^2W(T_{68})/dT_{68}^2$ when going from higher to lower temperatures, and the maximum variation for the seven thermometers.

% gives the percentage discontinuity in $d^2W(T_{68})/dT_{68}^2$.

δ_{90} gives the effect upon δ of an increase of W_{CCT-68}(90.188 K) with 29×10^{-6}.

δ_{373} gives the effect upon δ of an increase of W_{CCT-68}(100 °C) with 37×10^{-6}.

δ_{corr} gives the sum of δ, δ_{90} and δ_{373}.

the discontinuities, according to the present work, would almost vanish (δ_{corr} in table 4.4). For Bedford's group of thermometers, changes of W_{CCT-68} which are about a factor two smaller than indicated above would be sufficient to reduce the average discontinuity in $d^2W(T_{68})/dT_{68}^2$ at 90.188 K to zero.

It may be expected that in the next years data for many more thermometers, calibrated on IPTS-68, will become available.

8 Extrapolation of IPTS-68 below 13.81 K

The data of the intercomparisons of the thermometers below 13.81 K (see tables 5.4 and 5.5 in Chapter 5) was used to investigate the accuracy of temperatures obtained by extrapolation of IPTS-68 below 13.81 K. The procedure was to use the CCT-68 reference function and the deviation function for the range from 13.81 K to 20.28 K also at temperatures below 13.81 K.

The differences between the extrapolated IPTS-68 temperatures for the various thermometers are shown in fig. 4.9. Base line is the mean extrapolated IPTS-68 temperature ($\overline{T}$) of the thermometers Nos. 1 to 8.

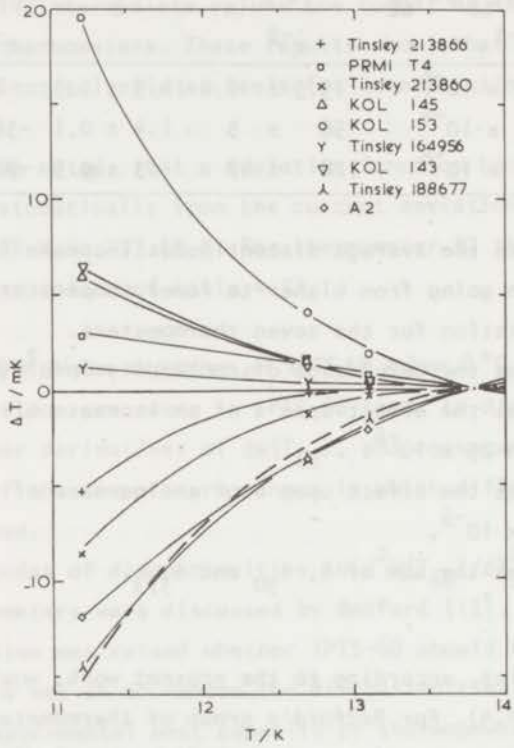

Fig. 4.9. Differences between extrapolations of the IPTS-68 below 13.81 K for various thermometers. The baseline is the mean of the extrapolated IPTS-68 for thermometers nos. 1 to 8. The dotted line gives the "thermodynamic extrapolation" of IPTS-68.

At 13 K the spread of the extrapolated IPTS-68 temperatures for the various thermometers is 4 mK and at 12 K about 16 mK. These values are slightly dependent upon the accuracy of the calibrations at the fixed points of IPTS-68. For example, a change in the calibration of a thermometer at 17.042 K or at 27.102 K with the equivalent of 0.1 mK, causes a change in the extrapolated IPTS-68 temperature of 0.3 mK at 13 K and of 1 mK

at 12 K. The effects of changes of 0.1 mK at the other fixed points are smaller. In view of the precision of the calibration-by-intercomparison, the maximum possible errors in the differences between the extrapolated T_{68} values, due to calibration errors, is estimated to be ± 1 mK at 13 K and ± 3 mK at 12 K.

Apart from the differences between the thermometers, it is interesting to know the deviations of the extrapolated IPTS-68 temperatures from the thermodynamic temperature. A temperature scale, which was a good approximation of the thermodynamic temperature, was accessible in the present experiments through five germanium thermometers calibrated on a magnetic temperature scale established by Van Rijn and Durieux (see ref. 14 and Chapter 5; the magnetic temperature used here is the temperature $\overline{T}_m(III)$ of ref. 14). The dashed line in fig. 4.9 represents the deviation of the magnetic temperature T_m from the average extrapolated IPTS-68 temperature $\overline{T}$.

The conclusion drawn from this experiment is, that temperatures below 13.81 K can be determined by extrapolation of the IPTS-68 calibration of a platinum thermometer with an accuracy which is about 5 mK or better at 13 K and about 15 mK or better at 12 K.

References

1. International Practical Temperature Scale of 1968, Metrologia 5, 35 (1969).
2. R.J. Berry, Can. J. Phys. 41, 946 (1963).
3. R. Muijlwijk and M. Durieux (private communication to H. Preston-Thomas, Febr. 1968).
4. H. Preston-Thomas and R.E. Bedford, Metrologia 4, 14 (1968).
5. M.R.M. Moussa, H. van Dijk and M. Durieux, Physica 40, 33 (1968); Commun. Kamerlingh Onnes Lab., Leiden, No. 367b.
6. M.P. Orlova, L.B. Belyanski, D.N. Astrov and D.I. Sharevskaya, Doc. No. 19, presented to working group II of the Comité Consultatif de Thermométrie (1966).
7. L.B. Belyanski, M.P. Orlova, D.N. Astrov and D.I. Sharevskaya, Doc. No. 16, presented to working group II of the Comité Consultatif de Thermométrie (1966).

8. R.E. Bedford and C.K. Ma, Metrologia 6, 89 (1970).
9. L.B. Belyanski, M.P. Orlova, D.I. Sharevskaya and D.N. Astrov, Metrologia 5, 107 (1969).
10. R. Muijlwijk, M. Durieux and H. van Dijk, Physica 43, 615 (1969); Commun. Kamerlingh Onnes Lab., Leiden, No. 373c.
11. D.I. Sharevskaya, M.P. Orlova, L.B. Belyanski, V.V. Getmanskaya and G.A. Galoushkina, Comité Consultatif de Thermométrie de la C.I.P.M., 9^{e} session, Sèvres, France, 1971; doc. CCT/71-57.
12. R.E. Bedford, Temperature, It's Measurement and Control in Science and Industry (Instrument Society of America, Pittburgh, 1972), Vol. 4.
13. Report of Working Group I of the Comité Consultatif de Thermométrie, January 1973.
14. C. van Rijn and M. Durieux, Temperature, It's Measurement and Control in Science and Industry (Instrument Society of America, Pittsburgh, 1972), Vol. 4.

CHAPTER 5

PLATINUM THERMOMETRY BELOW 13.81 K

1 Introduction

The platinum resistance thermometer is used to measure temperatures on the International Practical Temperature Scale of 1968 (IPTS-68) [1] in the range between 13.81 K and 903.89 K. Below 13.81 K, the platinum thermometer becomes less suitable for high-precision thermometry, that is, for measuring temperatures with a precision of the order of 0.1 mK, due to the rapid decrease of the sensitivity of the thermometer towards liquid-helium temperatures. However, for many applications for which a lower precision is sufficient, the extension of the use of platinum thermometers to temperatures below 13.81 K seems advantageous.

Only very few data on platinum thermometry below 14 K is available. This is probably partly caused by the lack of readily accessible temperature scales between 5 K and 13.81 K. A review of the available data is given in section 2.

In the present experiments, the resistances of ten platinum thermometers were determined between 2.1 K and 15.3 K. Temperatures were measured on a magnetic scale (see section 3). The experiments are described in section 4, results are given in section 5.

In section 6, it is investigated which accuracies in the range between 4.2 K and 13.81 K can be obtained with platinum thermometers which are calibrated at very few or none points in this range and at a few points outside this range.

In section 7, the retention of the low-temperature calibration of a platinum thermometer is discussed.

Finally, in section 8, the results of the present experiments are discussed in their relation to Matthiessen's rule; for different thermometers remarkably different deviations from this rule are found.

2 Review of earlier work on platinum thermometry below 14 K

In 1964, Van Dijk [2] reported upon measurements on twenty-seven platinum thermometers, made of platinum wire of different origin and purity, between 1.5 K and 4.2 K and between 9 K and 20.3 K. The data obtained between 1.5 K and 4.2 K could be represented within the experimental accuracy (which was estimated to be 1×10^{-7} in W(T)) with the formula

$$W(T) = W_0 + AT^2 + BT^5 \qquad (5.1)$$

in which W(T) is the reduced resistance $R(T)/R_{0\,°C}$. From the shapes of the W vs. T curves and, in particular, from the shapes of the ΔW vs. T curves (ΔW being the difference between W of different thermometers) it was concluded that, if between 4 K and 14 K a high interpolation accuracy is required, calibration at more than a few temperatures in this range is necessary.

It was shown by Berry [3] for six thermometers out of the group measured by Van Dijk, that the data below 4.2 K can often better be represented by the relation

$$W(T) = W_0 + AT^2 + BT^\gamma \qquad (5.2)$$

with values of γ other than 5.0. The estimated values of γ vary from 4.2 to 5.6 for five thermometers; for one thermometer the value of γ seems to be larger than 8.

Further, Berry [3,4] and Kos and Lamarche [5] reported upon two calibrated platinum thermometers. One of these (thermometer 320) had been calibrated by Martin and Berry with an accuracy better than 5 mK on a gas-thermometer scale between 4.2 K and 20 K. The other one (Pt 1) had been calibrated by De Haas and De Boer [6] in 1933; because of the large scatter of these data (maximum scatter ± 0.03 K) they were smoothed graphically by Berry [3]. Kos and Lamarche [5] and Berry [4] fitted polynomials of the form

$$W(T) = \sum_{n=0}^{k} A_n T^n \qquad (5.3)$$

to the data of the thermometers 320 and Pt 1. When calibration points covering the range from 2.0 K to 15.3 K were used, eq. (5.3) with k = 5 fitted the data for 320 within 3 mK and for Pt 1 within 10 mK. These deviations could be fully accounted for by uncertainties in the calibrations and, therefore, it was concluded that eq. (5.3) with k = 5 adequately represented the resistance functions. No lower-degree polynomial sufficed, a higher-degree polynomial did not improve the fit.

Kos and Lamarche and Berry further investigated the influence of the omission of all calibration data between 4.2 K and 10 K on the interpolation accuracy in this range. It appeared to be possible to interpolate with eq. (5.3) in the 4 K to 10 K range with an accuracy of 4 mK for thermometer 320 and of 13 mK for Pt 1, if two conditions were fulfilled. The first one was a weighting of the calibration data below 4.2 K by a factor of 25, the second one of the omission of calibration points below 2 K and above 15 K.

Muijlwijk [7] used eq. (5.2) to fit calibration data of eight platinum thermometers between 2 K and 5 K (on the 1958 - ^{4}He scale) and at 10.5 K and 11.7 K (on an extrapolated CCT-64 scale). The accuracy of the fits was about 10 mK above 4 K, which did not exceed the experimental error. At approximately 8.75 K, comparisons had been made between the platinum thermometers; with these data, temperatures were calculated from the interpolation formulae. The maximum deviation from the average calculated temperature was 9 mK. For the exponent γ in eq. (5.2), Muijlwijk found values between 4.52 and 4.75.

3 Temperature scale

For the temperature range between 5.2 K and 13.81 K no internationally adopted temperature scale exists. Several national temperature scales covering this range are in use or are being developed. The first of these, the NBS 2-20 K Acoustic Scale, was based on measurements of the velocity of sound in gases [8] (see also ref. 9). Other scales are based on the gas thermometer [10,11,12]. A third class is formed by the scales defined through magnetic thermometry. Magnetic scales for the range from 2 K to 30 K were recently developed by Swenson and Cetas [13] and, in this laboratory, by Van Rijn and Durieux [14]. Temperatures measured in the present experiments are based on a scale of these last authors; a short description

of this scale is given here.

In a magnetic thermometer the susceptibility of a paramagnetic salt is used as the thermometric parameter. Van Rijn and Durieux used gadolinium sulphate octahydrate and manganese ammonium sulphate hexahydrate, both as a powder of small crystals. The data for gadolinium sulphate could be described by the equation

$$n = A + \frac{B}{T_m + \gamma/T_m} \qquad (5.4)$$

where n is the number of turns of the Hartshorn bridge, used for the mutual-inductance measurements, and T_m is the magnetic temperature. The constants A, B and γ were determined by fitting T_m to IPTS-68 at 20.28 K and to the T_{58} - ^{4}He scale between 1.7 K and 4.2 K. This could be done by means of two germanium thermometers which had been calibrated at these temperatures, and which were also used in the magnetic-thermometer experiments. The thus defined magnetic temperature was denoted $^{Gd}T_m(I)$ in ref. 14; it will be denoted T_m or, when there is no ambiguity, T.

The two germanium thermometers, which had served to determine the constants in eq. (5.4), were calibrated in terms of T_m between 2 K and 30 K. Later, their calibration was transferred to other germanium thermometers. Four of these and one of the first set were incorporated in the present experiments. The calibration of the germanium thermometers is represented by polynomials of the form

$$\ln R = \sum_{n=0}^{k} A_n (\ln T)^n \qquad (5.5)$$

fitted to the calibration data. These polynomials are estimated to represent T_m within a few tenths of a millikelvin.

It should be noted that T_m, which is fitted to T_{58} and is equal to T_{68} at 20.28 K, differs from T_{68} at other temperatures: at 13.81 K the value of T_m is about 7 mK lower than that of T_{68}. This is caused by the fact that T_{58} and T_{68} are internally inconsistent. It was shown by the magnetic temperature measurements [13,14] and also by acoustic [8] and gas [10,12] thermometry that T_{58} deviates from the thermodynamic temperature, the deviation being linear in T and such that the normal boiling

point of ^{4}He in T_{58} should be raised by 8 mK. However, for the present experiments it suffices that T_m is a smooth temperature scale which differs probably not more than 15 mK from the thermodynamic temperature (see ref. 14), the differences being smooth in temperature. T_m is sufficiently well defined [14] that calibrations on this scale can be recalculated to other scales when necessary.

4 Experimental method

The apparatus has been described in Chapter 4 and the procedure of the measurements was similar to that outlined there. The temperature drift of the block during measurements was usually less than 3 mK per hour. Liquid helium was used a coolant throughout.

The measurements were made with ten platinum thermometers; nine of these are given in table 4.1, the tenth is the KOL thermometer 154, with $\alpha = 0.00392635\ K^{-1}$. The reduced resistances W(T) of these thermometers were determined at fourteen temperatures between 2.1 K and 15.3 K (in most cases twice at one temperature, with an interval of about an hour, which provides a check on the precision of the measurements).

Currents through the platinum thermometers were such that a maximum sensitivity was attained in conjunction with a tolerable temperature drift of the copper block, due to the joule heat of the thermometers, and an almost negligible self-heating of the thermometers (according to ref. 4, the self-heating in the range from 4 K to 16 K is expected to be smaller than 0.3 mK/μW; in the present experiments, a self-heating of 0.4 mK/μW at 13.81 K was found for the thermometers 164956 and T4).

The currents used are given in table 5.1, together with some thermometer characteristics below 16 K. The sensitivity of the platinum-thermometer resistance measurements, expressed in mK, for the voltage sensitivity of 5 nV of the d.c. amplifier, is shown in table 5.1. The precision of the temperature determination with the five calibrated germanium thermometers was 0.1 to 0.2 mK.

5 Experimental results

5.1 *Representation of data*

Polynomials of the form given by eq. (5.3) were fitted to the W-T

Table 5.1

Characteristics of platinum thermometers below 16 K.[a]

T	R	10^6 W	$\frac{dR}{dT}$	$\frac{1}{R}\frac{dR}{dT}$	i	$\frac{dV}{dT}$	$\frac{dT}{dV}$
K	Ω		μΩ/mK	K^{-1}	mA	nV/mK	mK/5nV
2	0.009[b]	360	0.13	0.01	10	1.3	4
4	0.009_5	380	0.33	0.03	10	3.3	1.5
6	0.011	430	0.67	0.06	9	6.0	0.8
8	0.013	510	1.3	0.08_5	8	10.4	0.5
10	0.016	650	2.3	0.12	7	16	0.3
12	0.023	900	4.0	0.16	6	24	0.2
14	0.034	1350	6.4	0.18_5	5	32	0.2
16	0.050	2000	9.6	0.19	5	48	0.1

[a] The ice-point resistance of the platinum thermometers is assumed to be 25 ohm. Values in columns 7 and 8 have been calculated for values of the measuring current given in column 6. V is the voltage across the thermometer.

[b] Values of R and W are only given as examples. The residual resistance can be much larger, that is by a factor of two or more.

data of the platinum thermometers between 2.1 K and 15.3 K. Calculations were performed with double precision (16 figures), using a modified and in ALGOL translated version of a CDC 3600 Fortran program from D.W. Osborne of the Argonne National Laboratory, Argonne, Ill., U.S.A.. In this program, based on a method described by Forsythe [15], a set of orthogonal polynomials $P_i(T)$ was generated, which satisfied the relations $\sum_{j,k} g P_j P_k = \delta_{jk}$ (the summation is taken over the measured points and g is a weight factor). The coefficients in the expansion $W(T) = \sum_i B_i P_i(T)$ were determined from minimizing the sum S of the weighted squares of the differences ΔW between calculated and experimental values of W. The weight factor varied from 4 at 2.1 K to 1 at 15.3 K, in accordance with the variation of the experimental accuracy in W. The final result was expressed as a polynomial in T (eq. (5.3)).

The sum S, the variance σ^2 (i.e. the sum of squares of ΔW divided by the difference between the number of the calibration points and the number of terms in eq. (5.3)) and the deviations of the data points from the fit, expressed as temperature differences ΔT, were calculated for polynomials

of different degree.

As best representation of the data, the lowest-degree fit was chosen for which the differences ΔT were not systematic and not larger than the experimental precision. In practice, the values of S or σ were a useful criterion, since these become virtually constant for fits of the desired and of higher degree.

5.2 *Discussion of the results*

Fits of eq. (5.3) with k = 5 and k = 6 to the experimental data of thermometer 164956 are given in fig. 5.1. These are representative for the eight thermometers with $\alpha > 0.003926\ K^{-1}$ (see section 4). Fits for the remaining two thermometers are shown in figs. 5.2 and 5.3. The deviations of the 6th-degree polynomials from the experimental data are comparable to the spread in these data, which is usually not larger than the equivalent of 5 nV in the voltage measurements (see table 5.1). With higher-degree fits no better agreement is found.

The convergence of the fits with increasing value of k is illustrated for one thermometer in table 5.2; the standard deviations of the fits with k = 6 for all thermometers are given in table 5.3. (A sensitivity of 5 nV

Table 5.2

Typical example of the standard deviations in W for fits of eq. (5.3) to W-T data between 2.1 K and 15.3 K

k	σ
2	5.5×10^{-5}
3	8.0×10^{-6}
4	2.7×10^{-7}
5	1.6×10^{-7}
6	5.2×10^{-8}
7	5.3×10^{-8}
8	4.7×10^{-8}
9	4.3×10^{-8}

Table 5.3

The standard deviations in W for fits of eq.(5.3) with k = 6 to W-T data between 2.1 K and 15.3 K of the platinum thermometers

thermometer	σ
T4	4.4×10^{-8}
213866	6.0×10^{-8}
213860	4.0×10^{-8}
154	9.6×10^{-8}
164956	4.8×10^{-8}
153	5.2×10^{-8}
145	5.3×10^{-8}
143	4.7×10^{-8}
188677	6.1×10^{-8}
A2	6.6×10^{-8}

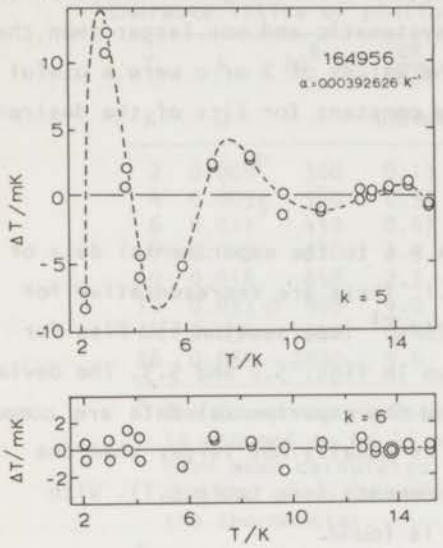

Fig. 5.1.
Fits of polynomials $W(T) = \sum_{n=0}^{k} A_n T^n$ with k = 5 and k = 6 to the experimental W-T data between 2 K and 15 K for thermometer 164956. $\Delta T = T_{polynomial} - T_{exp}$. The curves for k = 5 in this figure and in figs. 5.2 and 5.3 are hand-drawn through the points.

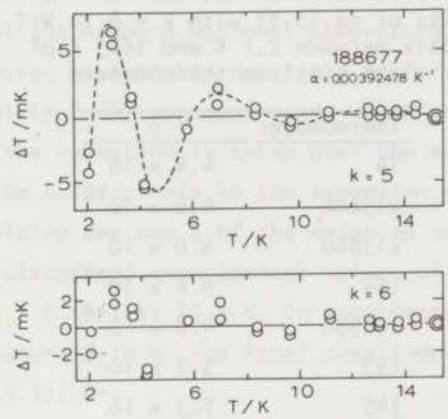

Fig. 5.2.
This figure is the equivalent of fig. 5.1 for thermometer 188677.

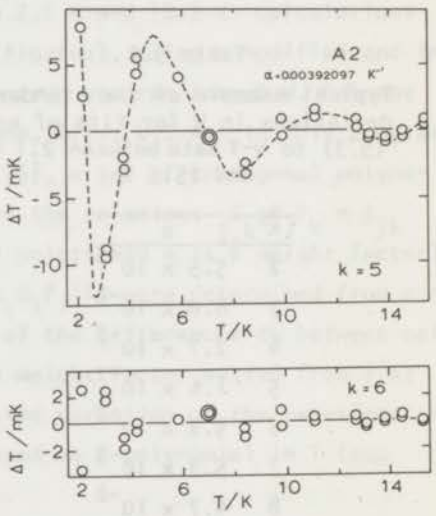

Fig. 5.3.
This figure is the equivalent of fig. 5.1 for thermometer A2.

in the voltage measurements corresponds to 2×10^{-8} in W at liquid-helium temperatures and to 5×10^{-8} in W at liquid-hydrogen temperatures.)

The deviations of the 6th-degree polynomial fits from the averaged experimental data at each temperature are (expressed as temperature differences) given in table 5.4 for all thermometers. Only 5 out of the 140

Table 5.4

Deviations of fits with $W(T) = \sum_{n=0}^{6} A_n T^n$ from the averaged experimental data. $\Delta T = T_{calc} - T_{exp}$.

	T4	213866	213860	154	164956	153	145	143	188677	A2
T K	ΔT mK	ΔT mK	ΔT mK	ΔT mK	ΔT mK	ΔT mK	ΔT mK	ΔT mK	ΔT mK	ΔT mK
2.1	-0.9	-0.1	-0.5	-0.2	-0.2	-0.2	-0.4	-0.7	-1.1	-0.5
3.0	2.1	0.0	1.4	1.2	-0.1	0.6	0.8	2.2	2.3	2.0
3.7	-0.4	0.5	-0.6	-2.2	0.7	-0.4	0.5	-1.7	1.0	-1.7
4.2	-1.4	0.2	-0.7	1.0	-0.1	-0.1	-0.5	0.3	-3.4	-0.4
5.7	-0.3	-1.4	-0.1	0.8	-1.3	0.1	-1.1	-0.7	0.4	0.3
7.0	1.1	0.9	0.9	-1.0	0.9	0.1	1.3	1.0	1.1	0.7
8.4	-0.2	0.4	-0.6	0.3	0.5	0.1	-0.1	-0.1	-0.4	-0.9
9.8	-0.5	-0.6	0.0	0.3	-0.8	-0.4	-0.5	-0.7	-0.6	0.3
11.2	0.2	0.0	0.1	-0.3	0.2	0.3	0.1	0.4	0.5	0.1
12.7	0.3	0.4	0.0	0.4	0.4	-0.1	0.3	0.1	0.0	0.2
13.1	-0.1	0.0	0.0	0.1	-0.2	0.0	-0.2	-0.2	0.0	-0.3
13.8	-0.2	-0.4	-0.1	-0.9	-0.2	-0.3	-0.3	-0.2	-0.2	-0.1
14.5	-0.1	0.1	0.1	0.6	0.1	0.3	0.1	0.1	0.1	0.3
15.3	0.1	0.1	0.0	-0.2	0.1	-0.1	0.0	0.0	0.0	-0.1

figures slightly exceed values corresponding to 10 nV; the majority of the figures is considerably smaller.

It may be concluded that eq. (5.3) with k = 6 represents the experimentally determined values of the reduced resistances of the group of ten platinum thermometers within the precision of the measurements, i.e. within about 2 mK at 4 K, 1 mK at 6 K, 0.5 mK at 8 K and 0.3 mK above 11 K. The polynomials are supposed to represent the W-T relations better than the experimental points due to the smoothing of the data. The coefficients of the fits are given in table 5.5.

The coefficient A_0 (see table 5.5) appears to be within a few times

Table 5.5

Values of the coefficients of fits with $W(T) = \sum_{n=0}^{6} A_n T^n$ to experimental W-T data of platinum thermometers between 2.1 K and 15.3 K. The units have been omitted (T is expressed in kelvin).

thermometer	$10^6 A_0$	$10^7 A_1$	$10^8 A_2$	$10^9 A_3$	$10^{10} A_4$	$10^{11} A_5$	$10^{12} A_6$
T4	357.467	21.873	31.764	319.542	-395.5940	392.2900	-81.3864
213866	364.287	14.269	59.435	272.520	-351.5148	369.3868	-76.7621
213860	384.575	- 1.178	127.211	141.350	-215.7752	302.9256	-64.2624
154	479.544	23.507	27.877	274.037	-300.2348	333.0470	-69.7289
164956	497.233	10.945	79.533	195.930	-228.8439	298.2787	-62.9429
153	498.999	17.013	58.503	192.081	-206.4745	283.8041	-59.8192
145	526.902	14.528	70.516	165.515	-167.8078	258.6805	-54.3204
143	586.524	13.991	79.021	126.695	-115.6218	232.5081	-49.8103
188677	717.798	-24.291	259.332	-164.474	202.4199	77.0798	-22.5933
A2	1322.942	-32.890	370.193	-682.073	927.5071	-333.0725	60.1831

10^{-6} equal to the value of the reduced resistance at T = 0 K, found by extrapolation of the experimental data between 2 K and 6 K (see table 5.6). Further, the coefficients A_1 to A_6 change, in general, in a regular way if A_0 increases. This type of regularity in polynomial fits to comparable data is not unusual: it has been found also for the polynomials which describe the temperature dependence of the resistance of germanium thermometers.

It may be noted that the experimental W-T data are not given, but the fitted polynomials and the deviations of the experimental data from these polynomials. This originated with the way in which the experimental data was taken and analyzed. The experimental data can, of course, easily be recovered from tables 5.4 and 5.5.

5.3 *The 2-20 K temperature range*

Fits of eq. (5.3) were also made to data in the range from 2 K to 20 K. As input for the range above 16 K, data given in table 4.2, Chapter 4, recalculated from IPTS-68 to T_m, was used. Polynomials of the 7th degree were invariably selected as best fits. At temperatures below 15 K, the fits were as good as the 6th-degree fits to the data in the 2-15 K range given in section 5.2, except for the point near 15 K where the calculated temperatures were about 0.8 mK higher than the experimental temperatures for all thermometers. This might have to do with the characteristics of the

W-T function of the thermometers ((1/W)dW/dT reaches a maximum value near 15 K). Above 16 K, the accuracy of the fits was about the equivalent of 0.15 mK, which was equal to the experimental precision.

5.4 *Validity of the formula* $W = W_0 + AT^2 + BT^5$

5.4.1 The range from 2 K to 6 K

Eq. (5.1), earlier used by Van Dijk [2] for temperatures between 1.5 K and 4.2 K (see section 2), has been least-squares fitted to the unweighted experimental W-T data between 2.1 K and 5.7 K of the ten platinum thermometers. Results are given in table 5.6.

Table 5.6

Coefficients and standard deviations for fits of the formula $W(T) = W_0 + AT^2 + BT^5$ to the unweighted experimental W-T data of the ten platinum thermometers between 2.1 K and 5.7 K.

thermometer	$10^6 W_0$	$10^6 A$ (K^{-2})	$10^9 B$ (K^{-5})	$10^8 \sigma$	$10^6 (A_0 - W_0)$
T4	358.88	1.554	1.519	3.0	-1.41
213866	364.92	1.559	1.507	4.4	-0.63
213860	383.85	1.585	1.547	5.2	+0.72
154	481.25	1.466	1.579	3.5	-1.71
164956	497.69	1.527	1.641	3.5	-0.46
153	500.25	1.433	1.612	1.8	-1.25
145	527.92	1.445	1.639	1.4	-1.02
143	587.63	1.425	1.625	2.6	-1.11
188677	715.30	1.726	1.921	3.8	-0.59
A2	1321.44	1.421	1.745	7.0	+1.50

The accuracy of the data below 6 K is estimated to be about 5×10^{-8} in W. The standard deviations of the fits show that eq. (5.1) can represent the present data below 6 K within the experimental accuracy.

The last column in table 5.6 gives the differences between W_0 (in eq. (5.1)) and A_0 (in eq. (5.3), see table 5.5).

5.4.2 The range between 2 K and 10 K

Eq. (5.1) has also been fitted to the data between 2.1 K and 9.8 K.

The standard deviations found in this case are on the average 15 times larger than those in table 5.6 and significantly larger than the experimental accuracy. The fitted equations differ systematically from the experimental data. As typical example, the differences between the experimental data and the fitted equation for thermometer 153 are given in fig. 5.4.

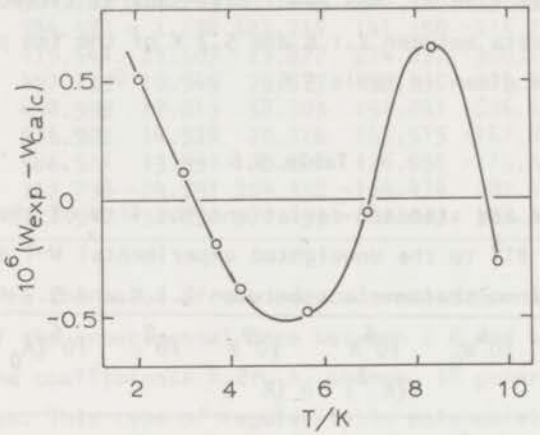

Fig. 5.4. Fit of the relation $W(T) = W_0 + AT^2 + BT^5$ to the experimental W-T data for thermometer 153 between 2 K and 10 K.

6 Reduction of the number of calibration points between 4 K and 14 K

6.1 *Introduction*

The method described in section 5.2 yields the accurate calibrations of the thermometers, but is rather elaborate. In particular, the acquisition of data points between 4 K and 14 K may sometimes be difficult (e.g., because of the lack of an accessible temperature scale). Therefore, it has been investigated which accuracies can be obtained with methods that require less calibration data between 4 K and 14 K. These methods are divided into two groups: 'individual' calibration procedures, in which a calibration is deduced from experimental W-T data for each individual thermometer, and procedures involving a reference function (such as e.g. in IPTS-68).

6.2 *Individual calibration procedures*

Polynomials $W = \sum_{n=0}^{k} A_n T^n$ were fitted to experimental W-T data for each thermometer at the four temperatures in the liquid-helium range and the three temperatures in the low liquid-hydrogen range (see table 5.4) and at a varying number of the experimental points between 4.2 K and 13.81 K. The differences between these polynomials and the 'full' calibrations of the thermometers (table 5.5) were investigated. It appeared that best results were obtained with fits with k = 6. Polynomials of higher degree showed markedly larger deviations from the full calibrations at temperatures between the calibration points.

In the following sub-sections, the differences between the 6th-degree polynomials, fitted to the limited number of points as described above, and the full calibrations are given; these are expressed as temperature differences $\Delta T = T - T_{\text{full calibration}}$.

6.2.1 Three calibration points between 4.2 K and 13.81 K

The differences ΔT are shown in fig. 5.5. It can be seen from the figure, that this method provides a calibration of the thermometers which differs very little from the full calibration. Because of the small number of points, the fitted polynomials represent closer the experimental data than the full calibration ; in fact, the fit is better than warranted by the precision of the data. Between the calibration temperatures, ΔT is, in general, not larger than twice the precision of the measurements. Apparently, there is overfitting at the experimental points, which means less smoothing of experimental errors compared to the full calibration.

If the calibration points are less evenly distributed over the interval between 4.2 K and 13.81 K, larger errors occur, e.g. with one calibration point at 5.7 K and two points above 11 K errors of at maximum 3 mK near 8 K occur.

6.2.2 One calibration point (at 7 K) between 4.2 K and 13.81 K

Except for one case, no interpolation errors (differences with the full calibration) larger than 5 mK occur. Only thermometer 154 showed a maximum error of 13 mK (at 10 K); this is probably due to incidental large errors in the calibration points in the liquid-hydrogen range (see

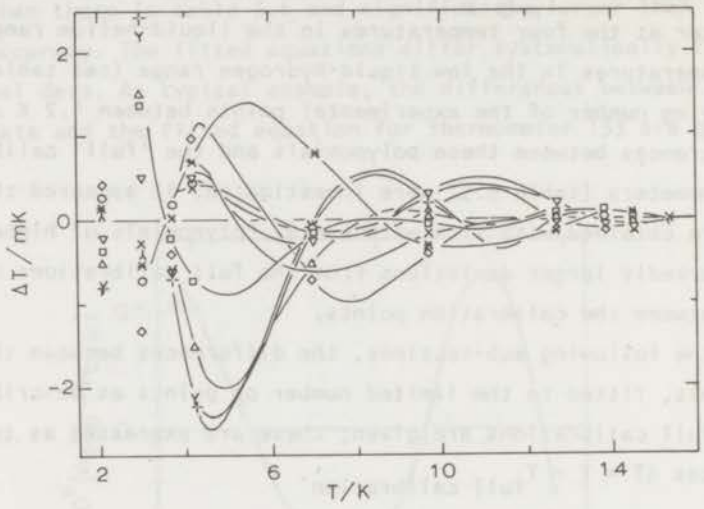

Fig. 5.5. Deviations of 6th degree polynomials fitted to data at a limited number of temperatures from the full (6th degree) calibration polynomials. Curves for different thermometers are marked with different symbols (see fig. 5.9) at the calibration temperatures.

table 5.4), caused by slight instability of this thermometer (which was also found at higher temperatures). This result illustrates the necessity for this method of accurate measurements at the hydrogen temperatures.

A very suitable fixed point for calibration would be the superconductive transition point of lead at a temperature of 7.201 K (on the NBS 2-20 K acoustic temperature scale). The experimental reproducibility of this point is 0.32 mK [16].

6.2.3 No calibration points between 4.2 K and 13.81 K

Interpolation errors are smaller than 0.03 K with a 6th-degree polynomial fitted to the four points at liquid-helium temperatures and the three points at liquid-hydrogen temperatures. With a 5th-degree fit errors up to 0.07 K arise.

6.3 *Calibration procedures involving a reference function*

This approach is similar to the definition of IPTS-68 between 13.81 K and 0 °C. The calibration is obtained by means of a deviation function ΔW of the type

$$\Delta W = \sum_{n=0}^{k} A_n T^n \qquad (5.6)$$

which gives the (small) differences between the reduced resistance W of a thermometer and a reference function. The constants in eq. (5.6) are determined from the values of W at k + 1 temperatures. The 6th-degree, full calibration, fit for KOL 153 (see table 5.5) is used as the reference function. The value of k is varied between 2 and 4.

For thermometers, of which the differences with the reference function deviate widely from Matthiessen's rule, such as for 188677 and A2 (see section 8), this method does not lead to satisfactory results: maximum interpolation errors are not smaller than 0.01 K in the cases considered, and therefore, these thermometers are excluded from the discussion.

6.3.1 One calibration point (at 7 K) between 4.2 K and 13.81 K

a) k = 4, two additional calibration points in the liquid-helium range and two in the low liquid-hydrogen range.

In this case, maximum errors of 2 mK occur near 10 K and 5.5 K, which are, respectively, six and two times as large as the present experimental precision. For suitable thermometers, this method is preferable above that in section 6.2.2; it requires less calibration points and is much more accurate.

b) k = 2, additional calibration points at 4.2 K and 13.81 K.

This method, requiring calibration only at three suitable fixed points, provides an accuracy of about 0.01 K.

6.3.2 No calibration points between 4.2 K and 13.81 K

For k = 4 and calibration at three temperatures in the liquid-helium range and at two temperatures in the low liquid-hydrogen range, an interpolation accuracy of about 0.01 K is found.

6.4 *Conclusions*

a) When an interpolation accuracy in the range between 4.2 K and 13.81 K is required, which is comparable to the experimental precision (i.e. 1.5 mK at 4 K, 0.5 mK at 8 K and 0.2 mK at 14 K), calibration at five or six temperatures in this range is necessary.

b) With two or three calibration points between 4.2 K and 13.81 K, the interpolation accuracy is a factor of two worse than under a).

c) With one data point (at 7 K) between 4.2 K and 13.81 K, an accuracy of 2 mK (at 10 K) can be attained for suitable thermometers by using a reference function.

d) If an accuracy of 0.01 K is sufficient, no calibration points between 4.2 K and 13.81 K are necessary (see section 6.3.2); in case of calibration at one temperature in this range (e.g. at 7 K), the total number of calibration points can be limited to three.

e) For the definition of an international practical temperature scale, a thermometer should be employed with which a temperature discrimination of the order of 0.1 mK is possible. This excludes the platinum thermometer as a candidate for temperatures below 12 K. For slightly less accurate work (1 to 2 mK) the platinum thermometer can very well be used down to, say, 5 K. The above analysis shows the necessary calibration. The calibration is probably less elaborate than would be required for germanium thermometers. Especially in those experiments where a platinum thermometer is used for temperatures above 13.81 K, it may be more convenient to use it, with a suitable calibration, also in the 5 K to 13.81 K range than to install a germanium thermometer.

7 Stability of the calibration

At not too low temperatures, say above 13.81 K, a platinum thermometer usually retains a once given calibration to 1 mK or better for prolonged periods. Since changes in the thermometer resistance are expected to follow to a first approximation Matthiessen's rule and the sensitivity of the thermometer decreases towards lower temperatures, the stability of a calibration such as given for the 2 K to 15 K range, may offer some problems.

The thermometers 164956 and T4 were used in all experiments described in this thesis. Repeated thermal cycling from room temperature to liquid-helium temperatures over a period of a year caused no detectable (> 2 x 10^{-8} in W) changes in the calibrations at liquid-helium temperatures. After careful mounting of the two thermometers from one into another apparatus, increases in W at 4.2 K of 1 x 10^{-7} (corresponding to 8 mK at this temperature) and 2 x 10^{-7}, respectively, were found.

These results are comparable to those of Berry [4] for six thermometers (average change at 4.2 K less than 1 x 10^{-7} per year). Durieux, Van Dijk and Muijlwijk [17] found for six thermometers an average drift of less than 2 x 10^{-7} per year, but larger shifts for six other thermometers (in the worst case 23 x 10^{-7} per year).

It follows from these data that, if the highest accuracy is required, it is necessary to check the resistance of the thermometers at a low temperature, say 4.2 K, regularly. The calibration can then easily be corrected, if necessary, by using Matthiessen's rule.

8 Description of the W(T) functions of the thermometers in terms of Matthiessen's rule

8.1 *Introduction*

The resistivity of platinum is often expressed by the relation

$$\rho(T) = \rho_{id}(T) + \rho_0 + \lambda(T)\rho_0 \qquad (5.7)$$

where $\rho_{id}(T)$ is the ideal resistivity, characteristic for the pure metal, and ρ_0 is the residual resistivity at T = 0 K. The term $\lambda(T)\rho_0$ represents the deviation from Matthiessen's rule. It is often assumed, that the deviations from Matthiessen's rule, and thus the function $\lambda(T)$, should be positive.

In practice, resistances are measured rather than resistivities. However, as shown by Berry [18], the differences between the reduced resistances $W(T) = R(T)/R_{0\,°C}$ and reduced resistivities $\rho(T)/\rho_{0\,°C}$ are not larger than 0.17% below 60 K; in fact, they are smaller than 1 x 10^{-8} in W below 15 K. It then follows that eq. (5.7) may be replaced by the expression

$$W(T) = W_{id}(T) + W_0[1 - W_{id}(T) + \lambda(T) - \lambda_{0\,°C} W_{id}(T)] \qquad (5.8)$$

where $W_{id}(T)$ is the reduced resistance for the pure metal, $R_{id}(T)/R_{id}(0\,°C)$, and W_0 is the residual reduced resistance at T = 0 K.

Eq. (5.8) may also be written as

$$W(T) = W_{id}(T) + W_0[1 - W_{id}(T)] + M(T) \qquad (5.9)$$

with

$$M(T) = W_0[\lambda(T) - \lambda_{0\,°C} W_{id}(T)] \; . \qquad (5.10)$$

When Matthiessen's rule holds, M(T) is equal to zero; eq. (5.9) then reduces to the so-called Nernst-Matthiessen rule:

$$W(T) = W_{id} + W_0[1 - W_{id}(T)] \qquad (5.11)$$

Differences $\Delta W(T)$ between reduced resistances of different thermometers can be expressed by the relation

$$\Delta W(T) = \Delta W_0[1 - W_{id}(T)] + \Delta M(T) \qquad (5.12)$$

where ΔW_0 is the difference in residual reduced resistance and $\Delta M(T)$ gives the differences in deviation from Matthiessen's rule for the thermometers.

It should be noted that values of $\lambda(T)$ cannot be unambiguously be deduced from measurements of W(T); they remain uncertain by an amount which is proportional to $W_{id}(T)$ (see ref. 18).

8.2 *The W(T) functions of the thermometers*

Differences between the reduced resistances of the platinum thermometers at temperatures below 15 K, calculated from the polynomials in table 5.5, are shown in figs. 5.6 and 5.7. If the differences did obey Matthiessen's rule, they would be virtually independent of temperature, since W_{id} varies from zero at 0 K to only 1.2×10^{-3} at 15 K (see eq. (5.12)).

For the ten thermometers, the deviations from Matthiessen's rule,

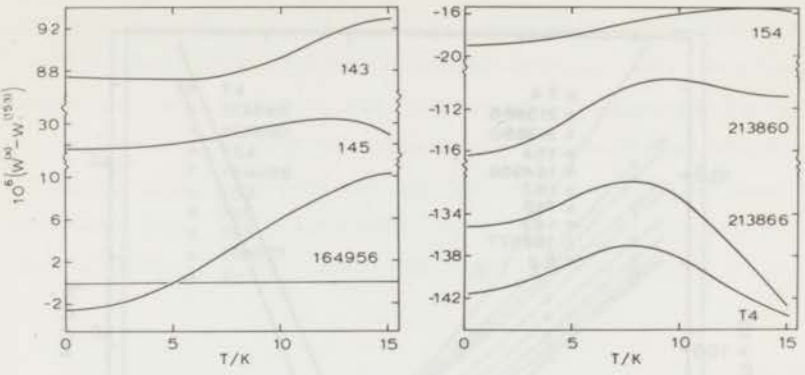

Fig. 5.6. Differences between the reduced resistances of platinum thermometers below 15 K.

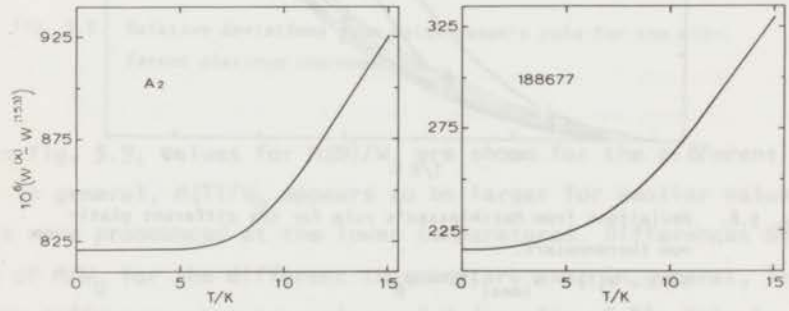

Fig. 5.7. Differences between the reduced resistances of platinum thermometers below 15 K.

calculated from eq. (5.9), are shown in fig. 5.8. In the calculations, the values given by Berry [3] have been used for $W_{id}(T)$.

The large values of M(T) which are found for A2 may be explained from the large residual resistance of this thermometer. The M(T) function for 188677 is, however, much larger than would be expected from its value for W_0.

Most thermometers (those with a temperature coefficient $\alpha > 0.003926$ K^{-1}) have values of M(T), which differ less than one would expect from the

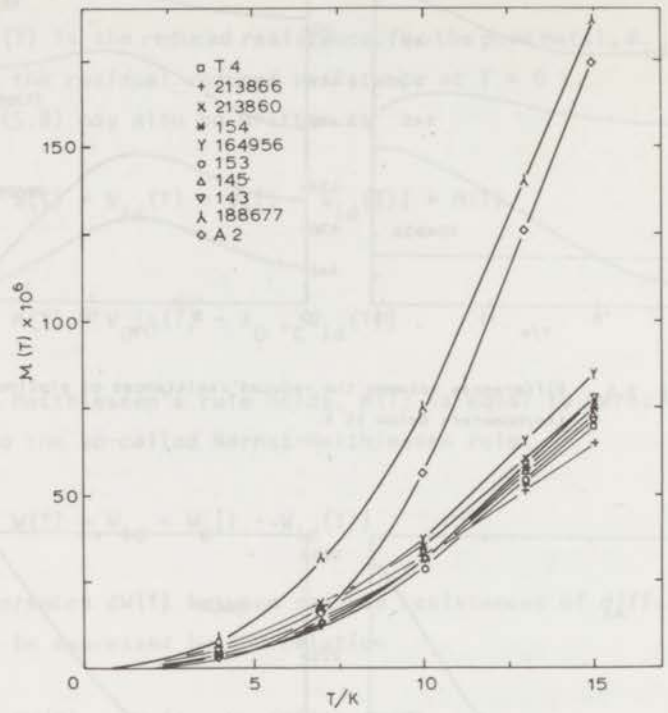

Fig. 5.8. Deviations from Matthiessen's rule for the different platinum thermometers.
$M(T) = W(T) - W_{ideal}(T) - W_0$.

differences in residual reduced resistance, assuming that the differences between the values of $\lambda(T)$ for the thermometers are small. This could mean that the assumed values of W_{id} are too low. (Berry's data for W_{id} should have been corrected for temperature-scale differences, however these corrections have been neglected since they amount to only a few times 10^{-6} near 14 K.) Berry estimated the values of W_{id} to be accurate within 1×10^{-6} near 4 K and within 6×10^{-6} near 13 K. Values of W_{id} reported by different authors (see ref. 2) show a spread of roughly $\pm 30 \times 10^{-6}$ at 14 K.

From fig. 5.8, as well as from fig. 5.6, the complexity of the deviations from Matthiessen's rule for the different thermometers becomes clear.

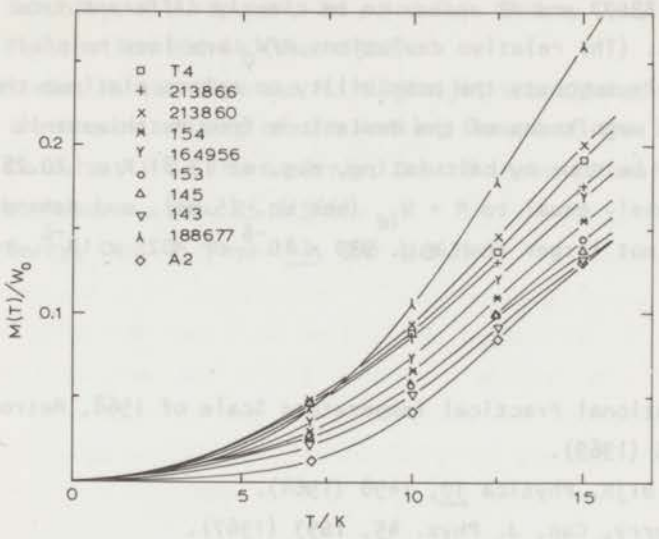

Fig. 5.9. Relative deviations from Matthiessen's rule for the different platinum thermometers.

In fig. 5.9, values for $M(T)/W_0$ are shown for the different thermometers. In general, $M(T)/W_0$ appears to be larger for smaller values of W_0; this is more pronounced at the lower temperatures. Differences between values of M/W_0 for the different thermometers are, in general, less complex than the differences between values of M (see fig. 5.8). This is in agreement with the representation of deviations from Matthiessen's rule by a term which is proportional to W_0 (or ρ_0 in eq. (5.7)).

As said before, thermometer 188677 shows an exceptional behaviour; its value of W_0 is much lower than that for A2 and yet its values of M are even larger than those for A2. Also its values of M/W_0 do not follow the trends of those of the other thermometers.

In Chapter 4, it is shown that temperatures measured on the International Practical Temperature Scale of 1968 with the thermometers 188677 and A2 differ up to 1 to 2 mK from those measured with the other thermometers. For A2, this is not surprising in view of its low value of α, which, in fact, disqualifies A2 for measuring temperatures on IPTS-68. For 188677 however, the value of α is only slightly below the required minimum value.

When the deviations of Matthiessen's rule at, say, 14 K are considered (see fig. 5.8), 188677 and A2 appear to be clearly different from the other thermometers. (The relative deviations M/W_0 are less helpful in this respect.) This suggests the possibility to select platinum thermometers on basis of the magnitudes of the deviations from Matthiessen's rule. This could easily be done by calculating, e.g. at 13.81 K or 20.28 K, $W - W_0$, which is closely equal to $M + W_{id}$ (see eq. (5.9)), and demanding its value to be not larger than e.g. 930×10^{-6} or 4025×10^{-6}, respectively.

References

1. International Practical Temperature Scale of 1968, Metrologia 5, 35 (1969).
2. H. van Dijk, Physica 30, 1498 (1964).
3. R.J. Berry, Can. J. Phys. 45, 1693 (1967).
4. R.J. Berry, Metrologia 3, 53 (1967).
5. J.F. Kos and J.L.G. Lamarche, Can. J. Phys. 45, 339 (1967).
6. W.J. de Haas and J. de Boer, Physica 1, 609 (1933-1934).
7. R. Muijlwijk, Physica 43, 419 (1969).
8. H.H. Plumb and G. Cataland, Metrologia 2, 127 (1966).
9. A.R. Colclough, Temperature, It's Measurement and Control in Science and Industry (Instrument Society of America, Pittsburgh, 1972), Vol. 4.
10. J.S. Rogers, R.J. Tainsh, M.S. Anderson and C.A. Swenson, Metrologia 4, 47 (1968).
11. D.N. Astrov, M.P. Orlova and G.A. Kytin, Metrologia 5, 111 (1969).
12. K.H. Berry, Metrologia 8, 125 (1972).
13. C.A. Swenson, Temperature, It's Measurement and Control in Science and Industry (Instrument Society of America, Pittsburgh, 1972) Vol. 4; T.C. Cetas and C.A. Swenson, Metrologia 8, 46 (1972); T.C. Cetas, Ph.D. Thesis, Iowa State Univ., Ames, Iowa, U.S.A. (1970).
14. C. van Rijn and M. Durieux, Temperature, It's Measurement and Control in Science and Industry (Instrument Society of America, Pittsburgh, 1972), Vol. 4.

15. G.E. Forsythe, J. Soc. Ind. Appl. Math. 5, 74 (1957).

16. J.F. Schooley, R.J. Soulen, Jr., and G.A. Evans, Jr., NBS Special Publication 260-44 (Dec. 1972).

17. M. Durieux, H. van Dijk and R. Muijlwijk, Unpublished report to the Moscow meeting of the Working Groups of the Comité Consultatif de Thermométrie, Comité International des Poids et Mesures, doc. 25 (1966).

18. R.J. Berry, Can. J. Phys. 41, 946 (1963).

APPENDIX

THE INTERNATIONAL PRACTICAL TEMPERATURE SCALE OF 1968

The International Practical Temperature Scale of 1968 (IPTS-68) [1] is used throughout this thesis. Therefore a short description of it, in the temperature range from 13.81 K to 273.15 K, is given here.

IPTS-68 in this range is based on the eight "defining fixed points" given in table A.1 and on the standard platinum resistance thermometer as an interpolation instrument between these fixed points.

The resistance of the platinum thermometer has to be determined at the eight defining fixed points. Then the complete calibration on IPTS-68 is derived as follows:

A reference function $W_{CCT-68}(T_{68})$ is defined by the relation

$$T_{68} = \{a_0 + \sum_{i=1}^{20} a_i [\ln W_{CCT-68}(T_{68})]^i\} \text{ K} \qquad (A.1)$$

where $W(T) = R(T)/R(0°C)$ and R is the resistance of the thermometer; the coefficients a_i are specified in the text of the scale (CCT-68 stands for Comité Consultatif de Thermométrie-1968). The range between 13.81 K and 273.15 K is divided into four parts in each of which a deviation function $\Delta W(T_{68}) = W_{thermometer}(T_{68}) - W_{CCT-68}(T_{68})$ is defined.

From 90.188 K to 273.15 K

$$\Delta W(T_{68}) = A_4 t_{68} + C_4 t_{68}^3 (t_{68} - 100°C) \qquad (A.2)$$

where the constants A_4 and C_4 are determined by the values of $\Delta W(T_{68})$ at the normal boiling points of oxygen and water ($t_{68} = T_{68} - 273.15$ K).

From 54.361 K to 90.188 K

$$\Delta W(T_{68}) = A_3 + B_3 T_{68} + C_3 T_{68}^2 \qquad (A.3)$$

where the constants are determined by the values of $\Delta W(T_{68})$ at the triple point and normal boiling point of oxygen and the value of $d\Delta W(T_{68})/dT_{68}$ at 90.188 K as obtained from eq. (A.2).

From 20.28 K to 54.361 K

$$\Delta W(T_{68}) = A_2 + B_2 T_{68} + C_2 T_{68}^2 + D_2 T_{68}^3 \qquad (A.4)$$

where the constants are determined by the values of $\Delta W(T_{68})$ at the normal boiling points of equilibrium hydrogen and of neon and at the

Table A.1

Defining fixed points in IPTS-68 for the range from 13.81 K to 273.15 K

Equilibrium state*	Assigned value of T_{68}
Triple point of equilibrium hydrogen**	13.81 K
Boiling point of equilibrium hydrogen at a pressure of 33330.6 Pa (25/76 standard atmosphere)	17.042 K
Boiling point of equilibrium hydrogen	20.28 K
Boiling point of neon	27.102 K
Triple point of oxygen	54.361 K
Boiling point of oxygen	90.188 K
Triple point of water	273.16 K
Boiling point of water	373.15 K

* Except for the triple points and the point at 17.042 K the pressures are 101325 Pa (one standard atmosphere).

** Equilibrium hydrogen means hydrogen which has its equilibrium ortho-para composition at the relevant temperature.

triple point of oxygen and by the value of $d\Delta W(T_{68})/dT_{68}$ at 54.361 K as obtained from eq. (A.3).

From 13.81 K to 20.28 K

$$\Delta W(T_{68}) = A_1 + B_1 T_{68} + C_1 T_{68}^2 + D_1 T_{68}^3 \qquad (A.5)$$

where the constants are determined by the values of $\Delta W(T_{68})$ at the triple point of equilibrium hydrogen, at T_{68} = 17.042 K and at the normal boiling point of equilibrium hydrogen and by the value of $d\Delta W(T_{68})/dT_{68}$ at 20.28 K as obtained from eq. (A.4).

The promulgation of IPTS-68 has been an important step in the improvement of temperature measurements. In the range above 90.188 K IPTS-68 replaces the former international practical temperature scale, which had not been revised significantly since its inception in 1927 and which deviated considerably from the thermodynamic temperature scale as was shown by modern gas thermometry. In the range from 13.81 K to 90.188 K IPTS-68 is the first internationally adopted scale and replaces the different "national scales" which were defined by sets of platinum thermometers calibrated, in some cases many years ago, against gas thermometers.

Below the temperature range of IPTS-68 there are two other internationally adopted temperature scales: The "1958 ^{4}He scale" and the "1962 ^{3}He scale" which are based on the vapour pressure-temperature relation of ^{4}He and ^{3}He. The upper limits of these scales are the critical points of ^{4}He (5.189 K) and of ^{3}He (3.324 K) respectively. In the range between 5.189 K and 13.81 K as yet no international practical temperature scale exists.

Reference

1. Echelle Internationale Pratique de Température de 1968, published by the Bureau International des Poids et Mesures, Sèvres, France; International Practical Temperature Scale of 1968, Metrologia 5, 35 (1969).

SAMENVATTING

Dit proefschrift beoogt in de eerste plaats bij te dragen tot de ontwikkeling van de thermometrie, die is te omschrijven als de fysica van het meten van temperaturen en het vastleggen van internationale praktische temperatuurschalen. Daartoe zijn met hoge nauwkeurigheid metingen uitgevoerd van dampspanningen van vaste en vloeibare neon tussen 19 K en 30 K en van vloeibare zuurstof tussen 54 K en 99 K, en is het gedrag van platina-weerstandsthermometers in het temperatuurgebied van 2 K tot 273 K bestudeerd. De beschreven metingen, voor zover betrekking hebbende op het gebied boven 13.81 K, zijn voor het eerst rechtstreeks gedaan op de Internationale Praktische Temperatuur Schaal van 1968 (IPTS-68). Tot voor kort werden metingen uitgevoerd op zogenaamde nationale of laboratorium temperatuurschalen, waarmee in het algemeen in verschillende laboratoria niet die reproduceerbaarheid kon worden bereikt die inherent is aan de IPTS-68.

In het temperatuurgebied, waarvan sprake is in de hier beschreven metingen, wordt de IPTS-68 gedefiniëerd met behulp van de platinathermometer. Deze dient dan te zijn geijkt bij een aantal vaste temperaturen, waartoe de temperaturen van de tripelpunten en normale kookpunten van een aantal stoffen behoren. Om deze reden is in de hoofdstukken 2 en 3 vrij uitgebreid aandacht besteed aan de techniek van het nauwkeurig en reproduceerbaar realiseren van deze punten voor neon en zuurstof.

De wijze, waarop de IPTS-68 is gedefiniëerd, brengt met zich mee dat met verschillende platinathermometers niet exact gelijke temperaturen worden gemeten. In hoofdstuk 4 wordt aangetoond, dat de verschillen tussen de thermometers in het hele gebied tussen 13.81 K en 273.15 K in het algemeen niet groter dan 2 mK zijn.

De verkregen dampspanningsrelaties van neon en (in iets mindere mate) van zuurstof kunnen, in hun temperatuurgebied, in plaats van de platinathermometer gebruikt worden voor temperatuurbepalingen. De dampspanningsrelaties bieden de interessante mogelijkheid tot een vergelijking met

andere thermische eigenschappen zoals de verdampingswarmte en de smeltwarmte, soortelijke warmten van de gecondenseerde en gasvormige fasen en viriaalcoëfficienten van het gas. De thermodynamische consistentie van beschikbare gegevens is onderzocht; in gevallen waar gegevens ontbraken, konden soms grootheden worden berekend.

Met gebruikmaking van bekende verschillen tussen de dampspanningen van de neon isotopen en van de toepasbaarheid van de wet van Raoult, zijn dampspanningsvergelijkingen voor ^{20}Ne en ^{22}Ne tussen 19 K en 30 K afgeleid uit de resultaten voor het 'normale' neonmengsel.

In hoofdstuk 5 zijn de resultaten beschreven van een onderzoek naar de temperatuurafhankelijkheid van de weerstand van tien platinathermometers in het gebied tussen 2 K en 15 K. Calibratieprocedures zijn uitgewerkt voor het gebied tussen 4.2 K en 13.81 K, waarmee de hoogste (gelijk aan de meetnauwkeurigheid) of een iets lagere (tot ongeveer 0.01 K) interpolatienauwkeurigheid kan worden bereikt. Duidelijke afwijkingen van de regel van Matthiessen, en opmerkelijke verschillen tussen de afwijkingen voor de verschillende thermometers, zijn gevonden.

Op verzoek van de Faculteit der Wiskunde en Natuurwetenschappen volgt hier een overzicht van mijn studie.

Nadat ik in 1960 het diploma gymnasium-B had behaald aan het Maerlant-Lyceum te 's-Gravenhage, begon ik in september 1960 mijn studie aan de Rijksuniversiteit te Leiden. In 1964 legde ik het kandidaatsexamen natuurkunde en wiskunde met bijvak sterrekunde (a') af. Ter voorbereiding op het doctoraalexamen volgde ik colleges bij Prof. Dr. J.A.M. Cox, Prof. Dr. J.A. Goedkoop, Prof. Dr. P.W. Kasteleyn, Prof. Dr. J. Kistemaker en Prof. Dr. P. Mazur. In mei 1967 legde ik het doctoraal-examen experimentele natuurkunde met bijvak klassieke mechanica af.

Sinds 1964 ben ik werkzaam op het Kamerlingh Onnes Laboratorium in de werkgroep Thermometrie, die tot 1965 onder leiding stond van Dr. H. van Dijk en sedertdien wordt geleid door Dr. M. Durieux. Aanvankelijk assisteerde ik Drs. C. van Rijn bij susceptibiliteitsmetingen ten behoeve van de ontwikkeling van een magnetische thermometer en bij de eerste onderzoekingen aan germaniumthermometers. Na mijn doctoraalexamen zette ik, daartoe in staat gesteld door subsidie van TNO aan de werkgroep Thermometrie, het onderzoek aan germaniumthermometers voort en breidde dit uit tot het temperatuurgebied van 0.5 K tot 100 K; tevens onderzocht ik temperatuurschalen voor het gebied van 2 K tot 20 K. Hierbij werd ik geassisteerd door mevr. Drs. J.A. Dorrepaal-Staas en mevr. Drs. M.C. Nieuwenhuys-Smit.

Vanaf 1964 assisteer ik bij het onderwijs aan pre-kandidaten, aanvankelijk bij het natuurkunde prakticum, vanaf 1966 bij werkcolleges behorende bij het college Elementaire Natuurkunde voor chemici van Dr. C.J.N. van den Meijdenberg en Dr. H. van Beelen; momenteel ben ik met de leiding van deze werkcolleges belast. In januari 1970 werd ik benoemd tot wetenschappelijk medewerker.

De in dit proefschrift beschreven onderzoekingen namen een aanvang in augustus 1970. Voor het tot stand komen van het proefschrift waren de voortdurende steun van en vele discussies met Dr. M. Durieux van bijzonder grote betekenis. Bij de experimenten werd ik met grote toewijding en vaardigheid terzijde gestaan door de heer

J. Mooibroek, technisch medewerker van de afdeling Thermometrie bezoldigd door TNO. Voor het uitvoeren van de talrijke computerberekeningen ben ik mevr. Drs. M.C. Nieuwenhuys-Smit en de heer J.E. van Dijk zeer erkentelijk. Deze laatste schreef o.a. de programma's voor de thermodynamische berekeningen. Dr. H. ter Harmsel was zo vriendelijk calibraties van platinathermometers bij het stoompunt en het tripelpunt van water uit te voeren.

De benodigde metalen apparatuur werd vervaardigd door de heer J.A.J.M. Disselhorst, die bijkomende technische problemen ondernemend oploste en die tevens de tekeningen voor dit proefschrift maakte. Voor de glazen apparatuur werd zorg gedragen door de glasblazerij van de heer B. Kret.

De samenwerking met de technische en administratieve staf van het Kamerlingh Onnes Laboratorium was steeds bijzonder plezierig.

Foto's voor het proefschrift werden vervaardigd door de heer W.F. Tegelaar. Het manuscript werd getypt door mevr. E. de Haas-Walraven.

Tenslotte wil ik mijn echtgenote bedanken voor haar steun in alle fasen van het ontstaan van het proefschrift.